



HAL
open science

structural basis of kinesin motility

Luyan Cao

► **To cite this version:**

Luyan Cao. structural basis of kinesin motility. Structural Biology [q-bio.BM]. Université Paris-Saclay, 2016. English. NNT : 2016SACLS267 . tel-01452845

HAL Id: tel-01452845

<https://theses.hal.science/tel-01452845v1>

Submitted on 2 Feb 2017

HAL is a multi-disciplinary open access archive for the deposit and dissemination of scientific research documents, whether they are published or not. The documents may come from teaching and research institutions in France or abroad, or from public or private research centers.

L'archive ouverte pluridisciplinaire **HAL**, est destinée au dépôt et à la diffusion de documents scientifiques de niveau recherche, publiés ou non, émanant des établissements d'enseignement et de recherche français ou étrangers, des laboratoires publics ou privés.

THESE DE DOCTORAT
DE
L'UNIVERSITE PARIS-SACLAY
PREPAREE A
L'UNIVERSITE PARIS-SUD

ECOLE DOCTORALE N° 569
Innovation thérapeutique : du fondamental à l'appliqué
Spécialité de doctorat : Biochimie et biologie structurale

Par

Mlle LuYan CAO

Structural Basis Of Kinesin Motility

Thèse présentée et soutenue à Gif-sur-Yvette, le 27 Septembre 2016 :

Composition du Jury :

M, MINARD, Philippe	Professeur, Université Paris-Sud	Président
Mme, MOORES, Carolyn	Professeur, Université de Londres	Rapporteur
M, PICOT, Daniel	Directeur de recherche, Université Paris Diderot	Rapporteur
M, LIPPENS, Guy	Directeur de recherche, LISBP	Examineur
M, KNOSSOW, Marcel	Directeur de recherche émérite, CNRS	Directeur de thèse
M, GIGANT, Benoît	Chargé de recherche, CNRS	Directeur de thèse



Acknowledgement

Many thanks to Prof. Philippe MINARD, Prof. Carolyn MOORES, M. Daniel PICOT, M. Guy LIPPENS, M. Marcel KNOSSOW and M. Benoît GIGANT for presenting as members of my thesis jury.

I would like to express my sincere thanks to M. Marcel KNOSSOW and M. Benoît GIGANT for their expert, sincere and invaluable guidance extended to me. Without their consistent and illuminating instruction, this thesis would not have reached its present form.

I am grateful to Valérie, Soraya, Weiyi, Shoeb and other members in our group. They provided their help and professional advice generously for this thesis. It's my honor to join the group and work with you.

I also thank Prof. Chunguang WANG. She shares her experience and knowledge which benefits me greatly.

In this thesis, diffraction data were collected at SOLEIL synchrotron (PX1 and PX2 beam lines). I am most grateful to the machine and beam line groups for making these experiments possible.

I sincerely thank Mme. Marie-France CARLIER and M. Julian PERNIER for sharing their Stopped-flow machine and their advices.

Supports on initial crystallization screening were provided by Mme. Armelle VIGOUROUX. DSC experiment has been done with the help of Mme. Magali AUMONT. The IMAGIF platform offered their professional supports to this work as well. I thank the HTX lab in Grenoble sincerely for their technical supports on crystallization screening.

Thank you, my dear friends, Quyen, Loïc, Abbas, Kai, Roman, Pierre for your supports and encouragements.

Thank you, Florian, for being there.

感谢我亲爱的爸爸妈妈，奶奶，姐姐，姑父姑妈，以及其他远在中国的亲人。没有你们的支持，也就不会有今天的我。

感谢建乔，周晗，毛毛，袁浩，和你们一起度过的那个夏天给了我希望和勇气。

Finally, I place on record, my sense of gratitude to one and all who have lent their helping hand in this thesis directly or indirectly.

Contents

Acknowledgement.....	1
Abbreviations.....	4
Preface.....	6
Introduction.....	7
1. Microtubules and tubulin.....	7
1.1 Microtubules.....	7
1.2 Tubulin.....	9
1.3 DARPin.....	12
2. Kinesin in general.....	15
2.1 Classification of the kinesin superfamily.....	15
2.2 Conserved motor domain.....	17
2.3 Other cytoskeletal motors.....	20
3. Kinesin-1.....	23
3.1 The kinetic mechanism of kinesin.....	24
3.2 Motility model of kinesin-1.....	28
3.3 Advancement of kinesin-1 structural studies.....	32
4. Kinesin-14.....	39
4.1 Kinesin-14 in general.....	39
4.2 Ncd.....	40
Objectives.....	45
Results and Discussion.....	46
1. Structure of apo-kinesin-1 bound to tubulin.....	46
1.1 Context.....	46
1.2 Paper: “The structure of apo-kinesin bound to tubulin links the nucleotide cycle to movement.”.....	48
1.3 Discussion.....	58
2. Structures of isolated apo-kinesin-1.....	66
2.1 Context.....	66

2.2	Paper: “The structural switch of nucleotide-free kinesin.”	67
2.3	Discussion	94
3.	Crystallization of kinesin-14 in complex with tubulin-DARPin.....	102
3.1	Objectives.....	102
3.2	Constructs	106
3.3	Characterization	109
3.4	Crystallization.....	114
3.5	Discussion	115
	Conclusions and Perspectives	118
	Materials and Methods	124
1.	Differential Scanning Calorimetry assay on kinesin-1 and its mutants.....	124
2.	Purification of Kinesin-14 heterodimer	124
3.	Production of Kinesin-Tubulin-DARPin complex.....	131
4.	Nucleotide state analysis	133
5.	Spin down assay	133
	References	134

Abbreviations

2YT	Yeast extract/bacto Tryptone medium
LB	Lysogeny Broth medium
DTT	Dithiothreitol
EGTA	Ethylene Glycol-bis(β -aminoethyl ether)- <i>N,N,N',N'</i> -Tetraacetic Acid
EDTA	EthyleneDiamineTetraacetic Acid
SDS-PAGE	Sodium Dodecyl Sulfate-PolyAcrylamide Gel Electrophoresis
Mes	2-(<i>N</i> -Morpholino) ethanesulfonic acid
Pipes	Piperazine- <i>N,N'</i> -bis(2-ethanesulfonic acid)
Hepes	4-(2-Hydroxyethyl)-1-piperazineethanesulfonic acid
PEG	PolyEthylene Glycol
ADP	Adenosine DiPhosphate
Mant-ADP	2'-(or-3')-O-(<i>N</i> -Methylantraniloyl) Adenosine 5'-DiPhosphate
ATP	Adenosine TriPhosphate
AMPPNP	Adenylyl-imidodiphosphate
Pi	Inorganic phosphate
GDP	Guanosine DiPhosphate
GTP	Guanosine TriPhosphate
GMPCPP	Guanosine-5'-[(α,β)-methyleno] triphosphate
K_D	Dissociation constant
k_{on}	Association rate
k_{off}	Dissociation rate
K_i	Inhibitory constant

K_m	Michaelis constant
K_a	Acid dissociation constant
EPR	Electron Paramagnetic Resonance
FRET	Fluorescence Resonance Energy Transfer
EM	Electron Microscopy
P-loop	Phosphate-binding loop
TEV	Tobacco Etch Virus

Preface

Microtubules are one of the main components of the eukaryotic cytoskeleton. Together with the actin-myosin system, and among other functions, they organize the intracellular transport, forming the filaments along which dyneins and kinesins travel. These motor proteins use the energy produced by ATP hydrolysis to walk along microtubule, carrying loads. The hallmark of kinesins is a relatively well-conserved motor domain, which comprises both the binding site for the nucleotide and the binding site for microtubule. Based on the position of the motor domain in the sequence, at the N-terminus, internal or at the C-terminus, kinesins can be divided into three subfamilies, N-type, internal and C-type, which are further divided into 14 classes according to differences in the motor domain sequence. N-type kinesins, including classes 1 to 12, move towards the plus end of microtubule, i.e. broadly speaking from the center to the periphery of interphase cells; whereas C-type kinesins, which kinesin-14 belongs to, move towards microtubule minus end. Kinesin-13s, internal kinesins, are not motile but depolymerize microtubule, showing that kinesins have roles beyond transport, for instance in the regulation of microtubule dynamics.

Kinesin binding to or dissociating from microtubules is tightly coupled with its nucleotide cycle. ADP-kinesin has a low affinity for microtubules and a low ADP dissociation rate. Binding to microtubules enhances ADP dissociation in kinesin and converts kinesin to a high affinity state for microtubules. Subsequent ATP binding triggers the conformational changes leading to the mechanical step. After ATP hydrolysis and Pi release, kinesin, back to ADP bound state, detaches from microtubules to complete the cycle. Although this general framework is well established, our understanding of several steps of this cycle is still incomplete, including how ADP dissociation is accelerated by microtubules and how ATP binding triggers the movement. Structurally, the conformation of ADP-kinesin detached from microtubule is known from X-ray crystallography whereas both crystal and electron microscopy structures have been determined for kinesin in an ATP state, bound to a microtubule (or to tubulin, which is the microtubule building block). What is missing are high resolution structural data on nucleotide-free kinesin, both isolated and as a complex with microtubules. These data should highlight the mechanism of ADP release from kinesin and complete our view of the kinesin structural cycle related to its mechanochemical cycle. This is the objective of my work.

Introduction

1. Microtubules and tubulin

In eukaryotic cells, combined with microfilaments and intermediate filaments, microtubules serve as cytoskeleton, providing cells with an inner framework, maintaining the shape of cells. Microtubules contribute to the structural formation of mitotic spindle, centrosome, cilia and flagella. Also, microtubules serve as a track for intercellular transport. Motor proteins, as kinesin and dynein, move along microtubules to transport cargoes. Microtubules are observed in all eukaryotes, playing important roles in different cellular functions including cell division, cell transport, morphogenesis etc.

1.1 Microtubules

Structure of microtubules

Microtubules have a cylinder-shaped structure with an external diameter of 24 nm. They are typically formed by 13 linear and parallel protofilaments that interact laterally. In vitro, they can consist of 9 to 16 protofilaments. Each of the protofilaments is composed of α/β tubulin heterodimers arranged head-to-tail (Fig. 1.1a), so in a protofilament, one end is an exposed α tubulin and the other is an exposed β tubulin. Because of the parallel arrangement of the protofilaments, microtubules are polarized: the end with the β subunit exposed is called the plus end; the other end with α tubulin exposed is called the minus end. Microtubules can be elongated at both the plus and minus ends, but it extends more rapidly at its plus end (Walker et al. 1988).

A standard microtubule with 13 protofilaments has a pitch of 3 monomers; consequently microtubule has a “seam”. Laterally, protofilaments contact each other with the same subunit (i.e. α tubulin to α tubulin, β tubulin to β tubulin), except the contacts in the “seam”, where α subunits are adjacent to neighbor β subunits (Fig. 1.1a).

Dynamics of microtubules

Dynamic instability of microtubules is studied as a foundation of cell physiology (Brouhard 2015). Figure 1.1b presents the dynamics of microtubule including several main processes: polymerization, depolymerization, catastrophe and rescue (Conde and Caceres 2009).

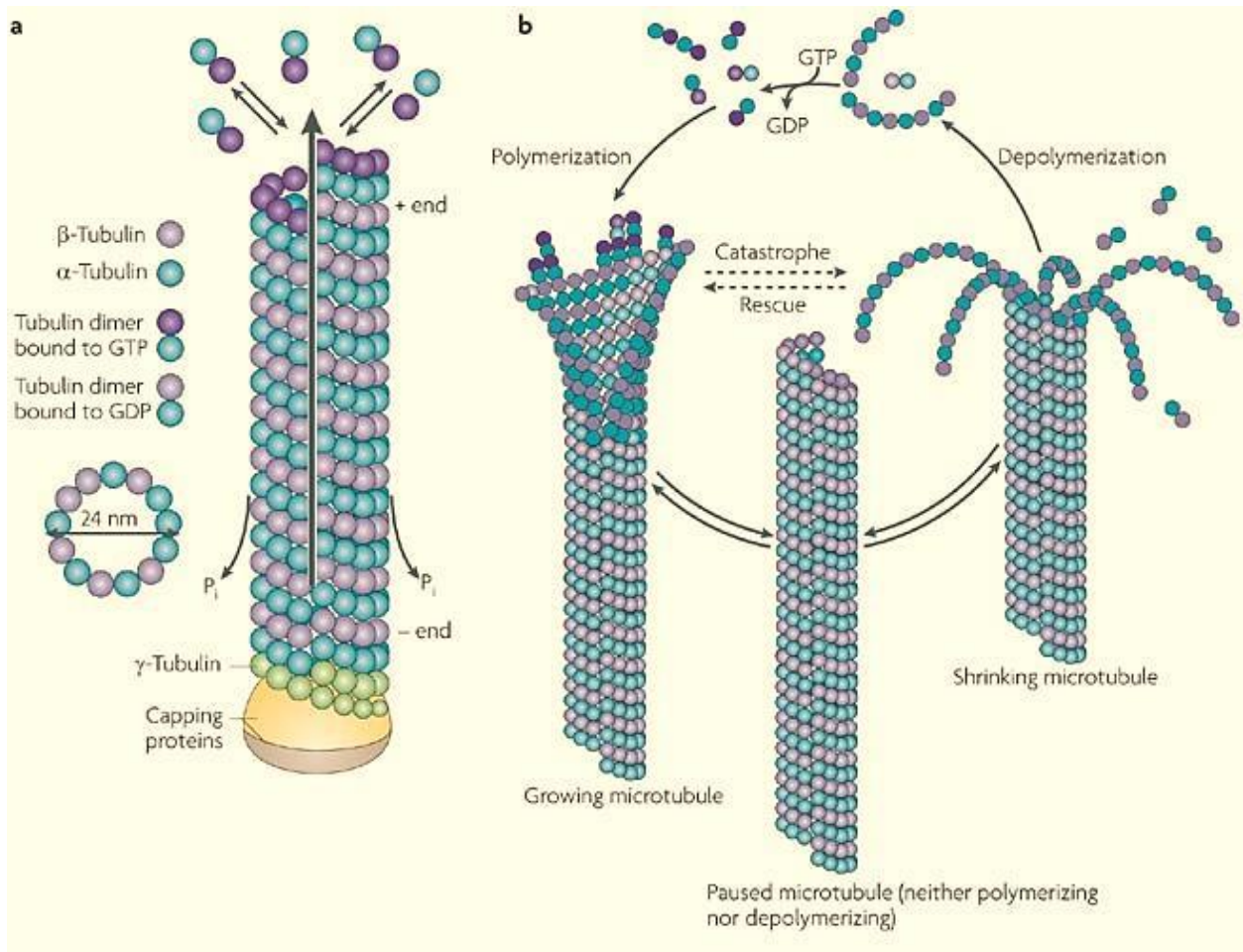


Figure 1.1 General information on microtubules. (Conde and Caceres 2009)

a) A microtubule is usually composed of 13 protofilaments, templated by the γ -tubulin ring complex. The straight arrow indicates the microtubule seam (where tubulins of adjacent protofilaments interact with a subunit of the other type).

b) The microtubule cycle.

In a tubulin heterodimer, each subunit binds a nucleotide, one of which is neither hydrolysable nor exchangeable GTP bound to α tubulin. Concerning the nucleotide in β tubulin, if it is a GTP, then the tubulin is called GTP-tubulin; if it is a GDP instead, the tubulin is called GDP-tubulin. That GTP-tubulins keep binding to microtubule ends is responsible for the growth of microtubules. This event is also called “polymerization”. The hydrolysis of the GTP molecule in GTP-tubulin, accompanying microtubule assembly, leads to the paradox that microtubules are composed mainly of GDP-tubulin, which tends to fall

off from the tip of microtubules. The paradox is resolved because of the delay between microtubule assembly and GTP hydrolysis, which leads to the formation of a “GTP-cap”, preventing microtubules from depolymerization at microtubule ends. When the GTP in the cap is hydrolyzed, microtubules will go through rapid shrinkage. The loss of the GTP-cap and its induced disassembly is called a “catastrophe”. It is observed by cryo-electron microscopy that protofilaments peel from the ends into ring-like structures during shrinkage (Mandelkow, Mandelkow, and Milligan 1991). GTP tubulin can also bind to the shrinking end to form a new cap preventing the microtubule from depolymerizing. The process that a microtubule stops shrinking and starts to grow is called a ‘rescue’. Microtubule growth and shrinkage is the basis of its functions.

1.2 Tubulin

Tubulin belongs to a protein family of several members sharing a conserved GTPase domain. There are seven different kinds of tubulin in eukaryotic cells: α , β , γ , ϵ , δ , ζ and η (Oakley 2000). Among them, δ , ϵ , ζ and η tubulin are considered as rare tubulins and do not have a ubiquitous distribution in eukaryotic organisms (Dutcher 2001). The other tubulins are found in all eukaryotes. γ tubulin, localized primarily in centrosomes and spindle pole bodies, is associated with microtubules nucleation and polar orientation. α and β tubulin are always associated in an heterodimer which is the building block of microtubule in all eukaryotic cells. The tubulin talked about in this thesis refers to the α/β tubulin heterodimer.

Characters of tubulin heterodimers

The sequence of α and β tubulins is highly conserved across species. For example, the comparison of tubulin sequences from human, *Drosophila*, *Chlamydomonas*, *Trypanosoma* and *Paramecium* indicates that α tubulins are 89-95% similar and that β tubulins are 88-94% similar (Dutcher 2001).

α tubulins and β tubulins, both having a molecular weight about 50 000 Dalton, share 40% amino-acid sequence identity. The isoelectric point of these subunits is between 5.2 and 5.8. Each monomer consists of about 440 amino acids upon which post-translational modifications play an important role in its dynamics and its organizations (Song and Brady 2015).

In cells, α/β tubulin colliding with the end of a protofilament extends a microtubule. The higher the concentration of tubulin is, the more frequently these collisions occur, and therefore the microtubule grows faster. For a single protofilament, α/β tubulin binds to its ends rapidly (at about $4 \mu\text{M}^{-1} \text{s}^{-1}$), but it falls off as rapidly when there is no lateral bond formed. Usually α/β tubulins entombed by their neighbors with a low off rate form open sheets at the ends of microtubules, which close into cylinders later. This process is usually

accompanied by GTP hydrolysis, though the hydrolysis of GTP is not obliged. With GMPCPP, a GTP non-hydrolysable analog, tubulin heterodimers can still form microtubules (Nogales and Wang 2006).

In solution, tubulin is instable and tends to form polymers. This process is GTP consuming and sensitive to the temperature. At 4°C, tubulins do not self-assemble and exist as heterodimers in the solution. When incubated at 37 °C with GTP and magnesium ions (Mg^{2+}) in the solution, tubulin heterodimers polymerize to form microtubules. If the temperature is decreased, microtubules start to depolymerize. This behavior of tubulin is used to purify it by several cycles of polymerization and depolymerization but also gives trouble for tubulin crystallization. Protein crystallization usually requires high homogeneity of samples, while tubulin heterodimers tend to polymerize and form various polymers. As a result, tubulin crystallization without any stabilizer is very difficult. Actually, so far there is no tubulin heterodimer alone without stabilizer that has been reported to be crystallized.

Structural studies on tubulin

Tubulin can exist in three major forms: straight protofilaments, as found in microtubule, heterodimers and curved oligomers. Different approaches have been used to characterize them structurally. The first near-atomic model of tubulin was determined by electron crystallography (Nogales, Wolf, and Downing 1998). In the presence of zinc ion, tubulin assembles into two-dimensional sheets made of antiparallel protofilaments. These Zn-sheets have been studied by electron diffraction. More recently, thanks to the progress in Cryo-electron microscopy, the structure of microtubules has been determined at about 3.5 Å resolution (Zhang et al. 2015). The structure of non-microtubular tubulin has also been determined but by X-ray crystallography with different tubulin stabilizers. Our lab published a crystal structure of a complex of GDP tubulin, two tubulins arranged head to tail, with the stathmin-like domain of RB3, a stathmin family protein (Ravelli et al. 2004). Following this, more high resolution crystal structures of tubulin oligomers and heterodimers in complex with stabilizers have been determined (Nawrotek, Knossow, and Gigant 2011).

As expected from their ~40% sequence identity, α tubulin and β tubulin present a similar overall structure (Fig. 1.2). They are globular proteins with a diameter of about 4 nm. Each subunit consists of two interacting β sheets surrounded by α helices. The subunit can be divided into three structural domains, including the nucleotide binding domain, an intermediate domain and the C-terminal domain. The nucleotide binding domain, also referred to as the N-terminal domain, forms a Rossmann fold where parallel β strands alternate with α helices. The Rossmann fold is typical for nucleotide-binding proteins. The nucleotide binding site on α - tubulin is called N-site (Non-exchangeable site); the one on β -tubulin is called E-site (exchangeable site). The intermediate domain, containing the taxol

binding site, also has a β sheet surrounded by α helices. The C-terminal domain, consisting of 2 α helices contacting the previous domains, is exposed to the outside surface of the microtubule and is usually the target of microtubule associated proteins (MAPs) and motor proteins (Downing and Nogales 1998).

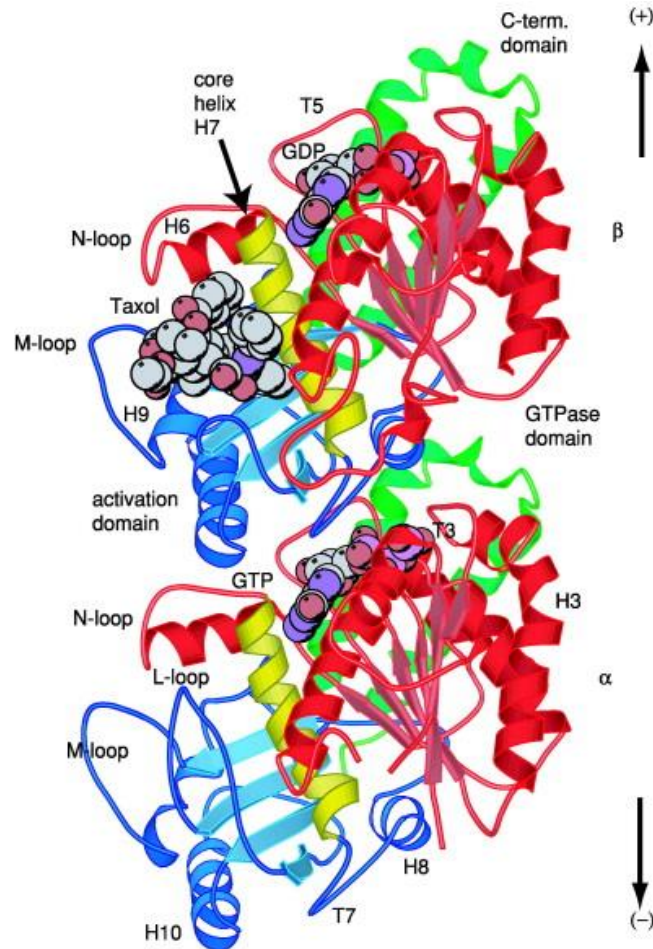


Figure 1.2 Structure of a tubulin heterodimer (Amos and Schlieper 2005)

A tubulin heterodimer is colored based on different domains. The GTP binding domains (red) are responsible for nucleotide binding. The activation domain colored in blue provides the catalytic α -tubulin Glu 254 residue which participates in the hydrolysis of the GTP in the next β -tubulin along a protofilament. The core helix (yellow) connects the two globular domains in each monomer. The C-terminal domain on the external surface is colored in green.

The last C-terminal residues of each subunit are flexible and are usually not seen in the structures. They are enriched in acidic residues. This part is also where the most differences among isotypes across species occur. Besides, these residues are the target of most of the post-translational modifications, including the removal of the last tyrosine of

the α subunit and the addition of glutamate chains (Wloga and Gaertig 2010). Nevertheless, these residues are removable by a protease called subtilisin which will reduce the total number of isoforms for tubulin consequently (Lobert and Correia 1992), so it's likely that subtilisin treatment may improve the possibility of tubulin's crystallization. For β subunit, there are more than one subtilisin site which have different accessibility to the protease corresponding to the heterodimer or polymer form of the tubulin.

Ligands of tubulin

Tubulin is the target of agents which can perturb microtubule dynamics with either a stabilizing or a destabilizing effect (Cormier et al. 2010). Some of these ligands are used clinically for cancer treatment. Different ligands target various sites in the tubulin heterodimer. Here I will present only two ligands of tubulin that I have used during my work either as a tubulin stabilizer for crystallization purpose, or as a microtubule stabilizer needed for kinetic studies.

Colchicine

Colchicine is originally extracted from plants of the genus *Colchicum*. It prevents tubulin heterodimer from polymerizing into microtubules. Structural studies identified the colchicine binding site on β tubulin; it is mostly buried in the β tubulin's intermediate domain (Ravelli et al. 2004). So as a tubulin stabilizer, colchicine has probably no direct impact on kinesin or kinesin-like protein binding. It has been checked afterwards by gel filtration chromatography that with or without colchicine a peak of kinesin-tubulin-DARPin complex shows at a similar position.

Taxane

Taxanes are originally found in plants of the genus *Taxus*. Taxol and Taxotere are used widely as chemotherapy agents because of their ability to interfere with cell division by stabilizing microtubules. These compounds are used to generate stable microtubules, when they are bound to tubulin heterodimers in a one to one ratio. The taxol binding site was identified by electron crystallography (Nogales, Wolf, and Downing 1998) on Zn-sheet tubulin, as a hydrophobic pocket located also in β tubulin.

1.3 DARPin

DARPin is the abbreviation for 'Designed Ankyrin Repeat ProteIN' (Fig. 1.3). Anti-tubulin DARPins have been selected in the lab to interfere with microtubule assembly in a unique manner. The ideal DARPins used in this thesis should be able to bind tubulin stably with a ratio of one to one forming a tubulin DARPin trimer, while not preventing kinesins from binding to tubulin.

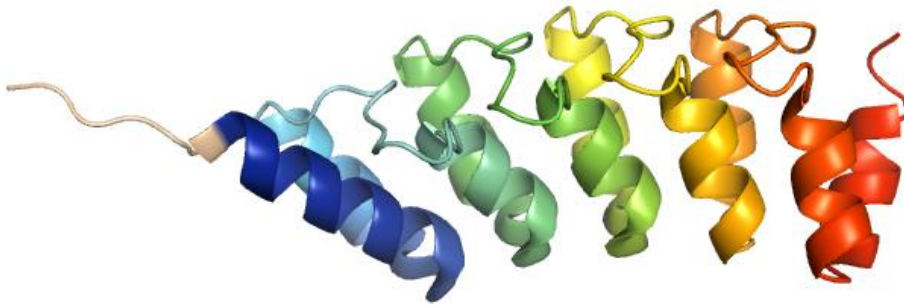


Figure 1.3 Structure of a DARPin named D1.

D1 is a typical selected DARPin, able to stabilize the tubulin heterodimer. It contains an N-cap (blue) and a C-cap (red), between which there are three internal ankyrin repeats. Its N-terminus also has six His (wheat) to facilitate purification.

Selection of DARPins

The DARPin library initially used for screening consists of DARPins having four or five ankyrin repeats. The N-terminal and the C-terminal ankyrin repeats stabilize the structure, between which there are two (N2C) or three (N3C) variable repeats. Tubulin was fixed on the surface of microtiter plates through its α subunit; consequently, its β subunit was exposed. The library was screened through four rounds of ribosome display. Then the cDNAs of selected DARPins were subcloned and clones producing tubulin binders were identified by ELISA on crude cell extracts (Pecqueur et al. 2012).

Several DARPins generating a strong signal during screening were expressed and purified. Because of the way tubulin was immobilized, the likelihood to obtain β subunit-specific DARPins was enhanced. However, the precise binding site remains unknown until the DARPin-tubulin complex structure is determined.

DARPin-tubulin complex

Several structures of DARPins in complex with tubulin heterodimer have been determined.

D1-tubulin structure at 2.2 Å resolution has been determined (Pecqueur et al. 2012). D1, binding a tubulin heterodimer with a one to one ratio, has a high affinity for tubulin regardless the nucleotide state of the tubulin. Its dissociation equilibrium constant from GDP tubulin is about 120 nM; that from GTP tubulin is about 155 nM. The structure shows D1 binds to the longitudinal interface of the β subunit. Five ankyrin repeats of D1 contact the helices H6, H11 and loop T5 of β tubulin, which explains the reason why D1 prevents

tubulin from polymerizing. In D1-tubulin, the kinesin binding site located on the lateral surface of a heterodimer remains uncovered. Hence, D1 is likely a good candidate to be a crystallization chaperone for tubulin-MAP complexes, in particular tubulin-kinesin complexes.

Another anti-tubulin DARPIn structure published is D2-tubulin in complex with kinesin and an ATP-analog at 3.2 Å (Gigant et al. 2013). It's the first successful case where a DARPIn is used to help crystallizing a tubulin-kinesin complex, in order to observe the conformational changes of kinesin when bound to tubulin. D2 binds to the β subunit's longitudinal interface, with a different binding mode compared with D1 (Fig. 1.4), stabilizing tubulin. It's proved that D2 doesn't modify the interaction between kinesin and tubulin, because kinesin's ATPase activities stimulated by tubulin or by D2-tubulin are similar with nearly identical catalytic constants and similar K_m . In the structure, kinesin with an ATP analog binding tubulin fits the previous 8 Å Cryo-EM map where a microtubule was decorated with kinesin-AMPPNP. Details of this structure, especially of kinesin, will be presented in the kinesin-1 part of this introduction. This complex structure points to a promising way to generate tubulin-kinesin crystal structures using DARPins as tubulin stabilizers.

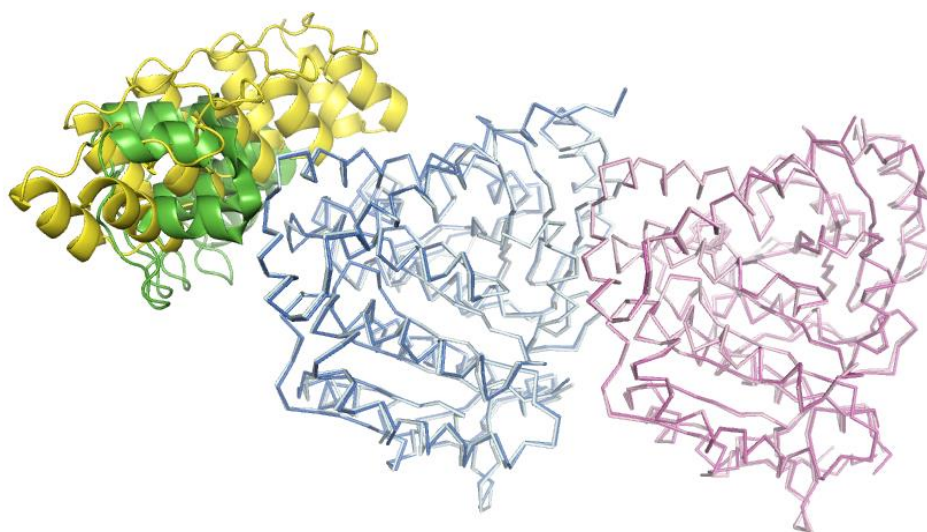


Figure 1.4 D1- and D2- tubulin structures. Tubulin heterodimers have been superimposed.

α tubulins (magenta) and β tubulins (blue) in both structures are almost identical with a low r.m.s.d of about 0.4 Å. Although D1 (yellow) and D2 (green) have a similar structure and both contact β tubulin, they don't bind identically.

2. Kinesin in general

Cytoskeletal motors play important roles in eukaryotic cells. They convert chemical energy into mechanical work and take nanometer steps along their tracks to transport a variety of cargos in the cytoplasm. Failures of motors can cause severe diseases or be lethal in some cases. Cytoskeletal motors are divided into three families: myosins, using actin filaments as tracks, dyneins and kinesins, both moving on microtubules to travel inside the cell (Schliwa and Woehlke 2003).

Kinesin superfamily proteins (KIFs) are reported to be able to transport organelles, protein complexes and mRNAs to specific destinations, using the energy produced by ATP hydrolysis. Thanks to them, the intracellular transport is spatially and temporally well controlled in cells. They also contribute to chromosomal and spindle movements during mitosis and meiosis (Hirokawa and Noda 2008).

KIFs share a conserved catalytic motor domain, also called head, containing an ATP binding site and a microtubule binding site. This part, where the chemical energy is converted into work, is responsible for ATP hydrolysis and kinesin's directional motility. Beside from the motor domain, kinesin also have a quiet variable non-motor domain, usually containing a coiled-coil segment, known as "stalk" region and a globular "tail" region. The tail region has a wide variety of functions in different kinesins, including interacting with cargo, regulating the ATPase activity of the motor domain; containing ATP independent MT binding sites and targeting kinesins to different locations (Ovechkina and Wordeman 2003). In some kinesins, the "tail" doesn't contact cargoes directly, but through light chains or associated protein instead (Hirokawa and Noda 2008).

2.1 Classification of the kinesin superfamily

Different KIFs have various structures and functions. Whereas the motor domain sequence of kinesins is relatively conserved and is the hallmark of this protein superfamily, sequence differences have led to the classification of kinesins in 14 sub-families (Fig. 2.1). The organization of their polypeptide chains has also led to the definition of 3 types of kinesins (Hirokawa et al. 2009).

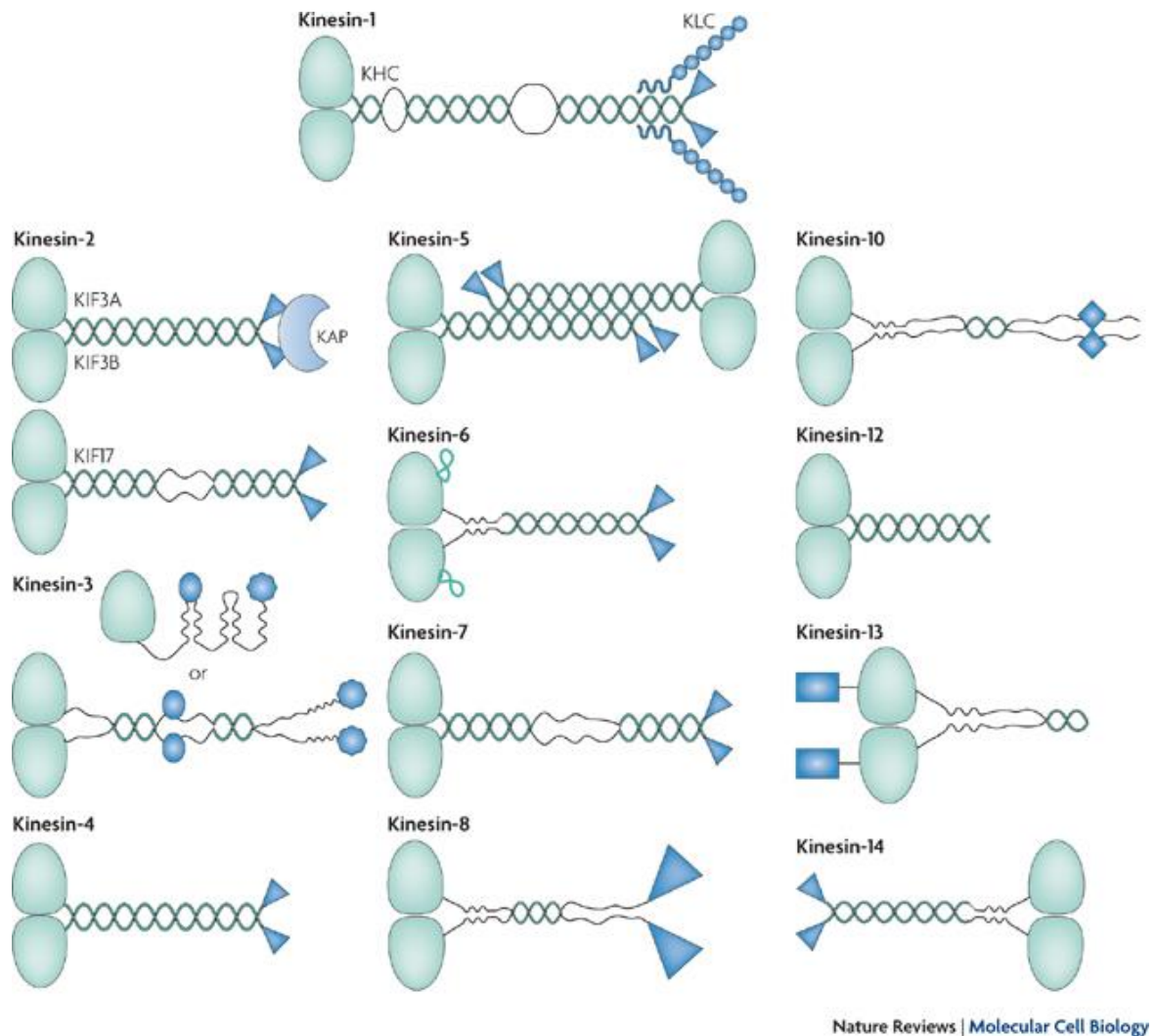


Figure 2.1 Members of the kinesin superfamily (Verhey and Hammond 2009).

The motor domains are colored in light green. Kinesin-1-12s, whose motor domain is located at kinesin's N-terminus, move toward the plus end of microtubule; Kinesin-14s, whose motor domain is located at its C-terminus, undergo minus end-directed motility; Kinesin-13s, whose motor domain is in the middle of the polypeptide sequence, don't move along microtubule actively; they diffuse instead. Kinesin-6's motor domain has a unique loop with approximately 65 amino acids insertion, colored in light green.

Many kinesins are oligomerized by their coiled-coil segments, colored in dark green. Most kinesins exist as dimers; some exist as either monomers or dimers (Kinesin-3 for example); some kinesins exist as tetramers (Kinesin-5 for example).

Non-motor domains, colored in dark blue, vary in kinesins. They are responsible for their isoform-specific regulation or functional properties or both. In addition to its-motor containing heavy chain, Kinesin-1 has a light chain contacting the C-terminal non-motor domain of the

dimerized heavy chain. The light chain allows Kinesin-1 to bind its cargoes indirectly. Some Kinesin-2s are heterotrimers, containing two motor subunits (KIF3A and KIF3B) and a Kinesin Associated Protein (KAP3). KAP3, either interacting with cargoes or regulating motor activity, contacts heterodimerized motor subunits through their non-motor tails (Marszalek and Goldstein 2000).

N-type kinesins, constituted of kinesins in classes 1 to 12, whose motor domains are located at the N-terminus of the sequence, have been found either to move towards the microtubule plus end or not to move. Most N-type kinesins, which move towards microtubule plus end, are processive. It means they are capable of taking hundreds of steps before dissociation. During the cycle of translocation, it's required that kinesin keeps attaching to microtubule. In this case, there is at least one motor domain that always binds to the microtubule. This type of kinesin is believed to move along microtubule in a hand-over-hand manner. The details of its motility will be introduced later.

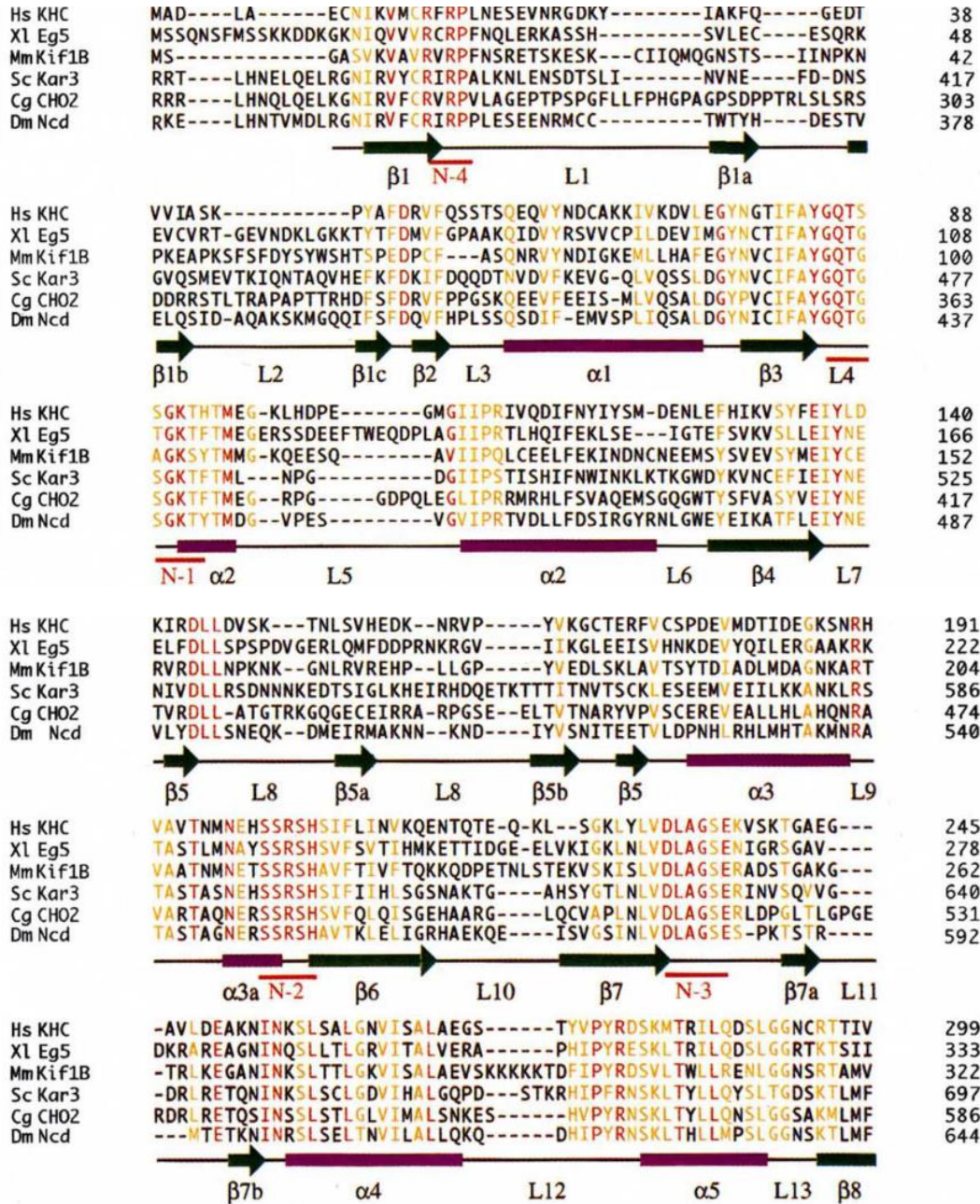
Kin-Is, for internal kinesins, all belonging to the 13th sub-family, are characterized by a motor domain that is internal to the polypeptide sequence. They hydrolyze ATP and use the energy to disassemble microtubules from both ends. This kind of kinesin doesn't generate movement; instead, they reach microtubule ends, either by direct binding or by diffusing along microtubules. There, they either induce or stabilize a depolymerizing-favoring conformational change in GTP tubulin dimer. Kinetic analysis also suggests that some Kin-Is can depolymerize microtubules processively, removing approximately 20 tubulin dimers from the end of a protofilament one by one before dissociation (Hunter et al. 2003).

The third type, called C-type, which coincides with the kinesin-14 sub-family, has a C-terminal motor; these kinesins move towards the microtubule minus end. Some of them contain a non-ATP dependent microtubule binding site in their non-motor region so that they can cross link microtubules. When their motor domain hydrolyzing ATP generates a movement, they are able to slide one microtubule with respect to another. Moreover, some members of kinesin-14 are also reported to have microtubule destabilizing ability (Wordeman et al., 2003).

2.2 Conserved motor domain

Although kinesin superfamily has a large number of members with different functions, they all share a conserved motor domain which is responsible for nucleotide consumption and microtubule binding. Among various KIFs, the motor domains have amino acid sequence similarity of about 30-60%. The sequence alignment of some most studied members is presented in Fig. 2.2 (Sablin et al. 1996).

Four conserved nucleotide binding motifs are marked, named N-1 to N-4. N-1, also called the P-loop (Phosphate binding loop) motif, with the conserved sequence GQTxxGKS/T, interacts with the α and β phosphates of the nucleotide; N-2, known as the Switch1 motif, whose pattern is NxxSSR, can bind the γ phosphate of ATP; N-3, Switch 2 motif (DxxGxE), is supposed to contact the γ phosphate as well; N-4, with the conserved sequence RxRP located near the N terminus of the kinesin, interacts with the adenine ring of the nucleotide through hydrophobic interactions. These nucleotide associated motifs are also observed in myosin and some GTPase proteins (Sack, Kull, and Mandelkow 1999).



Hs KHC	ICCS PSSYNE ETKSTLL FGQRA KTIKNTVCVNVELTAEQWKKKYEKEKEKNKILR--	355
Xl Eg5	ATVSPASINLEETMSTLDYASRAKNIMNKPEVNQKLTKKALIKYEYEEIERLKREL--	389
Mm Kif1B	AALSPADIN YDET LSTLR YADRA KQIKCNAVINED--PNAKLVRELKEEVTRLKDLLR	378
Sc Kar3	VNI SPSSSH INETLNSLR FASKVN -----STRLVSRK-----	729
Cg CHO2	VNI SPLEEN VSESLNSLR FASKVN QC-----VIGTAQANKK-----	622
Dm Ncd	INV SPFQDC FQESVKSLR FAASV NSCKMTKAKRRNRYLNNSVANSSTQSNNSGSFDK--	700




Figure 2.2 Sequence alignment of the motor domain of some kinesin family members (Sablin et al. 1996).

Residues with absolute conservation are marked in red; those with relatively lower (but still significant) conservative substitutions are marked in yellow. The positions of secondary structure elements are pointed, as well as the four nucleotide binding motifs (N-1 to N-4). Kinesins from different subfamilies and from different species are listed here as examples.

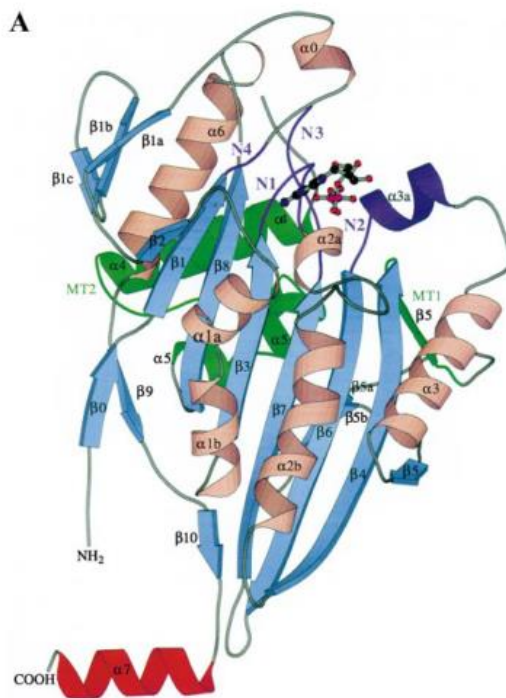


Figure 2.3 Structure of a rat-brain kinesin (Sack, Kull, and Mandelkow 1999).

In kinesin, central strands (blue) are surrounded by α helices (pink). α helices associated with microtubule binding are colored in green; the nucleotide binding region (purple) and the ADP are shown.

As the motor domains of various members in the kinesin superfamily are conserved, they share a similar structure. A typical kinesin motor domain structure (pdb id 2kin, (Sack et al. 1997)) is presented in the Figure 2.3. Generally, the kinesin motor domain consists of a series β strands locating in the middle of the structure with three α helices on each side. The nucleotide binding pocket with loops where conserved nucleotide binding motifs embed is clearly identified because in most cases the kinesin is co-crystallized with ADP.

2.3 Other cytoskeletal motors

In addition to kinesin, there are two other cytoskeletal motor families: myosins which move along actin filaments and dyneins which move along microtubules but usually towards the minus end. All of three use ATP as the source of energy. Among them, kinesins and myosins share a structural homology and a similarity in their mechanochemistry. Despite their low sequence identity, the topologies and tertiary structure of kinesin and myosin indicate they may derive from a common ancestor (Rayment 1996). By contrast, dyneins deviate from kinesins and myosins in both energy generation mechanism and in overall structure (Bhabha et al. 2016). In this section, a brief introduction on both myosin and dynein will be given.

Myosin

Myosin, responsible for actin-based motility, plays important roles in muscle contraction and motility processes in eukaryotes. It was found in both striated muscle tissue and smooth muscle tissue by Pollard and Korn (Pollard and Korn 1973). Myosins constitute a large and divergent protein family. Usually, myosins are heteromers consisting of one or two heavy chains and a variable number of light chains. A general structure of myosin V is presented in figure 2.4. Myosin heavy chain includes motor (head), neck and tail domain (Maravillas-Montero and Santos-Argumedo 2012). The motor domain is responsible for both actin filament binding and ATP hydrolysis. The neck domain serves as a linker between the catalytic motor domain and the tail; also, it is able to act as a lever arm for force transduction. The neck domain usually contains the myosin light chain binding site. The tail domain plays various roles in different myosin subfamilies. Most myosins move from the actin pointed (minus) end to its barbed (plus) end, except myosin VI which moves in the reverse direction (Sweeney and Houdusse 2010).

The motor domain structures of various myosins have been determined in different nucleotide state. In general, the myosin motor domain can be divided into four subdomains which are able to generate nucleotide-state associated movement (Coureux et al. 2003). The motor domain in myosin superfamily shares a similar catalytic pocket with that of the kinesin superfamily, including three conserved nucleotide associated motifs: P-loop, Switch 1 and Switch 2. Moreover, the secondary structure elements of kinesin are also found in myosin with a central β sheet surrounded by several α helices (Fig. 2.5).

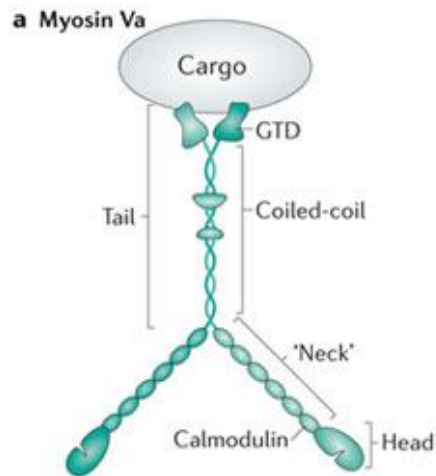


Figure 2.4 Domain structure of a myosin V (Hammer and Sellers 2012).

The head domain of myosin contains the nucleotide binding site and actin binding site. The neck domain is composed of α helices able to bind a calmodulin molecule. The tail domain consists of a coiled-coil stalk dimerizing the heavy chains, followed by two globular tail domains (GTDs). GTDs are responsible for cargo binding.

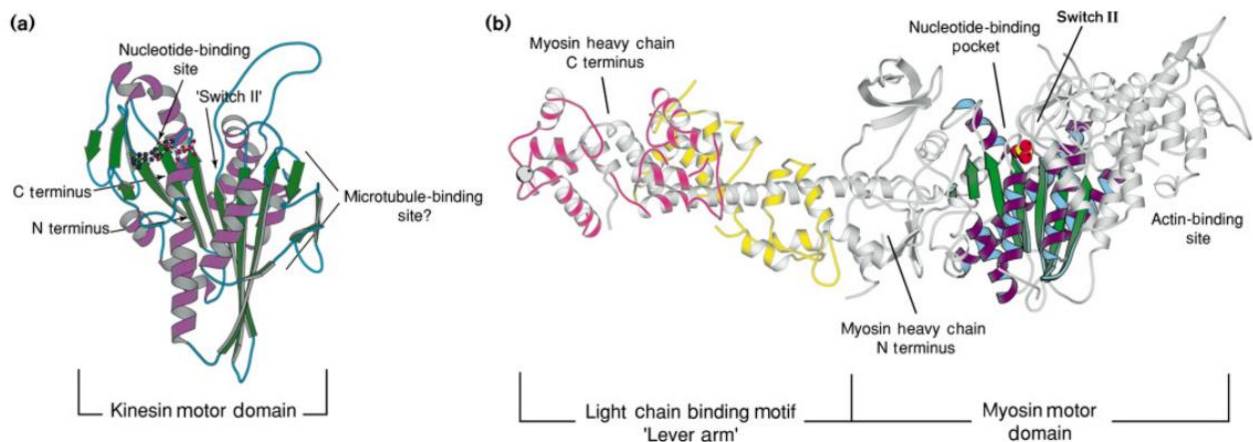


Figure 2.5 Comparison of the motor domains in kinesin and myosin (Rayment 1996).

- a) The kinesin motor domain. Central β strands are colored in green, with α helices (purple) surrounding. ADP is shown in balls and sticks.
- b) A subfragment of a chicken skeletal myosin in nucleotide-free state. A solvent (space-filling model in red and yellow) replacing ADP locates at the nucleotide binding site. In the motor domain, secondary structural elements similar to those found in kinesin are colored in the same pattern.

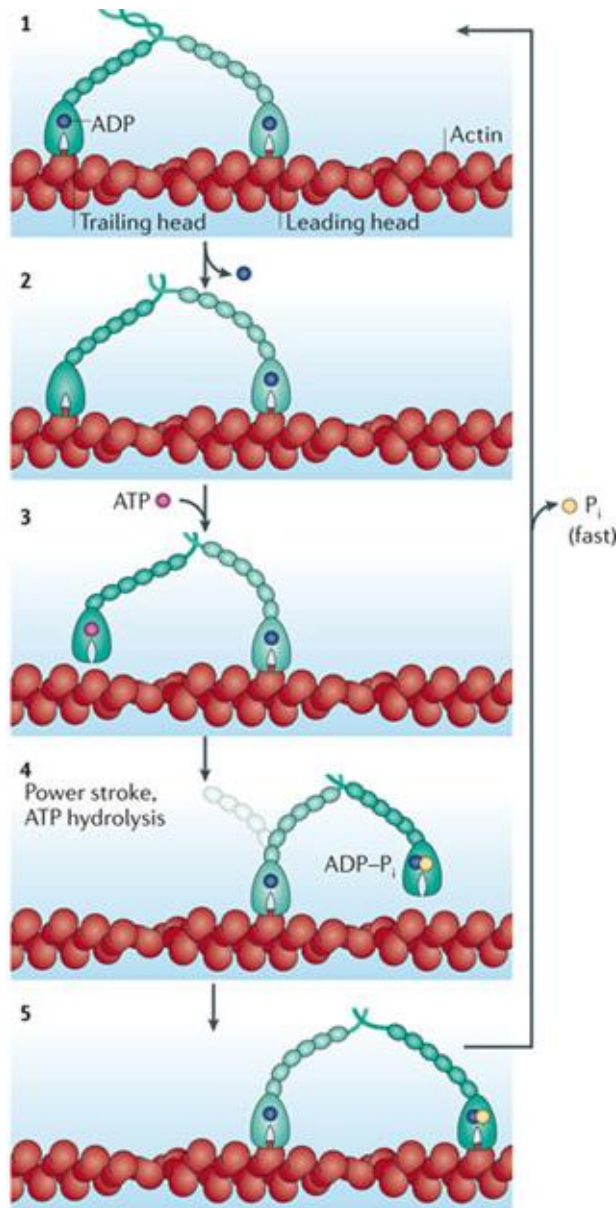


Figure 2.6 Processive movement of myosin Va motor (Hammer and Sellers 2012).

In myosin, movement corresponds to the nucleotide cycle of motor domains (Vale and Milligan 2000). The cycle alternates through high and low affinity for actin. Usually, the myosin motor domain in nucleotide-free state or ADP state is able to bind actin tightly; while in ATP or ADP and inorganic phosphate (P_i) state it dissociates from actin easily. Here, the processive movement of a myosin Va, corresponding to its nucleotide cycle, is presented as an example (Fig. 2.6). Myosin Va dwells in a state with both motor domain binding ADP attaching to the actin filament. The two motors exert intramolecular strain on each other. ADP releases from the trailing motor so that this motor is able to bind ATP.

After ATP binding, the dissociation of this motor occurs and so does ATP hydrolysis; meanwhile, the actin binding motor undergoes a power stroke, leading the dissociated motor, turning to its ADP-Pi state, to its forward binding site. Rebinding to actin filament, the ADP-Pi motor releases its Pi quickly and attaches to actin tightly. The cycle resets to the beginning and restarts all over again with myosin Va moving forward about 36 nm in each cycle.

Dynein

Cytoplasmic dynein belongs to the AAA (ATPases Associated with diverse cellular Activities) family. Although it is able to move along microtubules using the energy produced by hydrolysis of ATP, it is quite different from kinesin and myosin for the following aspects. First, structurally, its catalytic core (AAA ring) is separated from its microtubule binding domain (MTBD) by a long coiled coil. In both myosin and kinesin, the same motor domain is responsible for both ATP hydrolysis and microtubule binding. Second, unlike in kinesin and myosin in which two motor domains cooperate with each other during movement, the two dynein heads step independently of each other. Third, usually the movement of kinesin and myosin is processive; while dynein exhibits a weak directional bias and variable step sizes.

3. Kinesin-1

Kinesin-1, also called conventional kinesin, has been found in squid giant axon in 1985 (Vale, Reese, and Sheetz 1985). It was regarded as the only kinesin for a long time. It is the most studied kinesin, both through in-depth characterization of kinetic and motile aspects and through structural study.

As a typical N-type kinesin, once attached, kinesin-1 moves toward the (+)-end along the microtubule surface in 8 nm increments as it hydrolyzes one ATP per step (Howard 1996). As mentioned above, kinesin-1 can be described as a homodimer of heterodimers. It comprises two identical polypeptides which dimerize to form a rod-shaped coiled-coil stalk, with a tail at the C-terminal end and twin globular heads at the other end (Fig. 3.1). Each heavy chain contacts cargoes with the help of a partner “light chain”, which binds its C-terminal tail. Each head comprises the binding sites for both nucleotide and microtubule, which allows it to attach to microtubules with nucleotide-dependent affinity (Asbury 2005). Consequently, studies of kinesin-1’s motor domain of its heavy chain (KHC), bring insights into Kinesin’s conserved mechanisms, including those for ADP release and ATP binding and also into the mechanism of N-type kinesin’s motility.

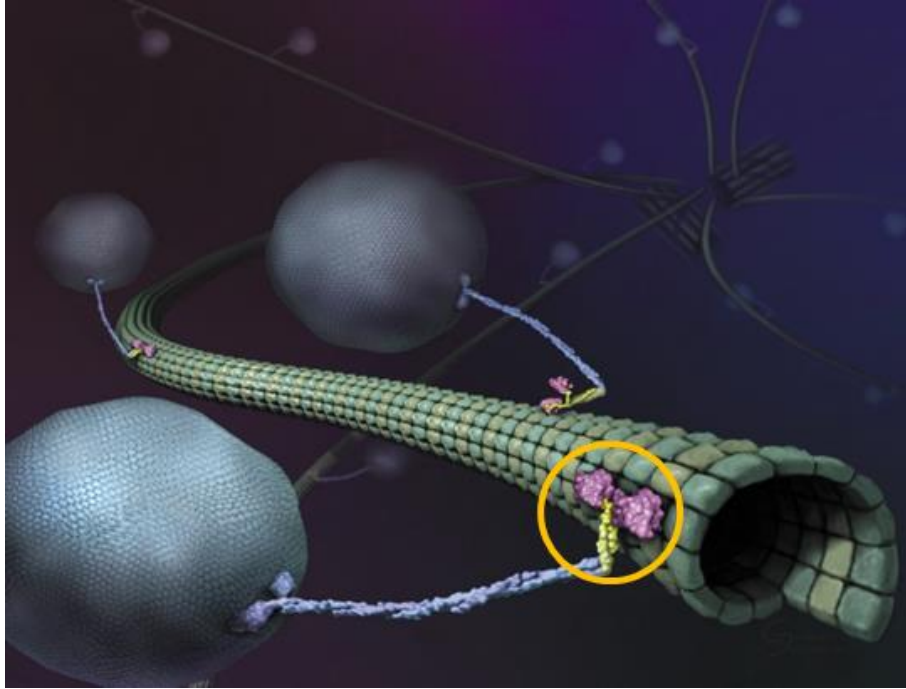


Figure 3.1 An artistic view of Kinesin-1 transporting cargoes along a microtubule (Johnson, G., et al. 2000).

Kinesin-1 light chain (KLC), connecting to the C-terminal tail of kinesin-1 heavy chain (KHC), contributes to cargo binding. Motor domains (magenta), located on the other side of the coiled-coil stalk, are responsible for walking along the microtubule. A neck linker embedded in the neck domain (yellow) of each motor plays an important role in kinesin-1's motility. Kinesin-1's motor domain plus its neck linker (orange cycle) is studied in this thesis.

3.1 The kinetic mechanism of kinesin

Kinesin is an ATPase whose motility is driven by its ATP turnover. Study of kinesin's kinetic mechanism is essential for understanding chemical energy consumption and motile force generation. The kinetic mechanism and relevant constants on kinesin-1 are summarized below (Cross 2004).

In the absence of microtubule

In the absence of microtubule, kinesin-1 binds ATP and hydrolyzes it on its own. When it is detached from the microtubule, kinesin-1 is trapped in an ADP-bound state, characterized by a low ADP dissociation rate (k_{off} about 0.01 s^{-1} for wild type dimers). ADP dissociation is the rate limiting step for an ATP turnover by isolated kinesin. The ADP dissociation rate is usually determined using the fluorescence variation signal of Mant-ADP which is a fluorescent analog of ADP with the same dissociation rate as ADP (Fig. 3.2).

After ADP dissociation, ATP is able to bind kinesin. For apo-kinesin-1, the rate of ATP binding is about $4 \mu\text{M}^{-1} \text{s}^{-1}$. For this measurement, apo-kinesin is required. To generate apo-kinesin in the absence of microtubules, EDTA and apyrase are used to accelerate the release of ADP and to hydrolyze it. But it is reported that apo-kinesin is prone to denature in the absence of a stabilizer (Sadhu and Taylor 1992; Huang and Hackney 1994). The K_D for ATP dissociation is about $75 \mu\text{M}$.

The rate of ATP hydrolysis by a microtubule-unbound single motor is about 7s^{-1} (Ma and Taylor 1997). After ATP hydrolysis, phosphate releases before ADP dissociation, as ADP is trapped tightly by kinesin.

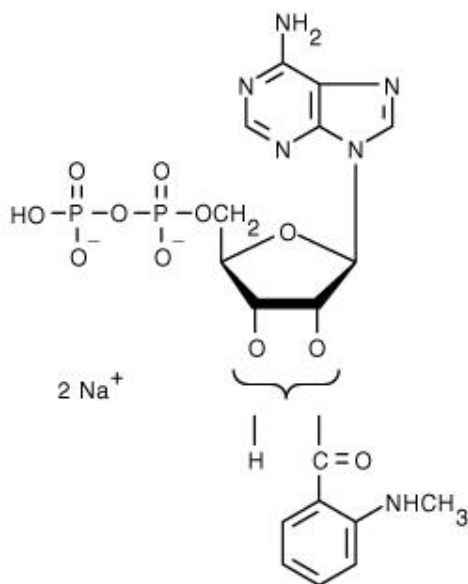


Figure 3.2 MANT-ADP (2'-(or-3')-O-(N-Methylanthraniloyl) Adenosine 5'-Diphosphate, Na Salt).

In the presence of microtubules

The relation of the nucleotide cycle with the interaction between kinesins and microtubules is summarized in Figure 3.3 (Ma and Taylor 1997; Vale and Milligan 2000; Wang et al. 2015).

ADP kinesin is not only characterized by its low ADP dissociation rate but by its relatively low affinity for microtubules as well (K_D is about $10\text{-}20 \mu\text{M}$). However, once it binds to microtubules, its ADP release is accelerated thousands of times (k_{off} increases from about

0.01 s⁻¹ to about 50 s⁻¹ for a monomer). A key discovery was made by Hackney that ADP release is sequential in a kinesin-1 dimer (Hackney 1994). He found that upon microtubule binding only one of the motors releases ADP directly, while the other head releases its ADP only after ATP binding to the first head (Cross 2004).

After ADP release, the apo-kinesin motor binds microtubules tightly with an unbinding rate constant of about 0.002 s⁻¹. The apo-kinesin in complex with microtubule, often called “rigor” following the equivalent state of myosin, is able to rebind ATP at a rate of 2-4 μM⁻¹ s⁻¹. ATP unbinding rate is about 150 s⁻¹. Actually ADP is also able to bind microtubule-attached kinesin with a rate of about 1.5 μM⁻¹ s⁻¹. Hence ATP and ADP actually bind to and dissociate from rigor complex with similar rates. So ADP is a competitive inhibitor of ATP binding to kinesin with an inhibition constant K_i of about 150 μM. Indeed it has been shown that ADP tends to detach kinesin-1 from microtubules and is able to reduce both the velocity and run length of walking kinesin-1 (Yajima et al. 2002). However, in physiological conditions, the concentration of ATP is at least five times higher than that of ADP (Tantama et al. 2013), so microtubule-bound apo-kinesin binds ATP preferentially and in this way completes its cycle.

Microtubule binding doesn't only stimulate kinesins' ADP dissociation but also accelerates ATP hydrolysis in an ATP turnover. The hydrolysis rate increase from 7 s⁻¹ to about 250 s⁻¹ (Ma and Taylor 1997). Then phosphate releases quickly with a rate higher than 100 s⁻¹. The low affinity between microtubule and the ADP-kinesin leads to its detachment from the microtubule.

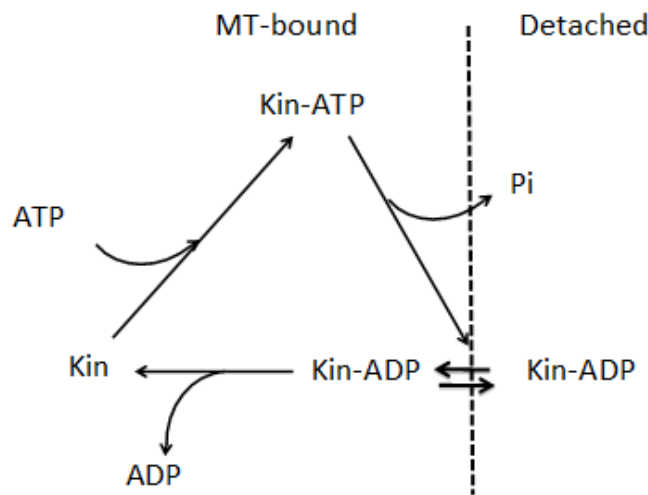


Figure 3.3 Kinesin's association with microtubules is coupled with its nucleotide cycle.

Although the frame of kinesin's nucleotide cycle is clear (Fig. 3.3), detail information on the effects caused by microtubule binding, including for instance how ADP dissociation is accelerated and how ATP hydrolysis is favored, is still missing.

Mutagenesis studies gives insights into kinesin's ADP release mechanism

Despite the unclearness of how ADP dissociation is accelerated by microtubule binding, some kinesin mutants are reported to have a higher ADP dissociation rate. These mutants may provide insights into kinesin's ADP release mechanism.

Most of these mutations, leading to a high spontaneous ADP release rate, are associated with its P-loop motif that interacts with the phosphates of the nucleotide. P-loop motif, a conserved nucleotide associated motif present in NTPases, including kinesin, myosin and G protein, has the sequence consensus motif GxxxxGKT/S. For kinesins there are two extra conserved residues in their P-loop motif so that their P-loop motif pattern is GQTxxGKS/T (Sack, Kull, and Mandelkow 1999).

Higuchi *et al.* mutated the first threonine of the P-loop motif to serine (GQTxxGKS/T) in *Drosophila* kinesin-1, because in myosin the equivalent residue is a serine (Higuchi *et al.* 2004). They found the T>S mutant releases ADP ($k_{\text{off}} \approx 0.0128 \text{ s}^{-1}$) faster than wild type ($k_{\text{off}} \approx 0.0035 \text{ s}^{-1}$) by 3.6 times without microtubules being involved.

A conserved residue of the so-called Switch 2 motif, E236 (in human kinesin-1 numbering) interacts with this P-loop threonine residue T87 (in human kinesin-1 numbering). If this glutamic acid is mutated to an alanine, its connection with the P-loop will be interfered. In the absence of microtubules, the E236A mutation increases the ADP dissociation rate from 0.01 s^{-1} to 1.1 s^{-1} (Rice *et al.* 1999). Interestingly, this mutation doesn't influence the microtubule-stimulated ADP release rate.

A related mutation is G234A, also located in the Switch 2 motif. This glycine is conserved in myosin and G protein; it forms a hydrogen bond with the γ phosphate of a tri-phosphate nucleotide. The G234A kinesin-1 mutant releases ADP very quickly with a k_{off} of around 10 s^{-1} . In addition, and in contrast to the case of the E236A mutant, in the case of G234A the microtubule-stimulated ADP release is disturbed. Moreover, this mutant is reported to be unable to undergo a conformational change corresponding to ATP binding so that its ADP dissociation cannot be accelerated by microtubules (Rice *et al.* 1999).

Another interesting mutant is associated with T92, another conserved threonine of the P-loop (GxxxxGKT/S). Nakata *et al.* found that if this threonine is mutated to an isoleucine or an asparagine, the mutant will bind microtubule strongly without capacity of detaching even in the presence of a high concentration of ATP (Nakata and Hirokawa 1995). Because of this character, T92N and T92I are used as a roadblock on microtubules in some studies (Crevel *et al.* 2004). It's also reported that T92N hydrolyzes ATP much more slowly (about

100 times) than wild type kinesin-1 (Krylyshkina et al. 2002). Interestingly, if the threonine is mutated to serine, as is the case in some kinesin subfamilies, i.e. kinesin-3, the mutant is still capable of moving along microtubules as wild type (Nakata and Hirokawa 1995).

These results highlighted the importance of nucleotide binding motifs on nucleotide trapping in kinesin. Nevertheless, in order to translate these results into microtubule-accelerated ADP release mechanism, more studies, especially structural studies, are required.

3.2 Motility model of kinesin-1

Kinesin-1 moves in a hand-over-hand way

Two main models of kinesins motility have been proposed (Yildiz and Selvin 2005).

One is called the inchworm model. Kinesin dimer walks with a leading motor always leading and always followed by the rear motor. The first motor steps about 8.3 nm once, which is about the length of a tubulin heterodimer; then the second motor steps the same distance while never bypassing the leading one. It suggests only one motor is catalytically active. It also means that both motors revert to the same conformation without requiring the rotation of the stalk.

The other model is called hand-over-hand, in which kinesin moves like people walk. The rear motor bypasses the leading motor to take a step, binding to the next binding site while becoming the leading motor. In this case, if the centroid position of the dimer moves 8.3 nm, a single motor moves twice this distance, 16.6 nm, as a step. In the next step, the former leading motor which is the rear motor now moves 16.6 nm forward, becoming the leading motor again. During this process, the other motor always sticks to its original binding site without moving until it's its own turn to step.

Evidences presented so far mostly support the hand-over-hand model. For example, Kaseda *et al.* found the movement of a heterodimeric construct, in which one motor contains a mutation decreasing its ATPase activity (18 times slower than WT) while the other one has the normal catalytic rate, is not uniform. The heterodimer makes one step with long dwell time following one step with short dwell time, because one of the motors takes more time to hydrolyze ATP. The overall moving speed of the heterodimer is 9 times slower than that of a wild type, which matches its average speed of ATP consumption (Kaseda, Higuchi, and Hirose 2003). If kinesin moves in an inchworm way, for each step the dwell time would be constant and the velocity of its movement would either be normal (with a normal motor as a leading head), or 18 times slower (with a mutated motor as a leading head). In another set of experiments, Yildiz *et al.* labeled one motor of a kinesin dimer with a Cy3 fluorophore, so the movement of the marked individual motor in the

dimer can be visualized (Fig. 3.4). They found that instead of moving about 8 nm for each step, as predicted by the inchworm model, one motor moves 16 nm in a step. This result matches the hand-over-hand model (Yildiz et al. 2004).

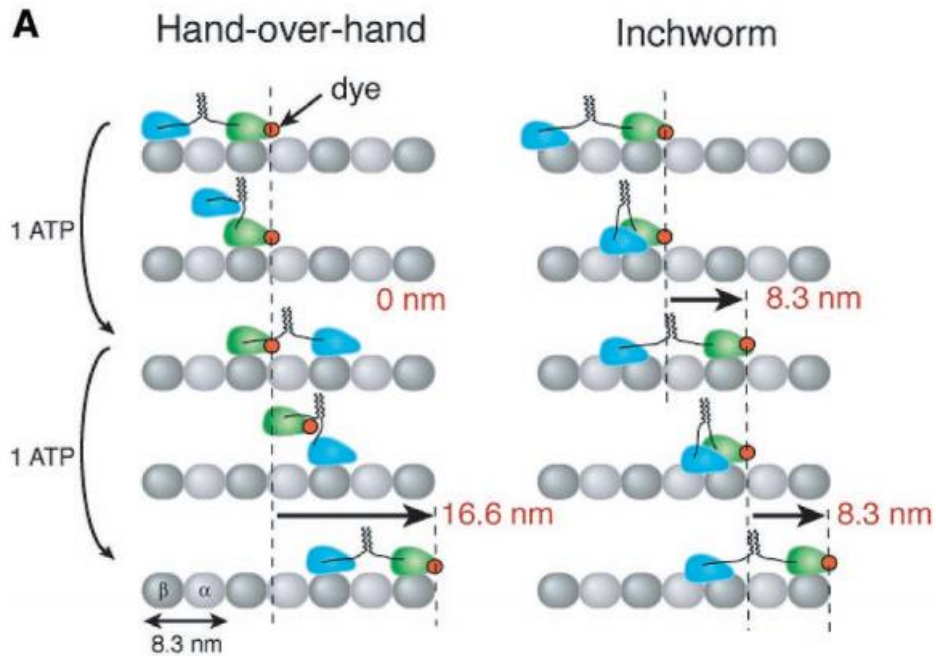


Figure 3.4 Different models of kinesin-1's motility (Yildiz et al. 2004).

In this figure, the motors of kinesin are colored in different colors to indicate the movement of each one. Although in both models, kinesin moves about 8.3 nm for each step; in hand-over-hand model, a single motor moves about 16.6 nm as a step, while in inchworm model, a step of a single motor is about 8.3 nm. Yildiz, et al. labeled one motor with a dye to observe the movement of a single motor.

Kinesin's motility coupled with its nucleotide cycle

Kinesin-1 walks towards microtubules plus end for hundreds of steps before dissociation. The processivity and unidirectional movement relies on the communication between the two motors. The neck linker model has been proposed and is generally accepted to account for this communication (Fig. 3.5a). The neck linker is a peptide of about 15 residues located at the C-terminus of a kinesin-1 motor domain and connecting each motor to the coiled-coil stalk. Previous studies indicate it can be either rigid and docked on the motor domain or

flexible. Furthermore, the conformational change of the neck linker is associated with kinesin's nucleotide state and also with its attachment to microtubule.

EPR spectroscopy and FRET studies on isolated ADP-kinesin suggest the neck linker is not attached to the catalytic core in a uniform rigid way. The neck linker may have a docked (Sindelar et al. 2002) or an undocked (Kull et al. 1996) conformation, both of which were observed in ADP-kinesin crystal structures. Upon kinesin binding to a microtubule coupled to ADP release, the neck linker is mainly in a detached and disordered conformation. However, when ATP binds to kinesin, the neck linker docks on the catalytic core. Neck linker docking requires both ATP (or an ATP analog, as AMP-PNP or ADP-AlF₄,-) and microtubule binding. After phosphate release, the neck linker turns back to a mobile state again and the ADP-bound motor dissociates from the microtubule to complete the cycle (Rice et al. 1999).

Taking both motors in a dimer into consideration, the processive and unidirectional movement of kinesin can be summarized as the followings (Fig. 3.5b). In the absence of microtubule, each motor of a kinesin dimer traps an ADP. Once one of the motors (motor A) binds a microtubule, its ADP dissociation is accelerated. Apo-motor A binds to the microtubule tightly, while being able to accept a nucleotide. During this process, the other motor (motor B) is always in its ADP state and keeps unbound from the microtubule, until ATP, whose concentration *in vivo* is higher than that of ADP, binds motor A. As discussed above, in a microtubule- and ATP-bound motor, the neck linker interacts with (docks on) the catalytic core, pointing towards the microtubule plus end. Neck linker docking on motor A narrows the distance between ADP-bound motor B and its next microtubule binding site, which is closer to microtubules plus end, favoring the attachment of motor B to the next binding site. Then ADP dissociates from motor B and ATP rebinding is allowed on apo-motor B; meanwhile, in motor A, ATP is hydrolyzed and ADP-motor A is able to detach from the microtubule. Afterwards, ATP binding induces neck linker docking on motor B, while ADP-motor A is driven to its next binding site. ADP-motor A rebinds to microtubule and its motile cycle continues, so does the cycle on motor B. Therefore, a kinesin dimer, with two motors going through alternative stages of the same cycle, walks step by step processively in one direction.

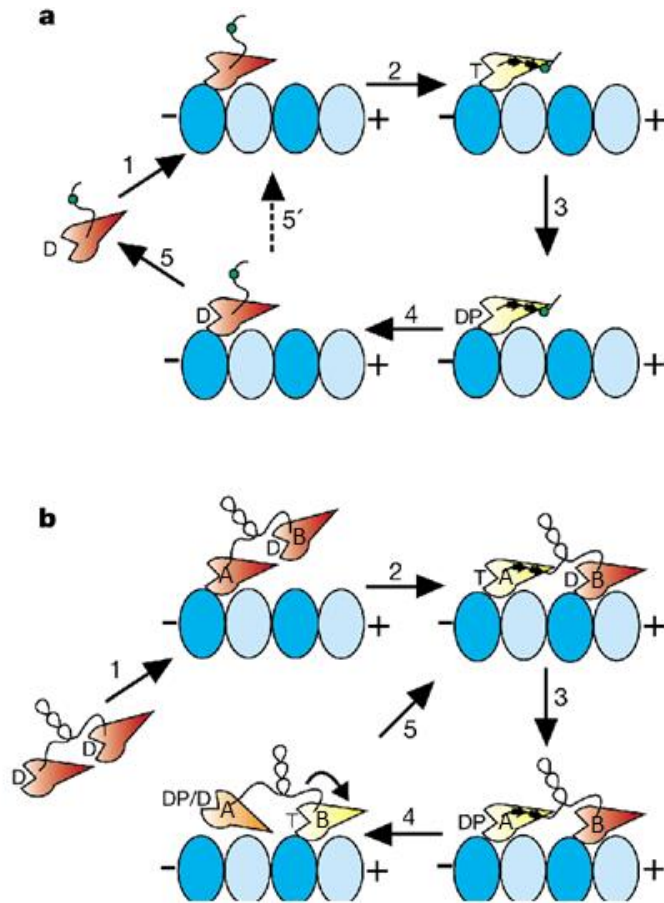


Figure 3.5 Kinesin-1 monomers and processive dimers' motility models (Rice et al. 1999).

The tubulins' two subunits are colored in light and dark blue. The motor domain is colored either in yellow, when it is in microtubule-bound and nucleotide triphosphate states; or in red, when it is in other states. The D marked on the motor domain refers to ADP binding; the T refers to ATP binding; and the DP refers to ADP-Pi state. A cysteine (Cysteine 333, in the neck linker, shown as a green spot) has been introduced for biophysical probes labeling.

a) Kinesin-1 monomer. The neck linker is disordered when the kinesin is in ADP or nucleotide-free state. Once the motor is bound to the microtubule, ADP release is accelerated. When ATP binds to the apo-kinesin motor, kinesin's neck linker docks on its catalytic core. The labelled cysteine, located at the tail of the neck linker moves towards the plus end of microtubule. After ATP is hydrolyzed, ADP-kinesin may dissociate from microtubule.

b) Kinesin-1 dimer. Initially, one motor (named motor A) attaches to the microtubule and then releases its ADP. Once ATP binds to this motor A, accompanied with neck linker docking, the partner motor (named motor B) moves forward with a chance to attach the next binding site, which is closer to microtubule plus end and 8.3 nm away from where motor A binds. ATP is hydrolyzed in motor A; in the meantime, motor B releases its ADP and binds a new ATP. When

the neck linker docks on motor B, motor A, now with bound ADP, can detach from microtubule and be displaced about 16 nm to the forward binding site. The cycle continues, allowing Kinesin-1 to move processively towards the plus end of microtubule.

3.3 Advancement of kinesin-1 structural studies

ADP kinesin-1

Since the first kinesin-1 structure was published, several ADP-bound kinesin-1 structures from different species have become available in the PDB. They are either monomers or dimers, from various species, with either a flexible or a rigid docked neck linker.

One of them is shown in figure 3.6 (pdb id 1BG2) (Kull et al. 1996). It consists of a central β sheet with a group of 3 α helices on each side. Most of the helices of kinesin are somehow unusual. One of them is interrupted by an inserted loop. At least two of them are 'distorted'. The nucleotide-binding pocket is formed by four regions of the polypeptide chain: P-loop, Switch 1, Switch 2 and N-4. The P-loop motif, as presented above, also called N-1 in kinesin, with the conserved sequence GQTxxGKS/T, interacts with α and β phosphates of the nucleotide. Switch1 motif forms a short α helice H3a in this ADP binding kinesin. Switch 2 motif is followed by a long flexible loop and the H4 (also called α 4) helix which has 4 turns. N-4, with the conserved sequence RxRP near the N terminus of the kinesin interacts with the adenine ring of the nucleotide through hydrophobic interactions (Sack, Kull, and Mandelkow 1999).

Sindelar *et al.*, using site-specific EPR measurement to detect the conformation of kinesin's neck linker in the absence of microtubules, found that both docked and undocked neck linker exists in the ADP-kinesin population. Following this, they determined the structure of ADP-kinesin (pdb id 1MKJ) with a docked neck linker (Sindelar et al. 2002). In general, this structure has a similar conformation as 1BG2: P-loop motif binds the ADP phosphates; Switch 1 forms the short H3a; Switch 2 is embedded in L11, most of which is disordered. By contrast, H4 tilts slightly and creates a space for the first residue of the neck linker to dock (Fig. 3.7). ADP-Kinesin-1 structures from different species also show a similar conformation (e.g. pdb id 2KIN).

Kinesin-1 dimers were also successfully crystallized with ADP bound (pdb id 3KIN, 2Y5W) (Kaan, Hackney, and Kozielski 2011). In both cases, the neck linker is rigid, which makes their motors' structure resemble to that of a monomer with a docked neck linker. For example, the r.m.s.d. of C α between 1MKJ and 2Y5W is only about 0.4 Å, despite the two kinesins are from different species (human and drosophila).

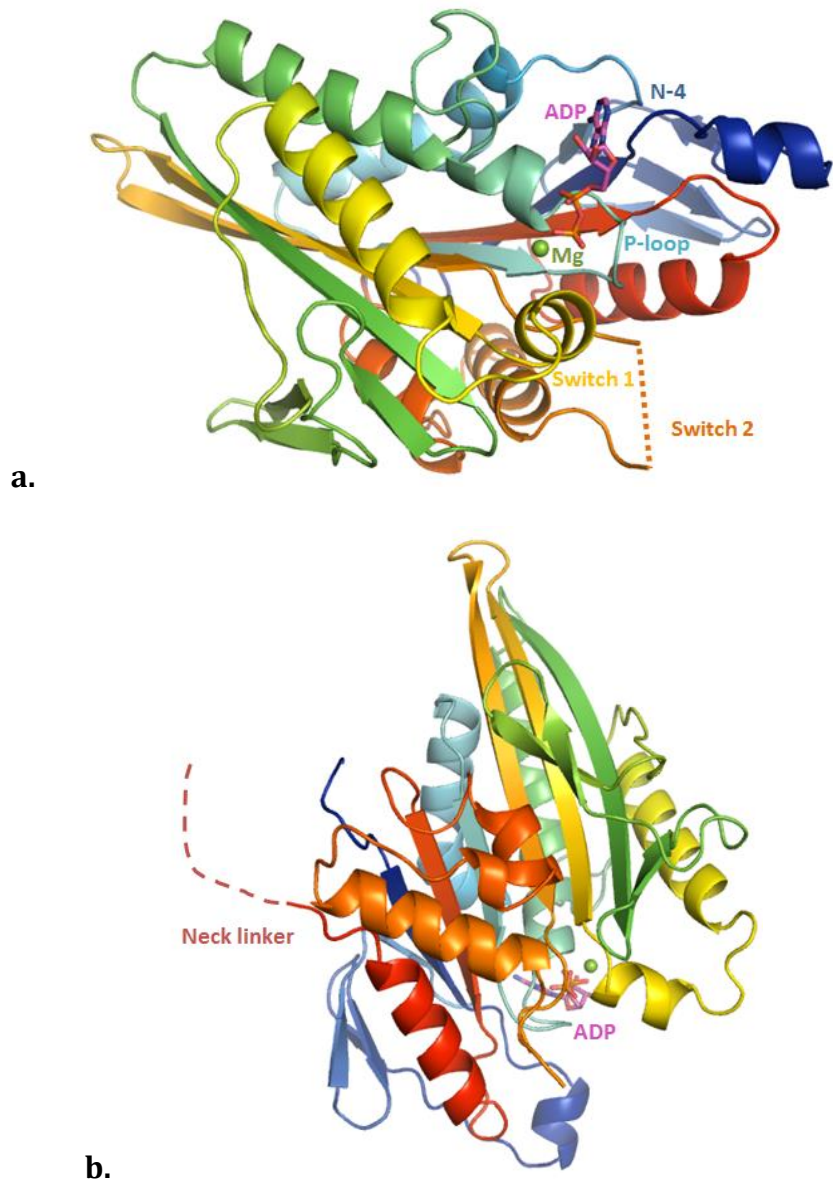
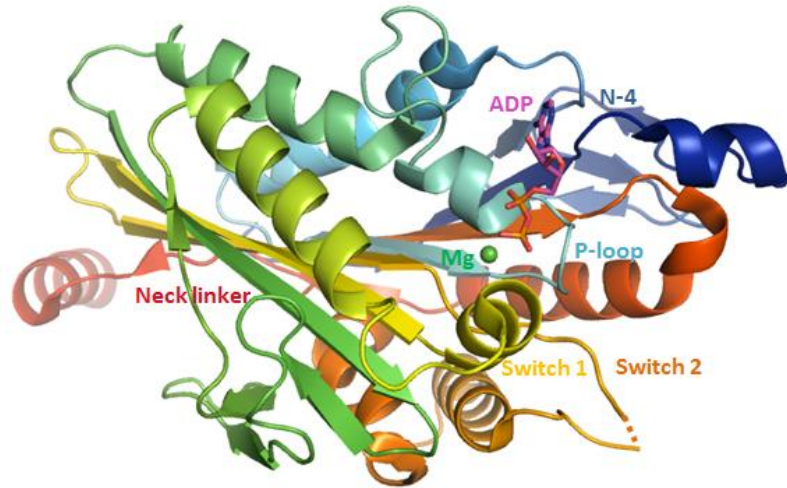


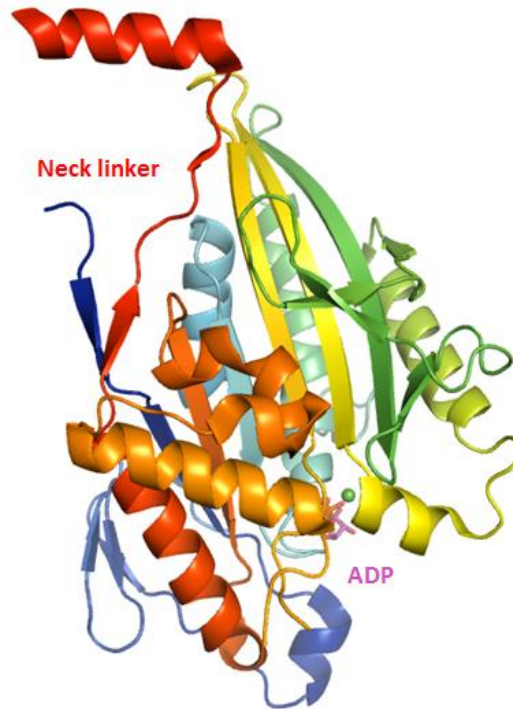
Figure 3.6 ADP bound human kinesin-1 (KHC) motor domain (pdb id 1BG2, rainbow colored from N-ter to C-ter) (Kull et al. 1996).

a) The neck linker which is located at the C-terminal of KHC motor domain is disordered and is not shown. The nucleotide binding motifs (Switch1, Switch2, P-loop and N-4) are labeled to indicate their locations. They define the environment of the nucleotide. Part of loop 11 (L11) in which Switch2 is embedded is disordered (shown as a dashed line).

b) View of 1BG2 from another side. The flexible neck linker is shown as a dashed line. The nucleotide is marked.



a.



b.

Figure 3.7 ADP bound human kinesin-1 (KHC) motor domain (pdb id 1MKJ), rainbow colored from N-ter to C-ter)(Sindelar et al. 2002).

a) The neck linker in this structure is rigid and interacts with the catalytic core in the same way as observed in microtubule-bound ATP-kinesin (Parke et al. 2010b). The nucleotide binding motifs (Switch1, Switch2, P-loop and N-4), which are labeled in different colors to indicate their locations, have similar conformations as those in the neck linker undocked ADP kinesin-1.

b) View of 1MKJ from another side. The C-terminal neck linker in this structure is ordered and attached to the catalytic core. The nucleotide is marked.

ATP analog kinesin-1

The structure of the kinesin motor domain in an ATP-like state in complex with tubulin (Fig. 3.8) has been determined in the laboratory (Gigant et al. 2013). It explains the mechanism of microtubule-stimulated ATP hydrolysis and also uncovers the connection between ATP, microtubule binding and the conformation of the neck linker. The main findings are summarized here:

- Upon tubulin binding, the Switch2 loop interacts with α tubulin and becomes ordered. This leads to the elongation of the H4 helix at its N-terminus, which in turns reinforces the binding to the microtubule. The analog of the third phosphate and the nucleotide-bound Mg^{2+} form several hydrogen bonds with conserved residues in Switch1 and Switch2, leading to significant conformational changes, mostly of Switch1.

- The conserved Glu236 residue, which is the C-terminal residue of Switch2, relocates and makes a salt-bridge with a conserved residue, Arg 203, of Switch1. The relocation of Glu236 puts it at the right place to activate the water molecule abstracting a proton from the water that has been proposed to be the nucleophile attacking the β - γ phosphodiester bond. As a consequence, the chemical step of ATP hydrolysis is accelerated. This two water ATP hydrolysis mechanism had been initially proposed based on the isolated Kinesin-5-ATP structure (Parke et al. 2010b).

- The structure also explained how the conformational change of ATP-kinesin allows the interaction of the neck linker with the core of the motor domain, which causes the docking of the neck linker and leads to the power stroke.

- It also defines the tubulin-kinesin interface (Fig. 3.9). Residues of L11, H4 and H6 in the kinesin contact H'3, H'11 and H'12 in α tubulin. On β tubulin, most of the interaction zone is located on H12, which interacts with L8, L12 and S5a on the kinesin.

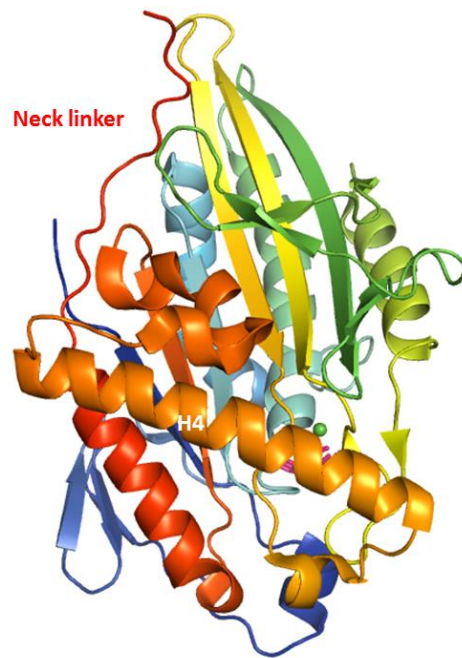
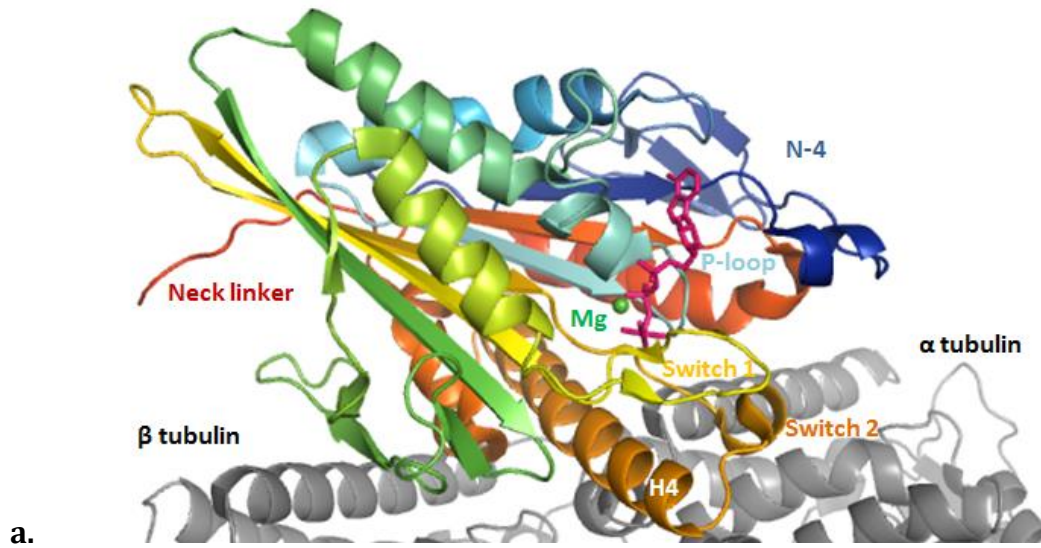


Figure 3.8 ATP analog bound human kinesin-1 (KHC) motor domain complex with tubulin heterodimer (pdb id 4HNA, rainbow colored from kinesin's N-ter to C-ter) (Gigant et al. 2013).

a) Loop L11 in which Switch 2 is embedded becomes ordered, extending in particular the H4 helix at its N-terminal end. The conformation of Switch 1 changes as well to contact the γ phosphate. As expected, the neck linker is docked on the catalytic core.

b) View of microtubule bound ATP analog kinesin from another side. The C-terminal neck linker in this structure is ordered and attached to the catalytic core. The tubulin heterodimer and DARPin in the complex structure are not shown here.

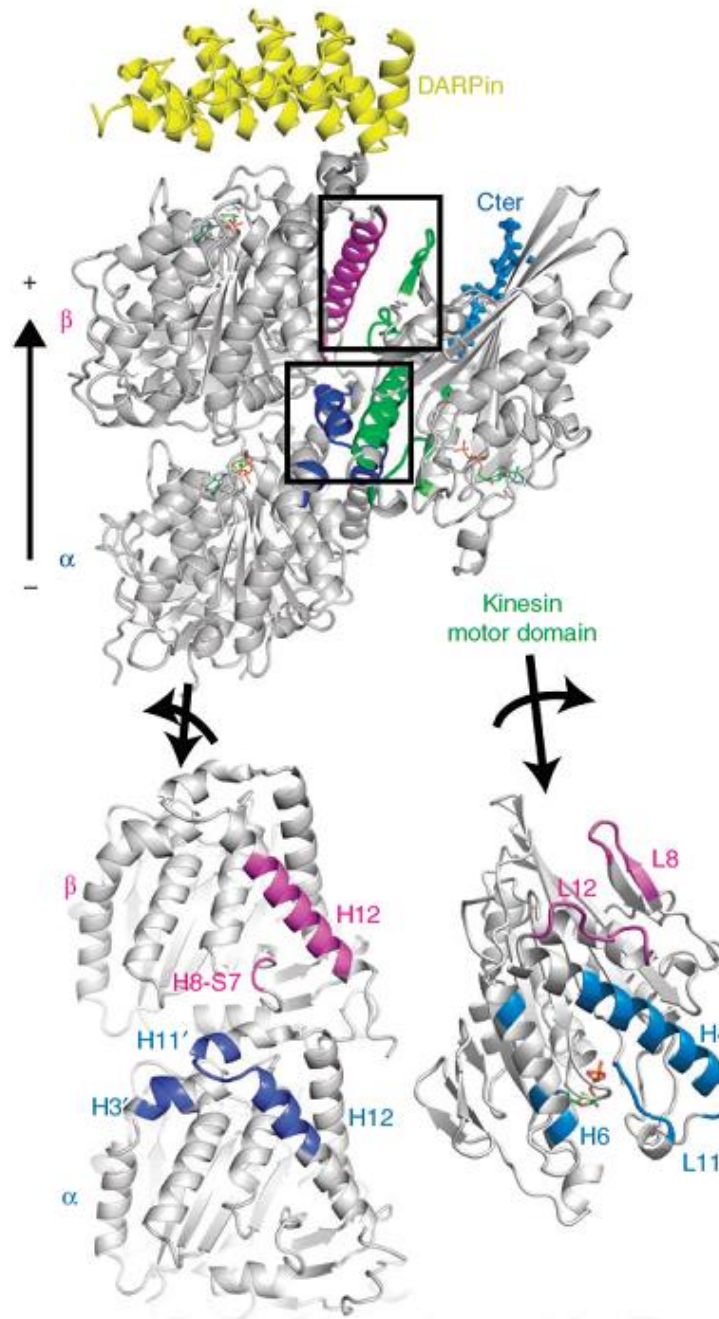


Figure 3.9 Tubulin-kinesin binding interface (pdb id 4HNA) (Gigant et al. 2013).

The contacting areas are highlighted on tubulin (left) and on kinesin (right). In the upper figure, the contacting area on α tubulin is colored in blue, on β tubulin it is colored in purple and on kinesin in green. In the lower figure, color code on tubulin remains the same, while in kinesin the interface is colored corresponding to the tubulin subunit contact. Relevant secondary structure elements are labeled on both tubulin and kinesin.

The missing structures of apo kinesin-1

Cryo-EM data of nucleotide-free kinesin-1 bound to microtubule structure have been obtained at 9 Å resolution (Sindelar and Downing 2007). At this resolution, only a rough orientation of the motor domain as well as the extension of H4 could be inferred. The resolution is too low to determine an atomic model. More detailed information can be offered by an atomic structure of nucleotide-free kinesin bound to a microtubule or to tubulin, especially to reveal the mechanism of ADP release.

Some kinesin subfamily has a relatively high spontaneous ADP release rate. An internal kinesin, pKinI (spontaneous ADP release $k_{\text{off}} \approx 8 \text{ s}^{-1}$), whose motor domain is in the middle of the sequence instead of at its N-terminus like most kinesins, was crystallized and reported to have a similar conformation as ADP kinesin (pdb id 1RY6 (Shiple et al. 2004)). Its insight on kinesin's ADP release mechanism in a general case is limited, because this kind of kinesin has a different power stroke mechanism from N-terminus kinesins, including kinesin-1.

There are only two microtubule-unbound apo N-type kinesin crystal structures in the PDB, probably due to the difficulty of generating stable apo-kinesin (Sadhu and Taylor 1992; Huang and Hackney 1994).

One is a structure of Eg5 bound to an inhibitor (pdb id 3WPN). In this case, an allosteric inhibitor able to suppress ATP binding is co-crystallized with Eg5 (Yokoyama et al. 2015). This inhibitor binds to the H4/H6 pocket which is 15 Å from the nucleotide binding pocket, leading also to a conformational change of the neck linker. As a consequence, conformational changes also occur around the nucleotide binding pocket and ATP binding is interfered. Hence, this structure doesn't represent a natural apo-like conformation.

The other apo-kinesin crystal structure (pdb id 3WRD) is generated by soaking ADP-Kif5C crystals with kinesin's C-terminal peptide (Morikawa et al. 2015). The structure is claimed to have an ATP-like conformation, in which a C-terminal neck linker docks into kinesin itself. In microtubule binding apo-kinesin EM structure, neck linker docking is not observed. The apo-Kif5C structure and ADP-Kif5C structure are very similar with an RMSD equaling 0.36 Å.

Determining the crystal structure of the complex of apo-kinesin-1 with tubulin is one of the objectives of this thesis. It is an intermediate state between ADP binding and ATP binding, and the main missing part in kinesin's nucleotide cycle coupled with microtubule binding (Fig. 3.10). Compared with ADP kinesin, it can give an insight to the ADP dissociation stimulated by microtubule binding; compared with ATP-analog-kinesin in complex with tubulin, it can help to explain the reason for neck linker docking.

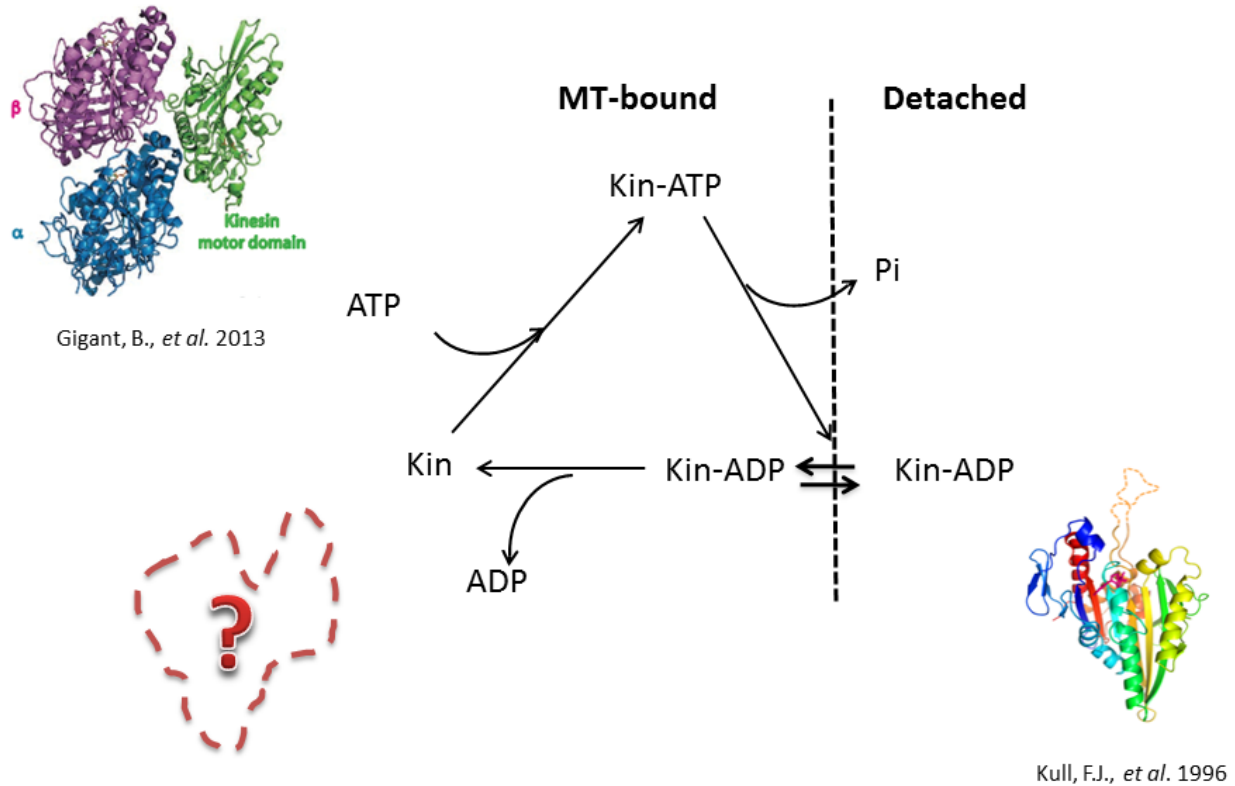


Figure 3.10 Kinesin's cycle.

The atomic structure of microtubule-unbound ADP kinesin has been determined long time ago. Recently, ATP analog-kinesin in complex with a tubulin heterodimer has been crystallized as well. As the main missing part of kinesin's cycle, the nucleotide-free kinesin in complex with tubulin can provide more information on i.e. microtubule stimulated ADP release mechanism and ATP associated neck linker docking.

4. Kinesin-14

4.1 Kinesin-14 in general

Kinesin-14, as presented before, is a subfamily of kinesins whose motor domain locating at the C-terminus of its sequence. They are dimerized through an N-terminal coiled-coil. Unlike most kinesins using an asymmetric hand-over-hand mechanism for a microtubule plus-end-directed processive movement, kinesin-14 subfamily members travel in a reverse direction, going through a different mechanism of motility. The force, allowing kinesin-14 to slide one MT relative to another, is generated by a rotation or bending of the coiled-coil stalk; while the rotation is likely coupled with the kinesin's nucleotide cycle.

Kinesin-14s play important roles during mitosis and meiosis. They are involved in spindle assembly and maintenance, are known to cross-link two parallel microtubules at the spindle poles, while cross-linking antiparallel interpolar microtubules in the spindle overlap zone.

The two most studied kinesin-14 motors are a *Drosophila* motor, Ncd (non-claret disjunctional), and a *Saccharomyces cerevisiae* motor, Kar3, serving as kinesin-14 models. Here, Ncd is taken as example to introduce kinesin-14's structure and motility cycle.

4.2 Ncd

Ncd (non-claret disjunctional) is a kinesin-14 in *Drosophila melanogaster*, playing a role in spindle organization and integrity during the early cleavages of the embryo and during female meiosis. It cross-links two microtubules, either parallel or antiparallel by its C-terminal ATP-dependent motor domains and its N-terminal ATP-independent tail. It is able to slide one microtubule relatively to another.

Ncd's motor domain has approximately 350 amino acid residues with 40% identity to kinesin-1, and previous studies indicate it has a kinetic mechanism similar to kinesin-1 as well (Pechatnikova and Taylor 1997). The rate-limiting step for both kinesins is the ADP dissociation in the absence of microtubules, while upon microtubule binding these kinesins can release ADP significantly faster. Although in *Drosophila* kinesin-1, ADP dissociation is much faster after binding to microtubules and is no longer the rate limiting step (Milic et al. 2014), in microtubule activated Ncd the hydrolysis of ATP is always rate-limited by ADP release (Mackey and Gilbert 2000). In general, Ncd's motor performs like a slow kinesin, its ATP hydrolysis speed and ADP dissociation rate are 15-20 times slower than those of a kinesin. In addition, the velocity of Ncd movement is about 100 nm s⁻¹, which is much slower than that of Kinesin-1 (about 1800 nm s⁻¹).

Structural studies of Ncd

First, the ADP bound Ncd monomer crystal structure was published in 1996 (Sablin et al. 1996), showing a remarkable similarity with kinesin-1, with a r.m.s.d of 1.21 Å. The position of Mg-ADP in both Ncd and kinesin-1 is identical. So are the central β sheet and six α helices, constituting the core in both motors. Moreover, the similarity of both structures suggests Ncd and kinesin-1 share a similar tubulin binding site. The main differences between kinesin-1 and Ncd happen in their surface loops. A group of loops (L1, L5 and L9) surrounding the entrance to the nucleotide-binding site are directed closer to the nucleotide in Ncd than in kinesin-1. Another different area in Ncd is found in L2, containing 10 more residues compared with kinesin-1. This loop extends from the main body of Ncd's motor. Sequence alignments indicate the length of the loop varies among members of the kinesin superfamily. L11, which is disordered in ADP-Kinesin-1 and is most other ADP-

bound kinesins, is ordered in this structure, which turned out in a later study to be caused by crystal packing (Sablin et al. 1998).

A crystal structure of an Ncd homodimer binding Mg-ADP (Fig. 4.1a) was determined two years later (Sablin et al. 1998). In that structure, the two motors are connected through their N-terminal “neck”, 13 residues preceding the first β strand of its catalytic core. The neck is helical and symmetrical so that it forms a parallel coiled-coil connected to the coiled-coil stalk domain without intervening loops, despite of being disordered in its ADP-monomer structure (Sablin et al. 1996). Together with part of the coiled-coil stalk, the neck contacts H1 and L6 in Ncd’s catalytic core. Based on the structure, mutations were introduced in the “neck” and in the part contacting the “neck” in Ncd’s catalytic core. Among these mutants, one whose 12 residues of its “neck” are randomly replaced by 12 hydrophilic residues moves towards microtubules plus end slowly, despite the mutant has a normal ATPase activity. These results indicate that the “neck” is essential for a minus-end-directed movement in Ncd.

Low angle X-ray scattering and Cryo-electron microscopy were used to study Ncd’s structure as well. These studies suggest that the ADP-Ncd dimer is symmetric in both crystal and solution; but once Ncd is bound to microtubules, the symmetry is broken (Endres et al. 2006). These studies indicate microtubule binding and ADP release from the microtubule-bound motor is associated with a symmetry breaking conformational change.

At least three Ncd mutants also show an asymmetric conformation even without a microtubule bound, although all these mutants bind ADP in the structure (Fig. 4.1b). In dimeric Ncd N600K mutant (pdb id 1N6M), where the mutation is located in the tubulin binding site, one of the motors and its coiled-coil stalk rotate about 75° while the other motor was superposed with one head of the symmetric Ncd dimer. The mutant dissociates ADP faster than wild type Ncd dimer (Yun et al. 2003). Another mutant, T436S (pdb id 1CZ7), shows a similar rotation of one of the motors together with its coiled-coil stalk as well. The mutation is located at the nucleotide binding site, leading to a high ADP dissociation rate (Heuston et al. 2010). A similar coiled-coil stalk rotation was also observed in the Ncd G347D mutant (pdb id 3L1C). In this case, a conserved glycine, the pivot point of stalk rotation was mutated to alter the stalk’s normal rotation (Liu, Pemble, and Endow 2012). The asymmetric conformation was generated by interfering with different aspects, microtubule binding, nucleotide binding and neck rotation, in these ADP-binding structures. A tubulin or microtubule bound Ncd structure would be most helpful to answer the remaining questions about how the asymmetric conformation is generated in wild type Ncd.

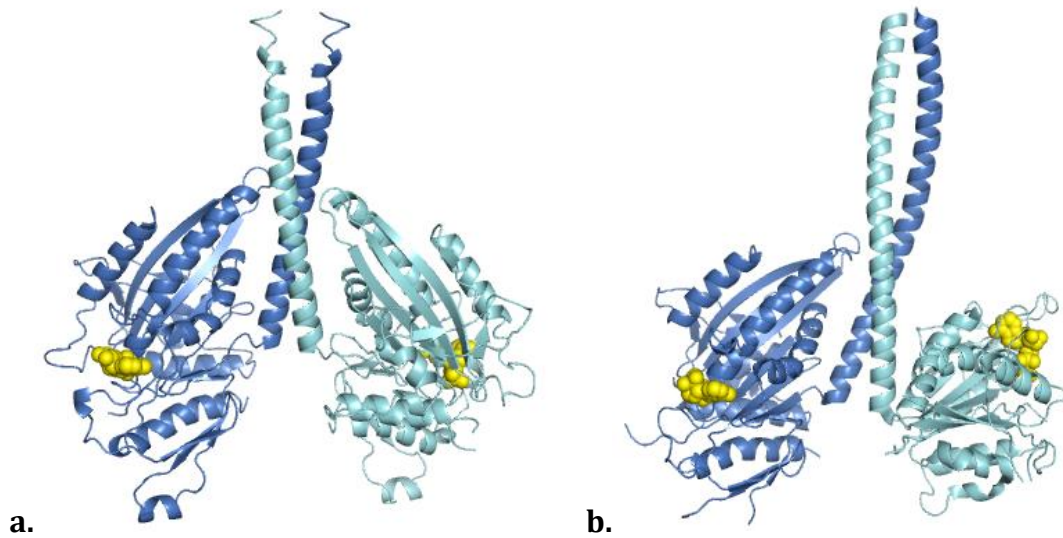


Figure 4.1 NCD homodimer in ADP state.

- a) *Wild type Ncd homodimer structure (Sablin et al. 1998). The motor domain of Ncd is similar to that of kinesin-1. Without being bound to a microtubule, the wild type Ncd homodimer is symmetric. Two ADP (yellow)-bound motor domains connect to each other with their N-terminal necks.*
- b) *In some mutants, the ADP-bound Ncd homodimer has an asymmetric conformation. The asymmetric conformation is also observed by EM when Ncd binds to a microtubule.*

Studies on Ncd's motility

Further studies on microtubule bound Ncd dimer's structure by Cryo-electron microscopy reveal the general mechanism of Ncd's motility (Endres et al. 2006). Three dimensional density maps of microtubule-bound dimeric Ncd in nucleotide-free state or in ATP analog state were calculated. A significant conformational change of Ncd's structure with or without ATP analog happens to its neck. Compared with those of apo-Ncd, the neck and unbound head of Ncd in ATP analog state rotate about 70° towards microtubules minus end (Fig. 4.2a). However, this clear ATP-caused rotation of the neck is not observed on an Ncd mutant, N340K, which can move along microtubule bidirectionally. Cryo-EM maps suggest that after ATP binding, the neck of the mutant rotates towards microtubules plus end or minus end with roughly equal probability.

These results lead to a theory that Ncd uses its neck as a lever arm to generate its power stroke (Endres et al. 2006). To prove it, the velocity of Ncd with different length of neck was measured and the results were compared, because for a lever-arm mechanism the velocity should be proportional to the length of the lever arm. Indeed, Ncd with a longer

neck turns out to move faster than that with a shorter neck, having the same ATPase turnover. If its neck is too short to form a dimer, Ncd almost loses its capability of movement, even consuming ATP normally. If a coiled-coil neck is kept while one of the motors is truncated, Ncd can still generate a “normal” movement with the same speed as a dimeric Ncd having the same length of neck. It is suggested that a stable coiled-coil stalk is required as a lever-arm to generate Ncd’s movement. But one motor seems to be sufficient for Ncd’s movement.

In general, Ncd moves in the following way (Fig. 4.2b). Ncd crosslinks two microtubules with one motor binding one microtubule while its N-terminal ATP-independent tail anchors to another microtubule. Once ATP binds to its microtubule-bound apo-motor, the neck rotates toward the motor-bound microtubule minus end. The neck plays a role as a lever-arm so that the motor-bound microtubule is drawn to slide over the tail-bound microtubule. Then ATP is hydrolyzed and the neck rotates back; as a consequence, the motor detaches from the microtubule and is able to bind to the next binding site, which is closer to the microtubule minus end. In this case Ncd slides one microtubule with respect to another, with its motor moving towards the motor-bound microtubule minus end.

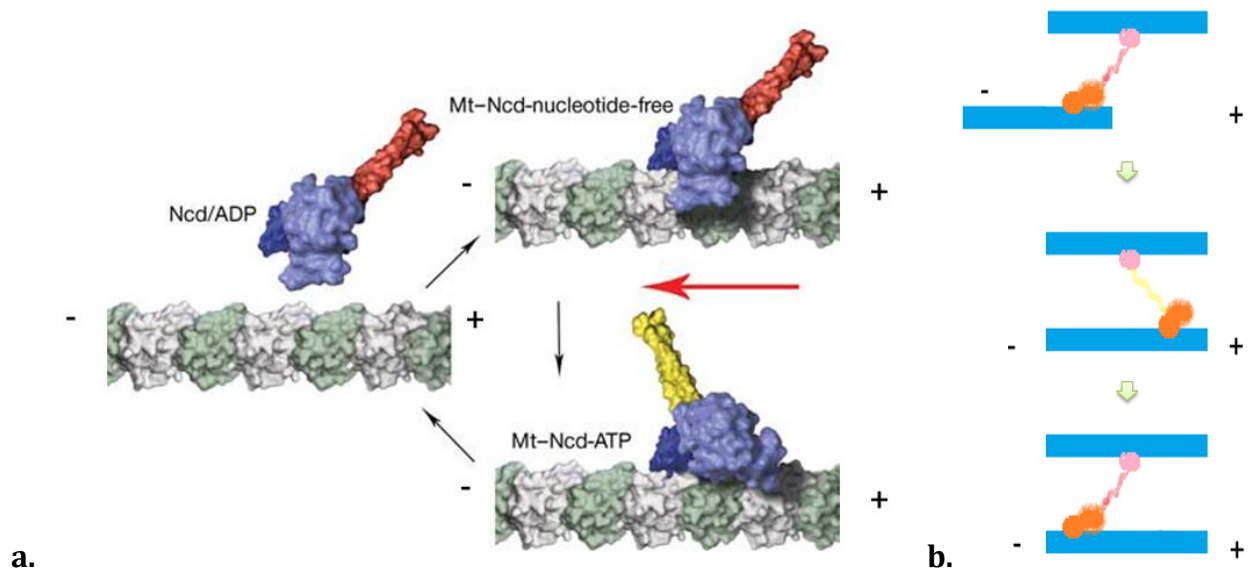


Figure 4.2 Motility model of NCD homodimer

a) A cryo-EM study on the microtubule-bound Ncd homodimer indicates that a neck rotation is caused by ATP binding (Endres et al. 2006). When ADP-Ncd motor (blue) binds a microtubule, its neck (red) points toward the microtubule plus end. Then the motor releases its ADP and is able to bind ATP. ATP binding leads a rotation of the neck (yellow) toward the microtubule minus end. After ATP is hydrolyzed, the neck rotates back to its original position (red) along with motor dissociation from the microtubule. Tubulin heterodimers are colored in green and white.

b) *The general model of Ncd's motility. Ncd's N-terminal ATP-independent microtubule binding tail (pink) attaches to one microtubule (blue), while its C-terminal motor (orange) binds to another microtubule. Once ATP binds to the microtubule-bound motor, a rotation happens to Ncd's neck (from red to yellow). As a result, the motor-bound microtubule is drawn to slide with respect to the other microtubule. After ATP hydrolysis, the neck rotates back (from yellow to red), allowing ADP-Ncd to detach from the microtubule and to rebind to its next binding site.*

Objectives

I am interested in the motility mechanism of kinesin, including its movement generation and its nucleotide consumption. Studying the structure of motor domain should provide information on the conformational changes of kinesin as a function of the nucleotide state and on their relation to the interaction with microtubules. Despite the advancement on kinesin-1's structure study, the main missing piece in the structural description on kinesin's cycle is an atomic structure of nucleotide-free kinesin in complex with tubulin. As an intermediate state between isolated ADP-kinesin and microtubule-bound ATP-kinesin, this structure will bring insights into microtubule stimulated ADP release mechanism, by comparison with ADP-kinesin structure. By comparison with tubulin-bound kinesin in the ATP state, such a structure should also identify the structural changes upon ATP binding which lead to neck linker docking.

The main objective of this thesis is to determine the crystal structure of a (+)-end directed motile kinesin in a nucleotide-free state, both isolated and in complex with tubulin heterodimer. In the latter case, a DARPIn will be used as a tubulin stabilizer.

These structural data will be complemented by the study of structure-based kinesin mutants. Moreover, mutagenesis study will be performed on kinesin-1 to test these analysis established on apo-kinesin-tubulin structure. Mutants and wild type kinesin will be studied structurally and biochemically. By analyzing the data on spontaneous ADP dissociation, ATPase activity of both kinesin mutants and wild type, I will know which residues are essential for kinesin's kinetic mechanism. For this objective, I have worked mainly with human kinesin-1 constructs. The results I have obtained are presented in the first (structure of apo-kinesin-1 bound to tubulin) and second (structures of isolated apo-kinesin-1) chapters of the results section.

The second objective is associated with kinesin-14, which differs from (+)-end directed kinesin as it moves towards the microtubule (-)-end. So far, there are only isolated kinesin-14s (not bound to tubulin) that have been crystallized. I will try to co-crystallize kinesin-14 in different nucleotide state (nucleotide-free or ATP-analog) in complex with tubulin. These data should allow one to compare the way that ATP binding triggers movement in these two kinds of kinesins (plus and minus-end directed kinesins). I will use both Ncd and Kar3 as representatives of kinesin-14 motors. Different DARPins will be used to enhance the chances of crystallization. Also crystallization of Vik1 (Kar3's motor-homology partner) in complex with tubulin will be tried. The advancement I have achieved so far will be presented in the third chapter of the results section.

Results and Discussion

1. Structure of apo-kinesin-1 bound to tubulin

1.1 Context

Kinesin-1 (kinesin or KHC) walks processively along microtubules in a hand-over-hand manner (cf. Introduction). The processive movement of kinesin requires each motor domain of the homodimer following the same mechanochemical cycle while in alternative stages.

The following short description summarizes the kinetic cycle relevant to the analysis made in this part of work (Cross 2004). The kinetic rate may vary because of different kinesin constructs studied.

In solution, kinesin in the ADP state has a slow release of ADP (off rate, k_{off} is about 0.01 s^{-1}) and weak microtubule binding (dissociation constant, $K_d \approx 10\text{-}20 \mu\text{M}$). Once the ADP-kinesin binds a microtubule, ADP release is stimulated. The off rate ($k_{\text{off}} > 100 \text{ s}^{-1}$) of microtubule-activated ADP release is several thousand folds of the ADP dissociation rate in the absence of microtubules (Hackney 1988; Hackney et al. 2003). Then, the affinity for microtubules of the kinesin, now in nucleotide-free state, is enhanced. After ADP release, Mg-ATP is allowed to bind the kinesin-microtubule complex (on rate, $k_{\text{on}} \approx 2 \mu\text{M}^{-1} \text{ s}^{-1}$). When ATP-kinesin is bound to microtubule, ATP hydrolysis is favored: the ATP hydrolysis in an ATPase turnover is accelerated from 7 s^{-1} (in the absence of microtubules) to $200\text{-}300 \text{ s}^{-1}$. Then, phosphate release happens (with a speed $> 100 \text{ s}^{-1}$). The low affinity for microtubule of the ADP-kinesin leads to its detachment from the microtubule. Although the framework of kinesin's nucleotide cycle is known, how microtubule stimulates both ADP release and the chemical step of ATP hydrolysis remains unclear. Structural study will help to figure out the conformational variations in the cycle.

Another point that remains to be clarified is how ATP binding to microtubule-bound nucleotide-free kinesin induces "neck linker docking". Neck linker, located at the C-terminus of kinesin motor domain, is a 15-amino-acid-long "linker" between kinesin motor domain and the coiled-coil stalk needed for kinesin dimerization. It's responsible for the communication between two motors.

In ADP-kinesin detached from microtubule, the conformation of neck linker varies. It can be either rigid and docked into the catalytic core or disordered. Both conformations have been observed in ADP-kinesin crystal structure (Sindelar et al. 2002). Using EPR spectroscopy and FRET approaches, Rice *et al.* have reported that, once kinesin binds

microtubule, the neck linker is disordered after ADP release (apo-kinesin) and becomes ordered upon ATP binding (Rice et al. 1999).

The ATP-induced neck linker docking in microtubule-bound kinesin is crucial for kinesin's processivity and unidirectional movement to microtubule plus end. Because when in the leading motor, ATP binds to the microtubule-attached catalytic core; the other motor in ADP state either binds microtubule untightly or is detached from microtubule. The neck linker docking ensures: 1) there is always at least one motor domain attaches tightly to the microtubule, because ATP doesn't hydrolyze efficiently without neck linker docking and ATP- or apo-kinesin, unlike ADP-kinesin, always has high affinity with microtubule. 2) the rear ADP-motor moves unidirectional. As the direction of neck linker docking points to the plus end of microtubule, the rear motor is led toward the plus end. 3) kinesin homodimer moves processively. The rebinding of the "rear" head to microtubule makes sure the mechanochemical cycle on that motor continue. In other words, when the "rear" head moves forward and rebinds microtubule, it become the new "leading" head releasing ADP and accepting ATP. The neck linker docking will happen in the new "leading" head, accompanied with the movement of the new "rear" head. However, details on the mechanism of neck linker docking remains ambiguous. In particular it remains unclear how the conformation of neck linker changes upon microtubule binding and nucleotide state. Structural study on kinesin's motor domain in different nucleotide state should provide detail information.

Although recently several structures of microtubule-bound kinesin in different nucleotide states have been obtained by Cryo-electron microscopy (Atherton et al. 2014; Shang et al. 2014); when I started my work, there was only one EM structure of nucleotide-free kinesin-1 binding microtubule (Sindelar and Downing 2007). Limited by resolution, it was hard to generate an atomic model. One can only infer a rough orientation of the motor domain and the extension of H4 helix.

Until then, most kinesin high-resolution structures obtained by X-ray crystallography in different nucleotide states are in the absence of microtubule or of tubulin (e.g. see (Kull et al. 1996; Parke et al. 2010b)). But some of the properties of the kinesin change so much upon interaction with microtubules that the structure of microtubule-unbound kinesin is likely not to be relevant to several steps of its nucleotide cycle. The first crystal structure of ATP analog- kinesin in complex with tubulin, as a previous work in our lab (Gigant et al. 2013), provided insights to the mechanism of ATP hydrolysis and neck linker docking. The main missing piece on the structural study of kinesin's microtubule associated nucleotide cycle is a microtubule-bound apo-kinesin structure, which is the intermediate state between ADP-kinesin and microtubule-bound ATP-kinesin.

Here, I further the structure study by determining a 2.2 Å crystal structure of a nucleotide-free kinesin in complex with tubulin. Compared with ADP kinesin structure, this structure shall provide information explaining how binding microtubule accelerates the ADP dissociation in kinesin motor. In addition, comparing apo-kinesin and ATP-analog kinesin, both in complexes with tubulin, we can distinguish the conformational changes caused by ATP binding from those led by microtubule binding. Furthermore, we may answer the questions including how neck linker docking is induced by ATP binding, how ATP hydrolysis is favored in microtubule-bound kinesin etc.

1.2 Paper: “The structure of apo-kinesin bound to tubulin links the nucleotide cycle to movement.”

ARTICLE

Received 23 Apr 2014 | Accepted 25 Sep 2014 | Published 14 Nov 2014

DOI: 10.1038/ncomms6364

The structure of apo-kinesin bound to tubulin links the nucleotide cycle to movement

Luyan Cao^{1,*}, Weiyi Wang^{1,2,*}, Qiyang Jiang^{2,†}, Chunguang Wang², Marcel Knossow¹ & Benoît Gigant¹

Kinesin-1 is a dimeric ATP-dependent motor protein that moves towards microtubules (+) ends. This movement is driven by two conformations (docked and undocked) of the two motor domains carboxy-terminal peptides (named neck linkers), in correlation with the nucleotide bound to each motor domain. Despite extensive data on kinesin-1, the structural connection between its nucleotide cycle and movement has remained elusive, mostly because the structure of the critical tubulin-bound apo-kinesin state was unknown. Here we report the 2.2 Å structure of this complex. From its comparison with detached kinesin-ADP and tubulin-bound kinesin-ATP, we identify three kinesin motor subdomains that move rigidly along the nucleotide cycle. Our data reveal how these subdomains reorient on binding to tubulin and when ATP binds, leading respectively to ADP release and to neck linker docking. These results establish a framework for understanding the transformation of chemical energy into mechanical work by (+) end-directed kinesins.

¹Laboratoire d'Enzymologie et Biochimie Structurales (LEBS), Centre de Recherche de Gif, Centre National de la Recherche Scientifique, 1 avenue de la Terrasse, 91190 Gif sur Yvette, France. ²Institute of Protein Research, Tongji University, 1239 SiPing Road, 200092 Shanghai, China. * These authors contributed equally to this work. † Present address: European Molecular Biology Laboratory Grenoble Outstation, 71 avenue des Martyrs, 38000 Grenoble, France. Correspondence and requests for materials should be addressed to C.W. (email: chunguangwang@tongji.edu.cn) or to M.K. (email: knossow@lebs.cnrs-gif.fr) or to B.G. (email: gigant@lebs.cnrs-gif.fr).

In the cell, the main function of kinesin-1 (previously named conventional kinesin and hereafter called kinesin) is to transport organelles. It does so by moving processively towards the (+) end of microtubules, a process tightly coupled to the ATP hydrolysis cycle¹. Kinesin consists of two identical motor domains connected by a coiled-coil stalk and a pair of light chains that bind to the tail C-terminal domains. The motor domain harbours microtubule- and ATP-binding activities. It comprises a catalytic core and an adjacent C-terminal neck region². Kinesin undertakes one step per ATP hydrolysed³. The corresponding processive movement is driven by two alternate conformations of the two kinesin neck linkers (the *ca.* 15 amino acids C-terminal to the motor domain core), docked and undocked, in correlation with the nucleotide bound to each motor domain⁴, giving rise to a transport rate at the level of 100 steps per second⁵.

To determine the mechanism for movement production, a detailed structural analysis of the kinesin in its different nucleotide states is required. Numerous X-ray structures of kinesins detached from their track protein are known; these kinesins are mostly bound to ADP (for example, see refs 5–7; for a review, see ref. 8) but in a few cases ATP-like structures have been determined^{9,10}. There is also a recent structure of ATP-like kinesin bound to tubulin¹¹ (ATP-like complex). In addition, kinesin motor domains in all their nucleotide states, bound to microtubules, have been studied by cryo-electron microscopy (EM) at resolutions up to *ca.* 9 Å^{12–15}. However, for a complete description of the kinesin nucleotide cycle, a high-resolution structure of the nucleotide-free kinesin bound to its track protein (nucleotide-free complex) is required.

Because of this missing structure, open questions remain about critical features of the kinesin mechanism. One such feature is that neck linker docking, which initiates each step taken, only happens on ATP binding to the motor domain⁴. The related specific question concerns the structural changes caused in tubulin-bound kinesin on ATP binding that lead to neck linker docking and result in movement. So far, it has only been possible to define the mixed effects on the kinesin structure of tubulin and nucleotide binding¹¹. The comparison of the atomic resolution structures of the nucleotide-free and ATP-like complexes would distinguish these effects and clarify how ATP binding initiates each step.

A second critical feature is that in the absence of microtubules, motile kinesins are trapped in an ADP-bound state, thereby minimizing futile ATP hydrolysis. Trapping terminates on microtubule binding, which accelerates ADP release by several orders of magnitude¹⁶. The corresponding mechanism remains elusive¹⁴. The comparison of kinesin-ADP with a structure of nucleotide-free kinesin would define structural changes in the nucleotide site that lower the affinity for ADP.

To address these issues, we have determined the structure of nucleotide-free kinesin bound to tubulin at 2.2 Å resolution and compared it with those of detached kinesin-ADP and of the complex of tubulin with kinesin-ADP-AlF₄⁻ (hereafter referred to as the ATP-like complex). These comparisons show that the kinesin structural changes along the nucleotide cycle are well described by rigid-body movements of three motor subdomains. As kinesin binds to tubulin, these movements distort the nucleotide-binding site and cause ADP release. The high-resolution structure we determined identifies the atomic interactions that are established in nucleotide-free kinesin by residues that interact with the nucleotide in kinesin-ADP. Our results also identify the interactions of ATP that cause subdomain movements resulting in the opening of a cavity in the motor core where the first residue of the neck linker gets buried, initiating neck-linker docking. In addition, our results suggest a connection between neck-linker docking and ATP hydrolysis. Therefore, the

structure of the nucleotide-free complex has allowed us to establish the reciprocal relationship between neck-linker docking on the one hand and ATP binding and hydrolysis on the other hand. Taken together, our results clarify the link between the kinesin nucleotide cycle and movement.

Results

Structure of nucleotide-free kinesin in complex with tubulin.

We determined the structure of an apo-kinesin motor domain bound to tubulin (Supplementary Table 1). For crystallization, the motor domain was truncated after the first amino acid of the neck linker, as this peptide has been shown to be disordered in nucleotide-free tubulin-bound kinesin⁴ (this means that the construct crystallized comprises residues 1–325). Furthermore, tubulin was complexed to a designed ankyrin repeat protein (DARPin)¹⁷ that prevents its assembly¹⁸ (Fig. 1a). As expected, there is no nucleotide in the kinesin nucleotide-binding site (Fig. 1b and Supplementary Fig. 1). Comparable to when ATP-like¹¹, the kinesin in its nucleotide-free form is able to bind to curved tubulin, whereas it moves along microtubules in which tubulin is straight. Nevertheless, the structure of apo-kinesin in the nucleotide-free complex is very similar to that of apo-kinesin monomers that decorate microtubules¹⁴ (Supplementary Fig. 2). As in cryo-EM reconstructions of microtubule-bound kinesin motor domains^{12,14}, the $\alpha 4$ helix at the interface with tubulin is longer at its amino-terminus than in detached kinesin-ADP; we find that similar to that in the ATP-like complex¹¹, it is extended by 2.5 turns (Fig. 1c). Furthermore, we compared the overall conformations of curved and microtubular tubulin residues at the interface with the kinesin, as had been done in the case of the ATP-like complex. We found that they are highly similar, the root mean square deviation of the C α s of tubulin residues at the interface with kinesin being 1.5 Å (34 C α s compared). Local or overall variations in kinesin structure corresponding to these small differences at the surface of tubulin are not detected at the *ca.* 9 Å resolution of cryo-EM maps currently available¹⁴. Therefore, both the kinesin and its interface with tubulin are similar in the nucleotide-free complex and in a microtubule-decorating kinesin. Thus, the structure we determined, in comparison with those of the ATP-like complex¹¹ and of detached kinesin-ADP^{5,6}, provides the basis for the identification of microtubule- and ATP-induced changes.

A remarkable property of the nucleotide-free complex is the plasticity of kinesin, which is notably more flexible than tubulin (Supplementary Table 2). The kinesin atomic temperature factors increase gradually from its tubulin interface to its tubulin distal surface (Supplementary Fig. 3). The kinesin temperature factors distribution in the nucleotide-free complex is unlikely to be due to the curvature of tubulin, as in the ATP-like complex¹¹, in which tubulin is just as curved as in the nucleotide-free complex, temperature factors of the tubulin and kinesin partners are similar (Supplementary Table 2). Instead, the flexibility seems specific to apo-kinesin, which is consistent with the notion that it is prone to denaturation¹⁹ unless it is stabilized on strong binding to tubulin (or microtubules) in the rigor state.

The mechanism by which ATP controls neck-linker docking.

The structure of the nucleotide-free complex was first compared with that of the ATP-like complex¹¹. The comparison shows that the motor domain binds to tubulin through the same interface in both nucleotide states. However, because of the higher resolution of the nucleotide-free complex crystals diffraction and as the tubulin-kinesin interface is highly ordered, additional interactions mediated by trapped water molecules were identified in the structure determined in this work (Fig. 1c).

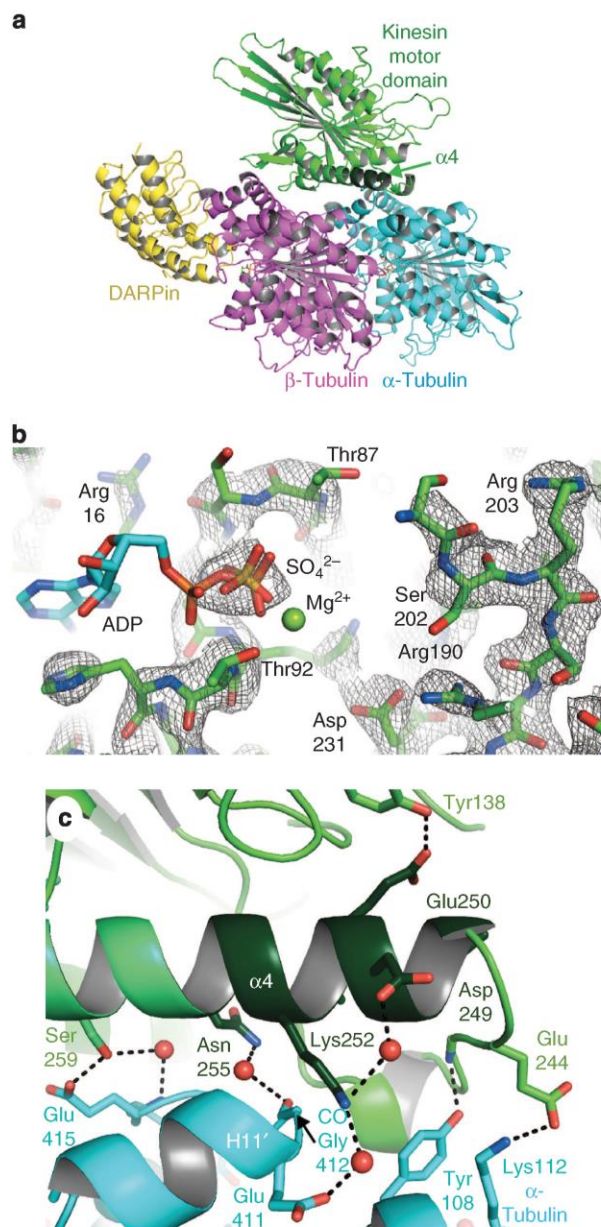


Figure 1 | The structure of nucleotide-free kinesin bound to tubulin.

(a) Overview of the complex crystallized. (b) Two Fobs-Fcalf map (contoured at the 1σ level) of the nucleotide-free complex centred at the nucleotide-binding site of (apo-) kinesin. ADP and Mg^{2+} are from kinesin-ADP (1BG2) after superposition of the kinesin P-loop subdomains (see Fig. 2a) in these two structures. In the apo-kinesin nucleotide site, no water molecule has been identified but an SO_4^{2-} ion that largely overlaps with the ADP β -phosphate and accounts for the observed electron density has been modelled. A stereo image of the electron density is presented in Supplementary Fig. 1.

(c) The $\alpha 4$ N-terminal extension is stabilized both by direct and water (red spheres)-mediated interactions with α -tubulin and the motor domain core. The kinesin is in green with the extension of the $\alpha 4$ helix, which forms in all nucleotide states on binding to tubulin^{11,14}, in darker green (as in a); α -tubulin is in cyan. All figures of structural models were generated with Pymol⁵¹.

The new structure differs from the structure of the ATP-like state by a considerable reorganization of the majority of the motor domain, as well as by local changes in the

nucleotide-binding motifs (Switch1, Switch2 and the P-loop). The general reorganization of the motor is best described by relative rigid-body movements of three subdomains: a tubulin-binding subdomain that lies at the kinesin-tubulin interface (helices $\alpha 4$ and $\alpha 5$, the intervening L12 loop and strands $\beta 5a$ and $\beta 5b$), a P-loop subdomain (constituted of both ends of the motor domain core—strands $\beta 1$ and $\beta 2$ of the core β sheet, helices $\alpha 1$ and $\alpha 2$ at the N-terminal end, and $\beta 8$ and $\alpha 6$ at the C-terminal end) and a Switch I/II subdomain ($\beta 3$ – $\beta 7$ and $\alpha 3$) (Fig. 2a and Supplementary Fig. 4; for the nomenclature of secondary structure elements, see these figures and refs 5,20). When the kinesin tubulin-binding subdomains in the nucleotide-free and ATP-like complexes are superimposed, additional 11° and 22° rotations are required to superimpose the Switch I/II and P-loop blocks, respectively (root mean square deviation after superposition are 0.64 and 0.58 Å, over 84 and 111 C α s, respectively) (Fig. 2b,c and Supplementary Movie 1). Movements of these two subdomains also account for the other structural changes in the kinesin nucleotide/microtubule binding cycle (Fig. 3) as well as for their functional consequences. In particular, when tubulin-binding subdomains in the nucleotide-free and detached ADP-bound kinesin are superimposed, the Switch I/II block is rotated 9° and the P-loop block is rotated 7° between the two structures. These rotations distort the nucleotide-binding site to cause ADP release (see ‘The acceleration of nucleotide release on tubulin binding’ in the Results section).

The effect of ATP binding on the relative orientations of the Switch I/II and P-loop subdomains may be analysed as follows. In the ATP-like complex¹¹, whereas the ADP moiety binds mostly to the P-loop subdomain, the γ -phosphate analogue and the nucleotide-bound Mg^{2+} establish a network of interactions with the P-loop and with completely conserved residues in the Switch I/II subdomain (Ser201 and Ser202 in the Switch1 motif and Asp231 in the Switch2 motif)^{9–11}. These interactions could not be made in the nucleotide-free complex (Supplementary Fig. 5). Only following relative reorientation of the Switch I/II and P-loop subdomains can the interaction of Asp231 with two of the groups that coordinate Mg^{2+} be established; this reorientation together with the new structure of the Switch1 loop allows Ser201 and Ser202 to interact with Mg^{2+} as well as with the γ -phosphate analogue (Supplementary Fig. 5). Therefore, ATP bridges the Switch I/II and P-loop blocks through the multiple simultaneous interactions it mediates, which favours the reorientation of the two subdomains.

Another consequence of ATP binding to the tubulin-bound kinesin is the docking of the neck linker. For the neck linker to be docked, the side chain of its first residue (Ile325, highly conserved in kinesins) needs to be buried in a cavity in the kinesin motor domain core that is boxed in by Ile9 in the P-loop subdomain and three highly conserved residues (Ile265, Leu268 and Leu290) in the tubulin-binding subdomain (Supplementary Fig. 6). In tubulin-bound kinesin this cavity is formed only in the ATP state, whereas it collapses in the apo state as the position of the first residue of the docked neck linker is largely occupied by the side chain of Ile9 (Fig. 2d). The residue at position 9 of the sequence is not as well conserved as the other residues that constitute the Ile325 cavity, but an isoleucine or a valine are most commonly found. Remarkably, in the recently determined rigor-like structure of the kinesin-3 KIF14 (ref. 21), the residue equivalent to Ile9 (a valine) is located as in the nucleotide-free complex and would interfere with neck-linker docking similarly to Ile9 in kinesin (Fig. 2d). Thus, taken together with structural evidence from the literature, our data lead us to propose that ATP binding triggers neck-linker docking by inducing the rotation of the P-loop subdomain. This will be further supported when additional structural data, for example, on apo-kinesin constructs with a longer neck linker, become available.

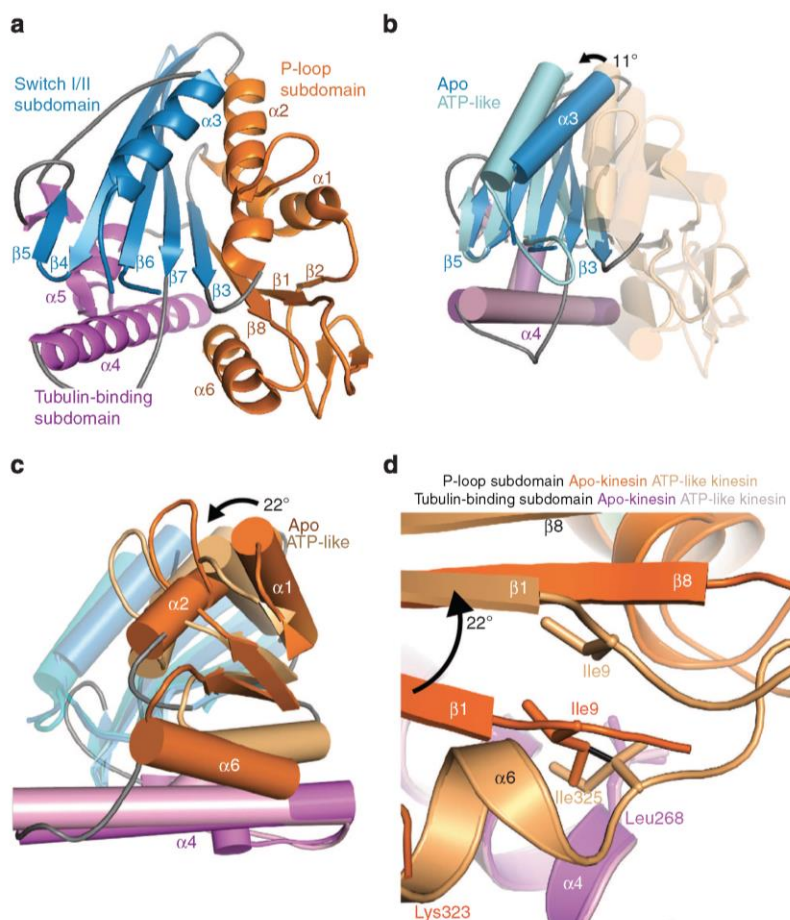


Figure 2 | Changes in tubulin-bound apo-kinesin on ATP binding. (a) The three subdomains whose movements account for structural changes during the nucleotide cycle. For clarity, the strands that are not part of the central β sheet are not labeled. The subdomains connecting loops are in grey. (b) The movement of the Switch I/II subdomain on ATP binding. In this and in c, the tubulin-binding blocks in ATP-like and in apo-kinesin have been superimposed and the subdomain that is not being compared is shown as a semi-transparent model. (c) The movement of the P-loop subdomain; for clarity, strands $\beta 1a$ – $\beta 1c$, which are not part of the central β sheet, have been omitted. (d) The effect of the P-loop subdomain rotation on neck-linker docking. P-loop subdomains in ATP-like and apo-kinesin are presented following superposition of the tubulin-binding blocks. The location of the first neck-linker residue (Ile325) in ATP-like kinesin is occupied by Ile9 in nucleotide-free kinesin (the atoms linked by a black solid line are 1.2 Å away). As a consequence, in the nucleotide-free complex the kinesin polypeptide chain is disordered after Lys323.

Neck-linker docking gates the kinesin ATPase. As mentioned above, when the neck linker is docked, its first residue (Ile325) would severely clash with Ile9 of the P-loop block in its nucleotide-free orientation (Fig. 2d), suggesting that neck-linker docking prevents the P-loop subdomain from rotating back from its ATP-like orientation towards the nucleotide-free one. As the structure of kinesin in the ATP-like complex is tuned for an efficient ATP hydrolysis chemical step^{10,11}, this means that neck-linker docking locks the structure in an ATPase-competent state. Indeed, deleting the neck linker (yielding the 1–324 construct) decreased the microtubule-stimulated ATPase by 60-fold compared with the 1–349 monomeric construct, which comprises the full neck linker in addition to the motor domain core (Table 1). Removal of the whole neck linker has been reported previously to have a substantial effect on microtubule-stimulated ATPase of another (+) end-directed kinesin, the kinesin-3 Kif1a²². We also found that incorporating the first residue of the neck linker (yielding the construct used for crystallization in this work) increased the ATPase rate by a factor of 20, the remaining difference from the 1–349 construct

(Table 1) being most likely due to the missing interactions mediated by the rest of the neck linker. These results strongly suggest that Ile325 contributes significantly to positioning the P-loop subdomain for efficient ATP hydrolysis when the neck linker is docked.

Our model leads to another prediction concerning the shortened constructs (1–324 and 1–325). As the neck linker is disordered⁴ and does not interfere with the P-loop subdomain in the nucleotide-free complex, the model predicts that ADP release should be much less affected than the ATPase chemical step in these constructs and become non-rate limiting. Indeed, we found that the maximum rates of microtubule-stimulated Mant-ADP release from both constructs (52.9 ± 7.4 and $43.0 \pm 3.3 \text{ s}^{-1}$, respectively; see Supplementary Fig. 7) are much higher than their respective k_{cat} kinetic constants and similar to the k_{cat} kinetic constant of the 1–349 construct (Table 1).

Interestingly, the ATPase of a triple mutant comprising residue changes I325A/K326A/N327A is unaffected²³. This result is well accounted for by the structures, as the C β of residue 325 in a docked neck linker clashes with Ile9 in apo-kinesin (Fig. 2d), so

that the ATPase-efficient positioning of the P-loop subdomain is still maintained in this triple mutant. To attenuate the clash between Ile9 and Ile325, we mutated the latter residue to a glycine in the 1–349 construct. This should lessen the interference of residue 325 with the nucleotide-free orientation of the P-loop subdomain and lead to a much decreased ATPase activity. This is what we observed: the ATPase activity of the I325G mutant was decreased by 27-fold (Table 1). This decrease of the ATPase activity could also be due to a general destabilization of the kinesin structure. If this was the case, one would expect ADP to

be less tightly bound in the mutated protein. However, such is not the case: the rate of spontaneous ADP release from the I325G mutant is very similar to that from the parent construct (0.015 s^{-1} versus 0.025 s^{-1}), implying that the effect of the I325G mutation on the ATPase rate is not due to an overall destabilization of the kinesin. Taken together, our results therefore suggest that when the neck linker is docked, the interference of Ile residues at positions 9 and 325 of the sequence locks the P-loop subdomain in its ATPase-competent orientation.

Our results are also consistent with a kinetic model of kinesin motility, which concluded that the rear head of a kinesin dimer, to which the neck linker is docked, has a much higher ATPase activity than the front head, in which the neck linker is undocked²⁴. They strongly support the proposal that neck-linker docking gates the ATPase activity of the kinesin motor domain.

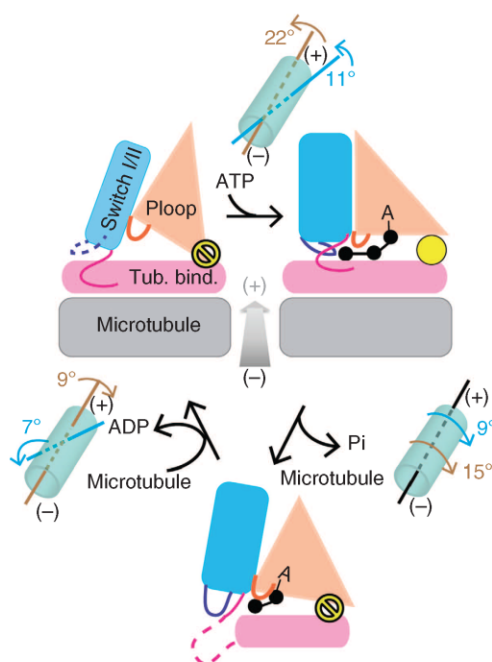


Figure 3 | Subdomains orientation changes along the kinesin mechanochemical cycle. The angles are those of the rotations needed to superimpose the P-loop (salmon, with the P-loop in orange) and Switch I/II (blue, Switch1/L9 in darker blue) subdomains, after the tubulin-binding blocks (pink) have been superimposed. The Switch2/L11 loop is in darker pink. The root mean square deviation of C α positions after superposition are all smaller than 1 Å. The rotation axes are schematized taking the microtubule (depicted as a cylinder, with its polarity indicated) as a reference. Note that the rotations that relate subdomains in detached kinesin and in the ATP-like complex are around nearly parallel axes so that the three subdomains were not readily identified based on these two structures. The yellow disk indicates the status of the neck linker, which docks along with ATP binding but does not in the nucleotide-free state. After phosphate release and detachment from the microtubule, kinesin-ADP undergoes recovery to a state in which the neck linker undocks and becomes disordered, as schematized.

The acceleration of nucleotide release on tubulin binding.

Next, we compared the structures of kinesin in the tubulin:apo-kinesin complex and of detached kinesin-ADP⁵. As mentioned above, when kinesin binds to tubulin, the α 4 helix extends by 2.5 turns (Fig. 1) at its N-terminal end, the corresponding residues being prone to disorder in detached kinesin (for example, see refs 5,6). When kinesin-ADP binds to tubulin and if the α 4 helix lengthened without additional changes, severe clashes would arise between the extension and the rest of the motor domain. In particular, Glu250, Asn253 and Ile254 in the extension would strongly clash with Tyr138 and Leu139 in the turn connecting strands β 4 and β 5 of the kinesin central sheet (Fig. 4a) and with Arg203 in the Switch1 motif (Supplementary Fig. 8). In apo-kinesin, these clashes are avoided through two main changes. Most of the Switch1-containing L9 loop is disordered, instead of forming a short helical segment as in kinesin-ADP⁵ (Supplementary Fig. 8). In addition, the Switch I/II subdomain rotates by 7° with respect to the tubulin-binding block (Fig. 3) so that Tyr138 makes a hydrogen bond with Glu250 and Leu139 does not interfere with the α 4 extension (Fig. 4a). This rotation is accompanied by a P-loop subdomain movement that allows the extensive interactions of the Switch I/II and P-loop blocks to be maintained (the buried surface area at their interface is larger than 2,000 Å² in all nucleotide states). These conformational changes of the kinesin on tubulin binding reorganize the nucleotide-binding site, as detailed below.

In kinesin-ADP⁵, similar to tubulin:kinesin-ATP¹¹, the nucleotide is bound by interactions with P-loop subdomain residues and by the completely conserved Switch2 N-terminal residue, Asp231. This residue makes hydrogen bonds with two of the groups that coordinate the ADP-bound Mg²⁺ ion^{22,25}, the Thr92 (in the P-loop) hydroxyl and a water molecule oxygen atom. As Asp231 belongs to the Switch I/II subdomain (Supplementary Fig. 4), the movements of the Switch I/II and P-loop blocks during the transition to the nucleotide-free state displace Asp231 by 2.6 Å with respect to the P-loop subdomain

Table 1 | Microtubule-stimulated ATPase kinetic parameters of truncation and substitution mutants of the kinesin motor domain.

Construct	1-349 (ref. 11)	1-325	1-324	1-349 I325G	1-349 D231A	1-349 R190A-D231A
k_{cat} (s ⁻¹)*	50.3 ± 1.6	16.8 ± 0.7	0.85 ± 0.02	1.88 ± 0.06	1.53 ± 0.06	11.0 ± 0.6
K_{M} (μM)†	1.3 ± 0.1	0.6 ± 0.1	0.11 ± 0.01	0.16 ± 0.02	0.06 ± 0.01	0.23 ± 0.05

*Kinetic parameters determined using nonlinear least squares to fit the variation of the ATPase rate as a function of microtubular tubulin concentration, using the Michaelis-Menten equation. Kinetic parameters are given as value ± s.e. (calculated from the fit).

†The lower K_{M} of the mutants seems an indirect effect of the mutations/truncations as the neck linker is not seen to contact tubulin or microtubules in the structures determined; similar observations have been reported for other kinesin neck-linker mutants²³.

(Fig. 4b). As a consequence, the simultaneous interactions of ADP-Mg²⁺ with the P-loop subdomain and Asp231 witnessed in detached kinesin cannot be maintained in tubulin-bound kinesin, where ADP release is substantially accelerated. These observations suggest that the tight binding of ADP in detached kinesin is, at least partially, due to the interactions made by Asp231.

To quantify the contribution of Asp231 to ADP trapping, we mutated it to alanine in the 1–349 construct and recorded the

spontaneous ADP release from this mutant. We found that the release rate ($0.15 \pm 0.01 \text{ s}^{-1}$, see Fig. 4c) is substantially faster than that of the parent construct ($0.025 \pm 0.01 \text{ s}^{-1}$), confirming a role for the Asp231 interactions with Mg²⁺ in ADP binding in tubulin-unbound kinesin. To evaluate the effect of the overall structural changes that accompany tubulin binding, we also measured microtubule-stimulated nucleotide release from the D231A mutant. The rate increases as a function of the tubulin concentration, its maximum value ($1.9 \pm 0.1 \text{ s}^{-1}$, see Fig. 4c) being similar to the ATPase rate (Table 1), meaning that nucleotide release limits the ATP hydrolysis rate in this mutant. The rate for microtubule-stimulated ADP release from D231A is much slower than that from the parent monomeric construct, which is at least as fast as the ATPase rate ($\sim 50 \text{ s}^{-1}$, similar to previously measured values³). A molecular explanation for this difference is provided below.

Asp231 makes a salt bridge with Arg190 in the nucleotide-free complex (Fig. 4b). Therefore, mutating it to an alanine leaves the positive charge of the arginine unbalanced. To eliminate a possible effect of this altered charge distribution, we produced the R190A-D231A double mutant of the 1–349 construct and measured the rate at which it releases ADP. The basal rate is accelerated compared with the D231A mutant (to $0.6 \pm 0.1 \text{ s}^{-1}$) as is the microtubule-stimulated rate ($13 \pm 0.5 \text{ s}^{-1}$, Fig. 4c), which still limits the ATPase rate (Table 1). Not unexpectedly, as kinesin is tuned for efficient microtubule-stimulated ADP release, the rate displayed by the double mutant is still slower than that by the 1–349 construct. The most probable explanation is that the interactions made by Asp231 and Arg190 in the nucleotide-free microtubule-bound kinesin also contribute to accelerating ADP release. To sum up, the overall structural changes caused by the re-orientations of the motor subdomains and, in particular, the change of Asp231 location lead to microtubule-stimulated ADP release from kinesin.

Discussion

In this study, we have determined the structure of nucleotide-free kinesin bound to tubulin. Comparison of this structure to that of ATP-like kinesin bound to tubulin¹¹ has led to the identification of three kinesin motor subdomains whose movements account for kinesin structural changes along the nucleotide cycle (Fig. 3). Of these, only the tubulin-binding subdomain had been identified for its most part, using two approaches: by alanine-scanning mutagenesis of the kinesin²⁶ and by structural studies using

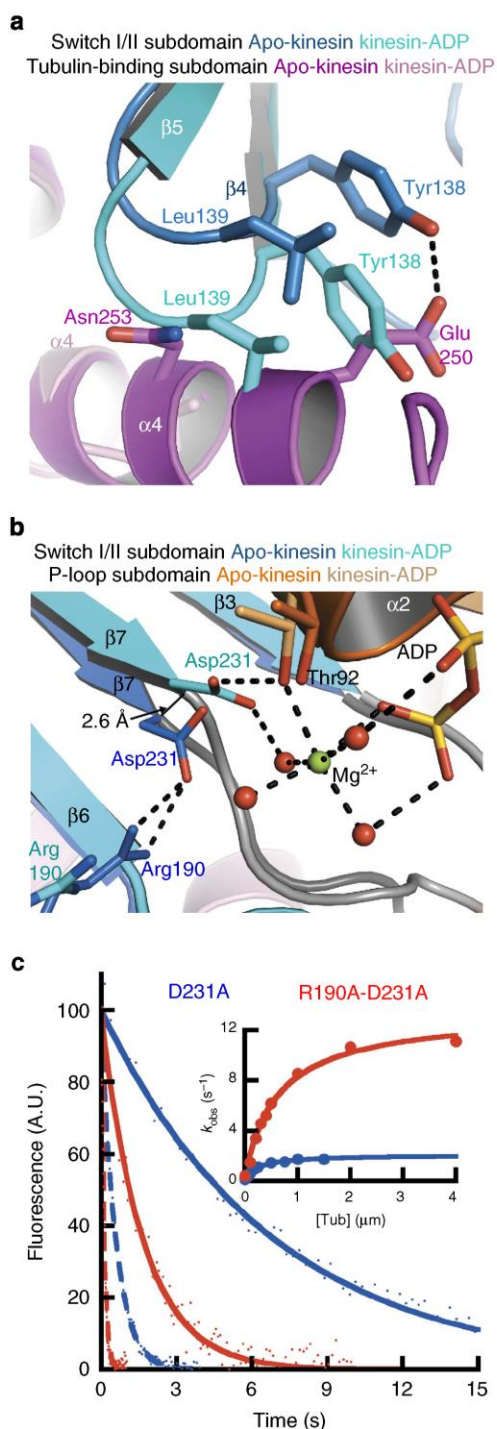


Figure 4 | Changes between detached kinesin-ADP and tubulin-bound apo-kinesin. (a) The $\alpha 4$ extension is not compatible with the structure of the $\beta 4$ - $\beta 5$ turn in kinesin-ADP. Kinesin-ADP⁵ has been superimposed on nucleotide-free kinesin in the tubulin complex by overlapping common $\alpha 4$ residues (residues 255 to 270). Residues of the $\beta 4$ - $\beta 5$ turn that clash with residues in the $\alpha 4$ extension are presented. (b) Changes in the nucleotide-binding site caused, on tubulin binding, by the rotations of the Switch I/II and P-loop subdomains. The P-loop subdomains have been superimposed to show the changes in the interactions of Asp231 with the Mg²⁺-coordinating ligands. For clarity, the Mg²⁺ coordinating water molecules are the only ones presented. (c) Kinetics of mant-ADP release from the D231A and R190A-D231A kinesin mutants. Fluorescence variations on release from the D231A (blue) and R190A-D231A (red) kinesins in the absence of microtubules (solid lines) or stimulated by 1 μ M microtubular tubulin (dashed lines) are shown (10% of the experimental points are displayed) after normalization following subtraction of a linear component due to photobleaching. The line is the fit by an exponential decay function. The inset to **c** gives the variation of k_{obs} as a function of microtubular tubulin concentration for both mutants.

X-rays and cryo-EM, in particular of a fast kinesin-1 from *Neurospora crassa*⁷. The three subdomains scheme differs from that deduced from cryo-EM studies, which depicted changes as rotations of the entire catalytic core of the motor domain, relative to the fixed $\alpha 4$ helix¹⁴. The identification of the subdomains was made possible because of the resolution of the structures we have determined and because of the large differences between tubulin-bound ATP-like¹¹ and apo-kinesin (Fig. 3). The distinction of three motor subdomains is also of interest in the context of the comparison of the kinesin and myosin families of motor proteins. The structural similarity of the kinesin motor domain core to the myosin catalytic domain surrounding the nucleotide was noticed when the first kinesin structure was determined⁵ and suggested a common evolutionary ancestor²⁷. However, whereas a substantial rearrangement of the core β sheet has been seen in nucleotide-free myosins^{28–30}, such a change has long been looked for unsuccessfully in kinesins³¹ and the resulting distortion was observed only recently in the KIF14-ADP structure²¹. Our data demonstrate that the core β sheets in nucleotide-free and kinesin-ATP are distorted in respect to each other (Supplementary Fig. 9a and Supplementary Movie 2). Remarkably, in both myosins and kinesin, the central β sheet is similarly partitioned into two subdomains (the Switch I/II and P-loop blocks in kinesin, which correspond to the upper 50 kDa and to the N-terminal myosin domains, respectively Supplementary Fig. 9b), and distorts when the subdomains change their relative orientation. This further strengthens the parallel between the two families of proteins, highlighting that they interact with the nucleotide through a common mechanism. The distinct insertions between the structural elements of the myosin and kinesin catalytic cores allow them to adapt to their different cycles of interaction with their tracks and to the different relations between their nucleotide and mechanical cycles³¹.

Our results clarify the mechanism for nucleotide release on tubulin binding, a mechanism that had remained elusive so far³². They suggest an important role of the Mg^{2+} ion in the binding of ADP to detached kinesin. Interestingly, Mg^{2+} is an inhibitor of ADP release from detached Kif1a²². The change of Asp231 location in microtubule-bound kinesin is expected to disrupt Mg^{2+} binding and to suppress its inhibitory effect. Indeed, Mg^{2+} has no inhibitory effect on ADP release from microtubule-bound Kif1a²². A mechanism similarly involving the disruption of the Mg^{2+} coordination has been demonstrated for the exchange-factor-mediated dissociation of GDP from the P21^{ras} GTPase^{33,34}. The high-resolution structure we determined also identifies a salt bridge established in nucleotide-free kinesin between Asp231 and Arg190, two residues that are, respectively, fully and highly conserved in kinesins. This salt bridge stabilizes the nucleotide-free structure, compensating at least in part for the interactions made between Asp231 and the nucleotide in kinesin-ADP. As we propose that nucleotide release results from relative movements of the Switch I/II and P-loop motor subdomains, interactions that hinder or alter these movements are predicted to influence ADP release. Such interactions were identified between the motor and the inhibitory tail domains in a kinesin^{35,36}. Taken together with the structure of tubulin-bound apo-kinesin, mutants analysis and inhibition data strongly argue that microtubule-stimulated ADP release is due to a distortion of the nucleotide binding site that, in particular, disrupts the Mg^{2+} coordination. This distortion is caused by microtubule-induced relative movements of the Switch I/II and P-loop subdomains.

The structural changes of tubulin-bound kinesin on ATP binding are also accounted for by our scheme. The direct effect of ATP binding is to bridge the P-loop and the Switch I/II subdomains (Supplementary Fig. 5), following which the orientations of these two blocks change. Therefore, neck-linker

docking is an indirect consequence of ATP binding, as the former only becomes possible following rotation of the P-loop subdomain (Fig. 2d). Indeed, kinetic studies have shown that neck-linker docking follows ATP binding³⁷. We also found that neck-linker docking gates the ATPase activity, because its first residue (Ile325) latches the motor domain in a hydrolysis-efficient conformation. This is also consistent with previous studies, suggesting a direct feedback of neck-linker docking to the catalytic site³⁸. Importantly, the connection between neck-linker docking and ATPase efficiency reduces the probability that in a dimer the microtubule-bound motor hydrolyses ATP before its companion head has been propelled in the direction of the movement. This contributes to the large processivity and thermodynamic efficiency of kinesin.

In summary, our work has enlightened three important aspects of motile kinesins mechanism that concern the three main reactions of their nucleotide cycle: the acceleration of nucleotide release on microtubule binding, the connection between ATP binding and neck-linker docking, and that between neck-linker docking and ATP hydrolysis. Taken together, these results set up a general framework for understanding the mechanism of kinesin-1. Because of the conservation of the sequences as well as of the regions involved in movement generation, the structural scheme, which we described for kinesin-1 mechanism, is likely to apply to other (+) end-directed kinesins.

Methods

Proteins. The monomeric kinesins used in this study (constructs 1–349, 1–325 or 1–324, and the D231A, R190A-D231A and I325G mutants based on the 1–349 construct) were obtained by standard molecular biology techniques from a *cys*-light version of human kinesin, which has been shown to have kinetic properties that are identical to those of kinesin⁴. They were produced in BL21 cells grown in 2YT medium. When A600 reached 0.7–0.8, protein expression was induced with 0.3 mM isopropyl β -D-1-thiogalactopyranoside at 18 °C overnight. Cells were suspended in 10 ml g⁻¹ of wet cells of 50 mM Mes-Na pH 6.0, 1 mM MgCl₂, 0.5 mM EGTA, 10 μ M ATP, 1 mM dithiothreitol (DTT) (Buffer A) to which 1 mM phenylmethylsulfonyl fluoride and protease inhibitors mix (complete EDTA free, Roche Applied Science) were added. Cells were lysed using a French press and cells debris were removed by centrifugation at 20,000g for 20 min at 4 °C. DNase (1 μ g ml⁻¹) was added for 15 min at room temperature, the kinesin-containing solution was centrifuged at 30,000g for 45 min at 4 °C and the supernatant was collected. Purification was performed on a Äkta Purifier system using two ion-exchange chromatography steps. First a Hitrap SP FF column (GE Healthcare) in Buffer A, eluting with a 0–30% Buffer B (Buffer A + 1 M NaCl) gradient. Second a Mono Q (GE Healthcare) column in a buffer containing 50 mM Tris-HCl pH 7.0, 1 mM MgCl₂, 0.5 mM EGTA, 10 μ M ATP, 1 mM DTT and 10% sucrose. The column was eluted with a 10–40% gradient of the Tris buffer to which 1 M NaCl had been added. The protein was then concentrated, quantified according to its optical density at 280 nm and stored in liquid N₂ until use.

Tubulin was purified by two polymerization/depolymerization cycles in a high-molarity buffer³⁹ and stored in liquid N₂ in 50 mM Mes-K pH 6.8, 33% glycerol, 0.25 mM MgCl₂, 0.5 mM EGTA, 0.1 mM GTP until use. Before use, an additional microtubule assembly/disassembly cycle was performed to remove any non-functional protein. The disassembly step was carried out in 15 mM Mes-K pH 6.8, 0.5 mM MgCl₂, 0.5 mM EGTA. Tubulin concentration was determined spectrophotometrically using an extinction coefficient at 278 nm of 1.2 mg⁻¹ ml⁻¹ cm⁻¹ assuming the molecular mass of the heterodimer is 100 kDa⁴⁰. The DARPIn was expressed in XLI1-Blue cells grown in 2YT medium. When A600 reached 0.7–0.8, protein expression was induced with 0.5 mM isopropyl β -D-1-thiogalactopyranoside for 4 h at 37 °C. Cells were suspended in 10 ml g⁻¹ of wet cells of 50 mM Tris, pH 8 (4 °C), 1 mM MgCl₂, 10 mM imidazole, 0.3 mg ml⁻¹ lysozyme and protease inhibitor mix (complete EDTA free, Roche Applied Science). Cells were lysed by sonication and cells debris were removed by centrifugation at 20,000g for 20 min at 4 °C. Purification was performed on a Äkta Purifier system using a Hitrap column (GE Healthcare). Eluted protein was subjected to size-exclusion chromatography on a Superdex 75 column equilibrated with 20 mM potassium phosphate pH 7.2, 1 mM MgCl₂, 0.5 mM EGTA, 100 mM KCl. D1 concentration was estimated by ultraviolet absorption using an extinction coefficient of 6,990 M⁻¹ cm⁻¹ derived from the peptide sequence using the ProtParam webserver (<http://web.expasy.org/protparam>).

To prepare the complex with apo-kinesin, kinesin was incubated with tubulin-DARPIn in a 1:1 ratio, then desalted through a PD10 column (GE healthcare) to remove unbound nucleotide. We checked that this procedure yields nucleotide-free kinesin by separating any remaining ADP from the tubulin nucleotides on a Mono

Q column (GE Healthcare) after trifluoroacetic acid denaturation of the proteins. ADP was then quantified based on comparison of the peak areas with those of an equimolar ADP:GDP:GTP sample of known concentration.

ATPase. The ATPase activities of kinesin were measured at 25 °C by using an enzyme-coupled assay⁴¹ in a buffer consisting of 20 mM Pipes pH 6.8, 1 mM MgCl₂, 0.5 mM EGTA, 1 mM DTT and 1 mM ATP. The enzymes and reagents for the assay (phosphoenolpyruvate, NADH, pyruvate kinase and lactate dehydrogenase) were from Sigma-Aldrich. Varying amounts of docetaxel-stabilized microtubules were added before addition of the kinesin (0.5 μM) and 20 μM docetaxel was supplemented in the buffer to stabilize microtubules. The variations of the stimulated ATPase rate as a function of microtubule concentrations were analysed according to the Michaelis–Menten equation to yield k_{cat} and K_M .

ADP release. As a means to evaluate the ADP release rate, kinesin constructs were loaded with Mant-ADP and the fluorescence decrease associated with dissociation from kinesin was monitored using a SX20 Stopped-Flow Spectrometer at 25 °C. Specifically, kinesin was incubated for 30 min on ice with a threefold excess of Mant-ADP in a buffer consisting of 25 mM Pipes-Na pH 6.8, 2 mM MgCl₂, 1 mM EGTA, 1 mM DTT, following which the kinesin was desalted using a Micro Bio-spin 6 column (BioRad) to remove unbound nucleotide. Next, 0.5 μM kinesin was mixed with an equal volume of buffer supplemented with 1 mM ADP, with or without microtubules, and the fluorescence intensity (excitation at 355 nm) was recorded using a 400 nm long-pass filter. We verified that superimposable time courses were obtained with 2 mM ADP or with 1 mM ATP (as used by others^{42–44}), confirming that the recorded process truly represents the dissociation of Mant-ADP, which kinetically limits the binding of ADP (and of ATP) in all the conditions tested. Data were fitted to determine an observed rate constant of the fluorescence decay, k_{obs} . For microtubule-stimulated Mant-ADP release, the variation of k_{obs} as a function of the tubulin concentration was fitted with a hyperbolic curve to determine the stimulated release kinetic constant k_{off} .

Crystallization and structure determination. The apo-kinesin–tubulin–DARPin complex was crystallized at 293 K by vapour diffusion with a crystallization buffer consisting of 30% (W/V) polyethylene glycol 5000 monomethyl ether, 0.1 M Mes-K pH 6.5 and 0.2 M ammonium sulphate. The crystal was harvested in the same solution supplemented with 20% glycerol, then flash-frozen in liquid nitrogen. A 2.2 Å data set was collected at 100 K at the Proxima1 beam line (Soleil Synchrotron, Saint Aubin, France). It was processed with XDS⁴⁵ and SCALA⁴⁶. The structure was solved by molecular replacement with PHASER⁴⁶ using tubulin–DARPin (pdb id 4DRX) and kinesin–ADP (1BG2) as starting models. The structure was refined with Buster⁴⁷ with iterative model building in Coot⁴⁸. The final model includes 1,331 residues, 99.2% of which are in favoured and allowed regions of the Ramachandran plots, while 0.8% are outliers, as evaluated with MolProbity⁴⁹. Data processing and refinement statistics are summarized in Supplementary Table 1.

Identification of the kinesin subdomains. Kinesin subdomains that are invariant in the nucleotide-free and the ATP-like complexes were identified with the programme RAPIDO⁵⁰ using a ‘low limit’ value of 1.

References

- Svoboda, K., Schmidt, C. F., Schnapp, B. J. & Block, S. M. Direct observation of kinesin stepping by optical trapping interferometry. *Nature* **365**, 721–727 (1993).
- Vale, R. D. & Fletterick, R. J. The design plan of kinesin motors. *Ann. Rev. Cell Dev. Biol.* **13**, 745–777 (1997).
- Coy, D. L., Wagenbach, M. & Howard, J. Kinesin takes one 8-nm step for each ATP that it hydrolyzes. *J. Biol. Chem.* **274**, 3667–3671 (1999).
- Rice, S. *et al.* A structural change in the kinesin motor protein that drives motility. *Nature* **402**, 778–784 (1999).
- Kull, P. J., Sablin, E. P., Lau, R., Fletterick, R. J. & Vale, R. D. Crystal structure of the kinesin motor domain reveals a structural similarity to myosin. *Nature* **380**, 550–555 (1996).
- Sindelar, C. V. *et al.* Two conformations in the human kinesin power stroke defined by X-ray crystallography and EPR spectroscopy. *Nat. Struct. Biol.* **9**, 844–848 (2002).
- Song, Y. H. *et al.* Structure of a fast kinesin: implications for ATPase mechanism and interactions with microtubules. *EMBO J.* **20**, 6213–6225 (2001).
- Marx, A., Hoenger, A. & Mandelkow, E. Structures of kinesin motor proteins. *Cell Motil. Cytoskeleton* **66**, 958–966 (2009).
- Chang, Q., Nitta, R., Inoue, S. & Hirokawa, N. Structural basis for the ATP-induced isomerization of kinesin. *J. Mol. Biol.* **425**, 1869–1880 (2013).
- Parke, C. L., Wojcik, E. J., Kim, S. & WorthyLake, D. K. ATP hydrolysis in Eg5 kinesin involves a catalytic two-water mechanism. *J. Biol. Chem.* **285**, 5859–5867 (2010).
- Gigant, B. *et al.* Structure of a kinesin-tubulin complex and implications for kinesin motility. *Nat. Struct. Mol. Biol.* **20**, 1001–1007 (2013).
- Bodey, A. J., Kikkawa, M. & Moores, C. A. 9-Angstrom structure of a microtubule-bound mitotic motor. *J. Mol. Biol.* **388**, 218–224 (2009).
- Peters, C. *et al.* Insight into the molecular mechanism of the multitasking kinesin-8 motor. *EMBO J.* **29**, 3437–3447 (2010).
- Sindelar, C. V. & Downing, K. H. An atomic-level mechanism for activation of the kinesin molecular motors. *Proc. Natl Acad. Sci. USA* **107**, 4111–4116 (2010).
- Skinotiis, G. *et al.* Nucleotide-induced conformations in the neck region of dimeric kinesin. *EMBO J.* **22**, 1518–1528 (2003).
- Cross, R. A. The kinetic mechanism of kinesin. *Trends Biochem. Sci.* **29**, 301–309 (2004).
- Binz, H. K. *et al.* High-affinity binders selected from designed ankyrin repeat protein libraries. *Nat. Biotechnol.* **22**, 575–582 (2004).
- Pecqueur, L. *et al.* A designed ankyrin repeat protein selected to bind to tubulin caps the microtubule plus end. *Proc. Natl Acad. Sci. USA* **109**, 12011–12016 (2012).
- Crevel, I. M., Lockhart, A. & Cross, R. A. Weak and strong states of kinesin and ncd. *J. Mol. Biol.* **257**, 66–76 (1996).
- Shipley, K. *et al.* Structure of a kinesin microtubule depolymerization machine. *EMBO J.* **23**, 1422–1432 (2004).
- Arora, K. *et al.* KIF14 binds tightly to microtubules and adopts a rigor-like conformation. *J. Mol. Biol.* **426**, 2997–3015 (2014).
- Nitta, R., Okada, Y. & Hirokawa, N. Structural model for strain-dependent microtubule activation of Mg-ADP release from kinesin. *Nat. Struct. Mol. Biol.* **15**, 1067–1075 (2008).
- Case, R. B., Rice, S., Hart, C. L., Ly, B. & Vale, R. D. Role of the kinesin neck linker and catalytic core in microtubule-based motility. *Curr. Biol.* **10**, 157–160 (2000).
- Clancy, B. E., Behnke-Parks, W. M., Andreasson, J. O., Rosenfeld, S. S. & Block, S. M. A universal pathway for kinesin stepping. *Nat. Struct. Mol. Biol.* **18**, 1020–1027 (2011).
- Yun, M., Zhang, X., Park, C. G., Park, H. W. & Endow, S. A. A structural pathway for activation of the kinesin motor ATPase. *EMBO J.* **20**, 2611–2618 (2001).
- Woehlke, G. *et al.* Microtubule interaction site of the kinesin motor. *Cell* **90**, 207–216 (1997).
- Kull, P. J., Vale, R. D. & Fletterick, R. J. The case for a common ancestor: kinesin and myosin motor proteins and G proteins. *J. Muscle Res. Cell Motil.* **19**, 877–886 (1998).
- Coureur, P. D., Sweeney, H. L. & Houdusse, A. Three myosin V structures delineate essential features of chemo-mechanical transduction. *EMBO J.* **23**, 4527–4537 (2004).
- Coureur, P. D. *et al.* A structural state of the myosin V motor without bound nucleotide. *Nature* **425**, 419–423 (2003).
- Reubold, T. F., Eschenburg, S., Becker, A., Kull, P. J. & Manstein, D. J. A structural model for actin-induced nucleotide release in myosin. *Nat. Struct. Mol. Biol.* **10**, 826–830 (2003).
- Kull, P. J. & Endow, S. A. Force generation by kinesin and myosin cytoskeletal motor proteins. *J. Cell Sci.* **126**, 9–19 (2013).
- Sindelar, C. V. A seesaw model for intermolecular gating in the kinesin motor protein. *Biophys. Rev.* **3**, 85–100 (2011).
- Boriack-Sjodin, P. A., Margarit, S. M., Bar-Sagi, D. & Kuriyan, J. The structural basis of the activation of Ras by Sos. *Nature* **394**, 337–343 (1998).
- Mittal, R., Ahmadian, M. R., Goody, R. S. & Wittinghofer, A. Formation of a transition-state analog of the Ras GTPase reaction by Ras-GDP, tetrafluoroaluminate, and GTPase-activating proteins. *Science* **273**, 115–117 (1996).
- Hackney, D. D., Baek, N. & Snyder, A. C. Half-site inhibition of dimeric kinesin head domains by monomeric tail domains. *Biochemistry* **48**, 3448–3456 (2009).
- Kaan, H. Y., Hackney, D. D. & Kozielski, P. The structure of the kinesin-1 motor-tail complex reveals the mechanism of autoinhibition. *Science* **333**, 883–885 (2011).
- Rosenfeld, S. S., Jefferson, G. M. & King, P. H. ATP reorients the neck linker of kinesin in two sequential steps. *J. Biol. Chem.* **276**, 40167–40174 (2001).
- Hahlen, K. *et al.* Feedback of the kinesin-1 neck-linker position on the catalytic site. *J. Biol. Chem.* **281**, 18868–18877 (2006).
- Castoldi, M. & Popov, A. V. Purification of brain tubulin through two cycles of polymerization-depolymerization in a high-molarity buffer. *Protein Expr. Purif.* **32**, 83–88 (2003).
- Correia, J. J., Baty, L. T. & Williams, Jr. R. C. Mg²⁺ dependence of guanine nucleotide binding to tubulin. *J. Biol. Chem.* **262**, 17278–17284 (1987).
- Huang, T. G. & Hackney, D. D. *Drosophila* kinesin minimal motor domain expressed in *Escherichia coli*. Purification and kinetic characterization. *J. Biol. Chem.* **269**, 16493–16501 (1994).
- Cheng, J.-Q., Jiang, W. & Hackney, D. D. Interaction of mant-adenosine nucleotides and magnesium with kinesin. *Biochemistry* **37**, 5288–5295 (1998).

43. Poster, K. A. & Gilbert, S. P. Kinetic studies of dimeric Ncd: evidence that Ncd is not processive. *Biochemistry* **39**, 1784–1791 (2000).
44. Ma, Y. Z. & Taylor, E. W. Kinetic mechanism of kinesin motor domain. *Biochemistry* **34**, 13233–13241 (1995).
45. Kabsch, W. Xds. *Acta Crystallogr. D Biol. Crystallogr.* **66**, 125–132 (2010).
46. Winn, M. D. *et al.* Overview of the CCP4 suite and current developments. *Acta Crystallogr. D Biol. Crystallogr.* **67**, 235–242 (2011).
47. Bricogne, G. *et al.* *BUSTER v. 2.10.0* (Global Phasing Ltd., 2011).
48. Emsley, P., Lohkamp, B., Scott, W. G. & Cowtan, K. Features and development of Coot. *Acta Crystallogr. D Biol. Crystallogr.* **66**, 486–501 (2010).
49. Chen, V. B. *et al.* MolProbity: all-atom structure validation for macromolecular crystallography. *Acta Crystallogr. D Biol. Crystallogr.* **66**, 12–21 (2010).
50. Mosca, R. & Schneider, T. R. RAPIDO: a web server for the alignment of protein structures in the presence of conformational changes. *Nucleic Acids Res.* **36**, W42–W46 (2008).
51. Schrodinger, L. L. C. The PyMOL Molecular Graphics System, Version 1.3r1 (2010).

Acknowledgements

We thank L.A. Amos (L.M.B., Cambridge U.K.) for her comments on the manuscript. We thank I. Mignot for assistance, D. Hamdane and J. Pernier for help with stopped-flow experiments and D. Mauchand (Unité Commune d'Expérimentation Animale, Institut National de la Recherche Agronomique, Jouy en Josas, France) for providing us with the material from which tubulin was purified. We gratefully acknowledge continuous support by A. Plückthun and B. Dreier (U. Zürich, Switzerland) in the selection and use of DARPinS. We also thank the staff at the LEBS/IMAGIF crystallization and biophysics platforms (CNRS, Gif-sur-Yvette, France). Diffraction data were collected at the European Synchrotron Research Facility (ID29) and at SOLEIL synchrotron (PX1 and

PX2 beam lines). We thank the machine and beam line groups for making these experiments possible. W.W. was supported by a Fondation ARC pour la recherche sur le cancer postdoctoral fellowship (PDF 20130606987). We gratefully acknowledge support by the Fondation ARC pour la recherche sur le cancer to B.G., Agence Nationale de la Recherche (grant ANR-12-BSV8-0002-01 to B.G.) and by the Science and Technology Commission of Shanghai Municipality (grant 11JC1413100 to C.W.).

Author contributions

B.G., C.W. and M.K. designed research; L.C. crystallized the tubulin–DARPin–kinesin complex and determined its structure; W.W. characterized all kinesin mutants biochemically; W.W. and Q.J. performed initial characterizations of the kinesin–tubulin interaction; L.C., W.W., B.G., C.W. and M.K. analysed the data; B.G., C.W. and M.K. wrote the manuscript with input from all other authors.

Additional information

Accession codes: Coordinates and structure factors have been deposited with the Protein Data Bank (accession code: 4LNU).

Supplementary Information accompanies this paper at <http://www.nature.com/naturecommunications>

Competing financial interests: The authors declare no competing financial interests.

Reprints and permission information is available online at <http://npg.nature.com/reprintsandpermissions/>

How to cite this article: Cao, L. *et al.* The structure of apo-kinesin bound to tubulin links the nucleotide cycle to movement. *Nat. Commun.* **5**:5364 doi: 10.1038/ncomms6364 (2014).

1.3 Discussion

Kinesin's processivity

When kinesin-1 homodimer moves along microtubules, each head goes through the same mechanochemical cycle (Fig. 5.1A) continuously and alternately. This is the key point for kinesin's processive movement which evinces that a single kinesin homodimer is capable of taking hundreds of steps before dissociation from microtubule. The processivity of kinesin relies on gating mechanisms which include a series of tightly coordinated biochemical and mechanical events (Block 2007).

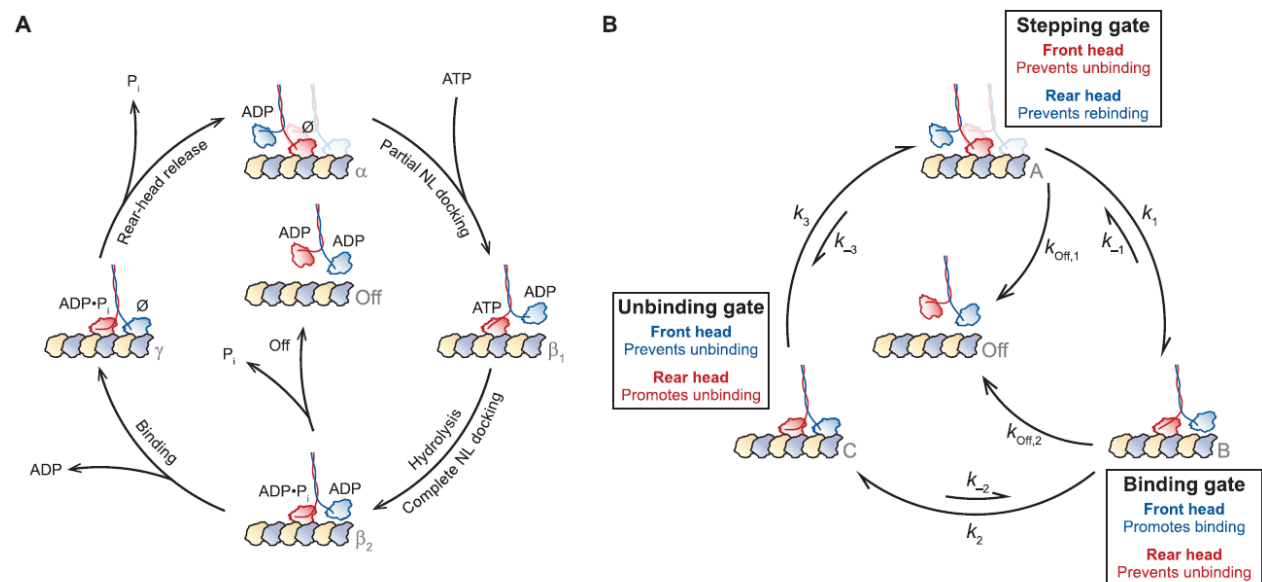


Figure 5.1 A general gating framework of kinesin dimer's mechanical state (Andreasson et al. 2015a).

- A) A summary on kinesin mechanochemical cycle. (α) The front head (red) binds to microtubule and has released its ADP. (β_1) The nucleotide-free (\emptyset) front head attached to microtubule is able to accept ATP. ATP binding leads to the partial docking of neck linker. (β_2) Afterwards ATP hydrolysis completes the neck linker docking and enables the rear head (blue) to bind the forward binding site. (γ) Microtubule binding stimulates the ADP dissociation in the new leading head; meanwhile, in the former leading head, phosphate release and motor domain dissociation happens. The dimer goes back to ATP-waiting state (α), with the former rear head moving about 16 nm forward and taking the leading position.
- B) A general gating framework based on kinesin's mechanochemical cycle. Stepping, binding and unbinding gates are shown. When the front head first binds to microtubule, the stepping gate prevents it from unbinding and promotes the rear head

binding to the forward binding site. When the rear head moves forward, the binding gate favors its binding, while preventing the unbinding of the bound head. When both heads bind microtubule, the unbinding gate promotes the unbinding of the rear head and prevents the unbinding of the leading head.

To simplify the gating mechanism (Fig. 5.1B), there are three principles ensuring the processivity of kinesin movement (Andreasson et al. 2015a):

- 1) If there is only one head bound to microtubule, its dissociation should be prohibited.
- 2) The on-pathway transitions, including attaching towards the forward binding and detaching from the rear binding site, are promoted.
- 3) The off-pathway transitions, including rebinding of the rear head to its rear binding position and dissociation of the head from its leading position, are prohibited.

Tubulin-bound apo-kinesin structure presented here, compared with ADP-kinesin structure and tubulin-bound ATP-like kinesin structure, may provide some structural interpretations to the gating mechanism, including in the one-motor-bound state how the dissociation is prohibited and how the off-pathway transition is avoided.

One-motor-bound state

In the mechanochemical cycle of kinesin dimer, the one-motor-bound state includes “ATP-waiting-state” following the dissociation of ADP bound rear head and “ATP-state” leading the rebinding of the former rear head towards the forward binding site. During this procedure, the microtubule bound head is either in nucleotide-free state or binding ATP. Previous biochemical study has already shown that both apo-kinesin motor ($K_D \approx 0.62 \mu\text{M}$) and ATP-kinesin motor ($K_D \approx 0.27 \mu\text{M}$) are able to bind microtubule tightly (Crevel, Lockhart, and Cross 1996). Analyzing both tubulin-bound apo-kinesin and ATP-analog-kinesin structures, we confirmed an elongated α helix (H4) is responsible for their high affinity with microtubule. H4, located in the tubulin-binding subdomain, in microtubule-unbound ADP kinesin is short and followed by a flexible loop. When kinesin binds tubulin part of the disordered loop becomes rigid leading to the extension of H4. The extended part of H4 interacts with tubulin. The interaction between H4 extended part and tubulin is observed in both ATP analog-kinesin and apo-kinesin, despite of slight differences. In ATP-analog kinesin, the N-terminus of H4 helix is curved, instead of straight, so that N-terminal L11 can connect Switch 1 which is ordered and contacting the γ phosphate of ATP (or ATP analog). The elongation of H4 is also observed in electron microscopy studies (Atherton et al. 2014; Shang et al. 2014).

In physiological conditions, microtubule-bound apo-kinesin binds ATP (and not ADP) because 1) of a lower concentration of ADP compared with that of ATP (Tantama et al.

2013) and 2) of a slightly higher affinity of microtubule-bound apo-kinesin for ATP ($K_D \approx 75 \mu\text{M}$) than for ADP ($K_D \approx 120 \mu\text{M}$) (Cross 2004).

Off-pathway transitions are prohibited

There are two main off-pathway transitions that should be avoided in kinesin cycle.

- 1) When there is one head attached to microtubule, the rebinding of the rear head upon the rear-binding site should be prohibited.
- 2) When both heads bind microtubule, the ATP hydrolysis in the leading head should be prohibited so that the leading head will not detach from the microtubule.

For the first coordination mechanism, it has been shown that the rebinding of the rear head is controlled by the interhead tension caused by the neck linker docking. In kinesin mutants whose neck linker is elongated artificially, the rear head has more chance to rebind to its former binding site (Isojima et al. 2016).

The second coordination mechanism is much more complicated. There are two controversial gating mechanisms. One is the “front-head gating” model in which ATP binding or hydrolysis in the front head is prohibited. The other is the “rear-head gating” model which suggests ATP hydrolysis or MT release in the rear head are accelerated. Furthermore, there are two theories about the gating mechanism that is either tension dependent or orientation dependent. When both heads bind microtubule, the heads are separated by 8.2 nm. The neck linker of the front head points backwards, while that of the rear head points forwards and docks onto the catalytic core. Consequently, intramolecular tension is developed between the heads. Some people proposed the tension “pulls” the rear head, accelerating the dissociation of the rear head, responsible for the “rear-head gating” mechanism. The other interpretation is that the backward orientation of the neck linker in the front head inhibits the ATP binding or ATP hydrolysis in the front head, causing the “front-head gating”.

Recently, more and more results on single-molecule study support the front-head gating mechanism caused by the neck linker backward orientation. Isojima *et al.* found that the dwell time of the two-heads-bound state is independent of the concentration of ATP. It indicates that the two-heads-bound state is not gated by the fast ATP hydrolysis in the rear head. They also found it's rare that the leading motor dissociates from microtubule before the dissociation of the rear head in both wild type kinesin dimer and a mutant where the neck linker is elongated. This result rules out the possibility that the gating mechanism is led by the interhead tension (Isojima et al. 2016). Dogan *et al.* found that a small backward tension, as low as 2pN, is necessary to inhibit the nucleotide binding to a single head, although the tension between two microtubule-bound motor domains is up to 15 pN.

Based on that, they proposed that the gating mechanism is caused by the back ward orientation of the front head's neck linker (Dogan et al. 2015).

My results, indicating that neck-linker docking in the forward head is the necessary condition for ATP hydrolysis, are able to provide a structural interpretation to this theory. For a single microtubule-bound motor domain, there is no space for neck linker to dock in apo-state; while the subdomain rotations induced by ATP binding create a potential hydrophobic site allowing the first residue of neck linker to dock into. The docked, even if partially docked, neck linker, as a pin, stabilizes the structure at a subdomain-rotated state in which ATP hydrolysis is favored. This theory is supported by the facts that if neck linker is truncated or the first residue is mutated, the ATPase hydrolysis efficiency is significantly interfered (see table 1 of the article).

Taking both motor domains into consideration, we find that if the rear head still binds its rear binding site or doesn't move forward enough, the neck linker is always backward oriented, which means the neck linker cannot dock into the front head. The front head will act as the KHC 324 mutant, in which there is no neck linker docking, with very low ATPase activity. As a result, the binding or hydrolysis of ATP in the leading motor domain is prohibited.

Furthermore, the partial docking of the neck linker, promoting the ATP hydrolysis, probably leads neck linker to fully dock into the catalytic core. In this case rebinding of the rear head to its original binding site is prohibited and binding of the rear head to its forward binding site is favored. But more evidence should be provided to support this hypothesis.

Kinesin and myosin

The first determined kinesin structure reveals the topological similarity between kinesin and myosin, despite that these two proteins have a low sequence identity (Kull et al. 1996).

Myosin motor domain in different nucleotide state have been analyzed structurally (Coureux et al. 2003). These results have revealed that myosin can be divided into several subdomains. The rotation of these domains, including N-terminal subdomain, upper and lower 50 kDa subdomains, the converter subdomain, is associated with the nucleotide state, with actin attachment and with the closure of a major cleft between upper and lower 50 kDa subdomains (Fig. 5.2).

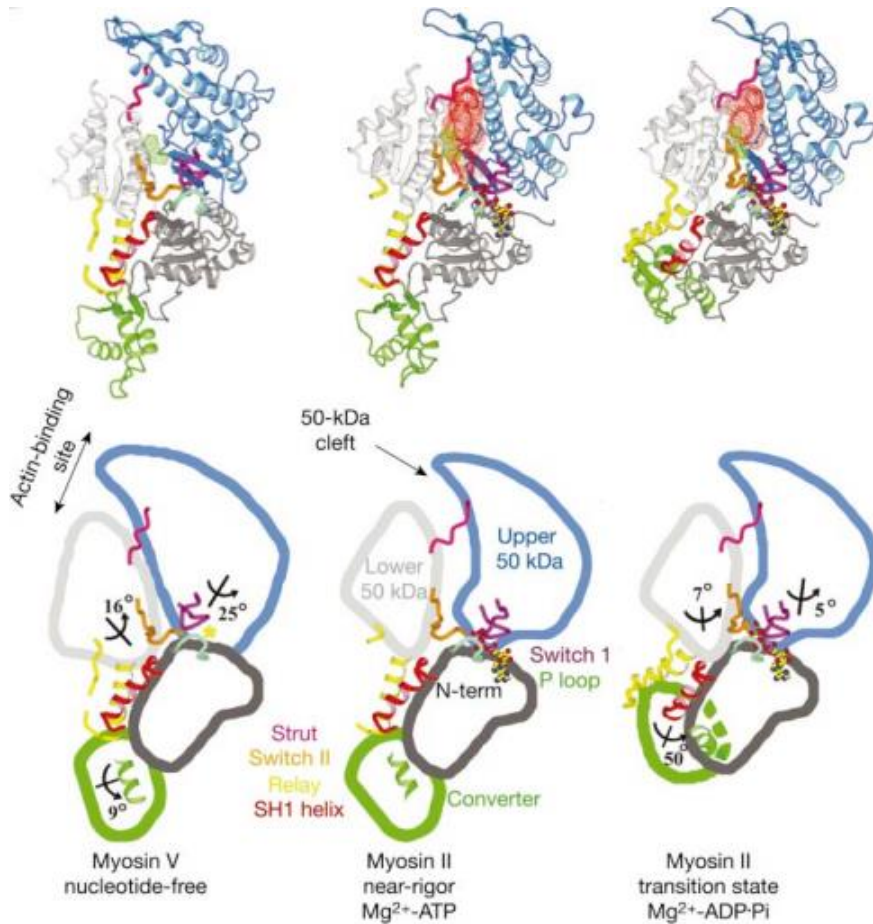


Figure 5.2 Positions of subdomains and connectors in different myosin states (Coureux et al. 2003).

The structures of nucleotide-free myosin V, myosin II in near-rigor and transition state are presented here. The structures have been superimposed on their N-terminal subdomains. The rotation necessary to move from nucleotide-free myosin V to the near-rigor myosin II is marked on the each subdomain of myosin V; the rotation necessary to move from the near-rigor to the transition station in myosin II is indicated on the subdomains of myosin II in transition state.

However, due to lack of the intermediation state structure, the subdomains in kinesin similar to myosin had not been identified until this work. Those subdomains close to nucleotide binding site of kinesin and myosin are compared and presented in figure 5.3. Besides, myosin and kinesin share a similar distortion of the central β sheets along with their nucleotide cycles (Fig. 5.4). These common features confirm the reliability of three-subdomain theory in kinesin, also strengthens that kinesin and myosin share a same ancestor.

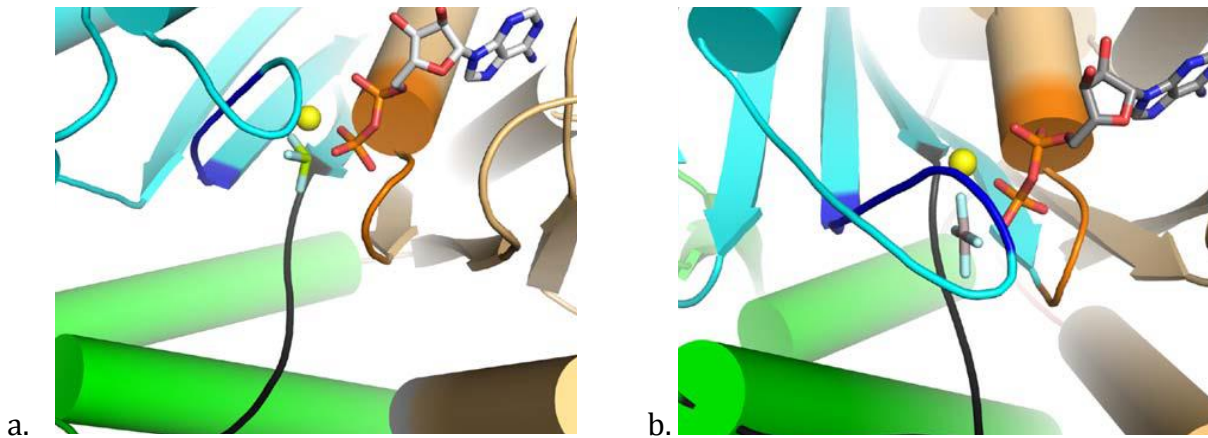


Figure 5.3 Comparison between subdomains in kinesin and in myosin (Wang et al. 2015)

The similarity of subdomains in kinesin (pdb id 4HNA) and myosin (pdb id 1W7J) is presented here, with an ADP-BeFx bound myosin (a) (Cecchini, Houdusse, and Karplus 2008) and an ADP-AlFx bound kinesin (b) (Gigant et al. 2013). The lower 50 subdomain of myosin and tubulin binding subdomain of kinesin are colored in green. Myosin's N-terminal subdomain and kinesin's P-loop subdomain are colored in wheat, with P-loop motifs (orange) highlighted in both structures. The upper 50 subdomain of myosin and Switch 1/2 subdomain of kinesin are shown in cyan with both Switch 1 motifs (blue) highlighted. In both structures, the loop containing Switch 2 motif is shown in grey.

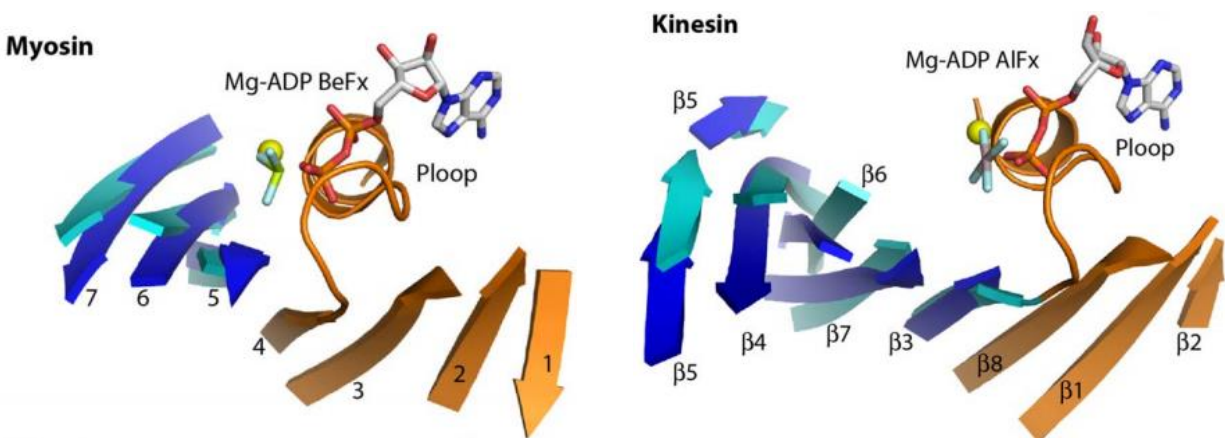


Figure 5.4 Distortion of the central β sheet upon ATP binding in myosin and kinesin. (Wang et al. 2015)

Distortion of the central β -sheets upon ATP-binding in myosin and in kinesin is presented here. For myosin, β strands (sheet 1-4, in orange) of N-terminal subdomains are superimposed, and strands of the upper 50 subdomains are colored in cyan (ATP-like structure, pdb id 1W7J)

(Cecchini, Houdusse, and Karplus 2008)) or in blue (nucleotide-free structures, pdb id 10E9 (Coureux et al. 2003)). For kinesin, strands ($\beta 1$, $\beta 2$ and $\beta 8$, in orange) of P-loop subdomains are superimposed, and strands of Switch 1/2 subdomains are shown in cyan (ATP-like structure, pdb id 4HNA (Gigant et al. 2013), or in blue (nucleotide-free structure, pdb id 4LNU,(Cao et al. 2014)).

Nevertheless, along with these structural and mechanochemical similarities, there are a lot of differences between these two motor proteins. The major one associated with subdomain definition is the binding mode of myosin or kinesin to their track. Kinesin motor binds one tubulin with its tubulin binding subdomain; while myosin attaches to one actin molecule through its upper and lower 50 subdomains, and to another actin of the same filament through its lower 50 subdomain. As a result, myosin and kinesin are able to track actin filaments and microtubules respectively.

Perspectives

Kinesin's processivity

As discussed, kinesin's processivity is a complicated but subtle process involving kinesin's mechanochemical cycle. Each step is controlled spatially and temporally. Our work provides possible structural explanation to kinesin's processivity which matches the theory proposed based on biophysical results. But questions still remain to be answered including how the rear head detachment is favored, how the microtubule binding stimulated ADP dissociation is prevented from the rear head etc. A possible way to generate the answers is to determine ADP-kinesin structure in complex with tubulin heterodimer. Both co-crystallization of ADP-kinesin with tubulin and soaking apo-kinesin-tubulin complex crystals with ADP can be tried.

ADP release mechanism

Although we present the evidence that Switch 1/2 subdomain rotation led by elongation of H4 is involved in high ADP dissociation rate, more study is necessary to reveal the proper microtubule stimulated ADP release mechanism.

The spontaneous ADP dissociation rate of the double mutant R190A D231A ($k_{\text{off}} = 0.6 \text{ s}^{-1}$) is still far lower than the microtubule stimulated ADP release rate of its parent constructs ($k_{\text{off}} = 50 \text{ s}^{-1}$), despite the fact that it's already about 20 times more than the spontaneous ADP dissociation rate of the WT kinesin. Moreover, beside the Switch 1/2 subdomain rotation, there are other parts of kinesin that go through significant structural changes i.e. P-loop subdomain rotates as well. These evidences indicate that there must be other factors involved in the microtubule stimulated ADP dissociation.

Comparing the structure of apo-kinesin in complex with tubulin to that of ADP-kinesin, we can know the structural changes involved in the microtubule and nucleotide binding. Nevertheless, having a kinesin structure with nucleotide without microtubule and another kinesin structure without nucleotide with microtubule, we cannot tell which conformational change is associated with nucleotide release or which is involved in microtubule binding. As a result, mutagenesis studies are necessary to identify more residues involved in this process. As well, more structural studies on apo-kinesin will be helpful to clarify the structural influence caused by the microtubule attachment. This is the objective of the next chapter.

2. Structures of isolated apo-kinesin-1

2.1 Context

Previous biochemical study indicated that ADP dissociation from kinesin is significantly accelerated upon microtubule binding (Cross 2004; Hackney 1988). However the molecular mechanism remains unclear. The structure of apo-kinesin-1 in complex with tubulin which I determined, making up kinesin's mechanochemical cycle, provided important information on the linkage between ATP binding and hydrolysis and kinesin movement, and as well on the ADP release mechanism. Structural analysis indicates that, upon microtubule binding, the binding environment of magnesium in kinesin is disrupted so that ADP release is favored. This hypothesis is further supported by mutagenesis study on kinesin. When R190 and D231, residues stabilizing magnesium indirectly via its water ligand, are mutated to alanine, the mutants have higher spontaneous ADP release compared with WT. In WT kinesin these two residues' interaction with magnesium is interfered by microtubule binding, which contributes to the enhanced ADP dissociation.

However, whereas the comparison between apo-kinesin-1-tubulin complex and ADP-kinesin in the absence of tubulin is very informative, questions on the ADP dissociation mechanism remain. One reason is that the presence or absence of ADP is not the only variable in these two structures. Indeed it is difficult to discriminate which conformational changes are caused by tubulin binding and which are caused by ADP release. Consequently, more study is necessary to characterize further the mechanism of microtubule-stimulated ADP dissociation from kinesin.

As presented in the introduction part, several kinesin mutants are able to release ADP much faster than WT in the absence of microtubule but without obvious structural explanations (Rayment 1996; Higuchi et al. 2004; Heuston et al. 2010). Most of these residues belong to the conserved nucleotide binding motifs, including P-loop motif and Switch 2 motif, of kinesin. Among them, there are two mutants drawing my attention. One is the T92 equivalent mutant. The P-loop residue T92 interacts directly with the Mg^{2+} ion. It also interacts with D231 (from Switch 2). Further analysis on T92-associated mutants may provide supporting evidence to our previous study. The second one is the E236A mutant which has a spontaneous ADP release rate significantly higher than that of WT; meanwhile this switch 2 glutamic acid residue doesn't contact magnesium nor the nucleotide directly (Rice et al. 1999). Instead it interacts with the P-loop, in particular with T87.

In order to gain new information on ADP release from kinesin and on the underlying structural consequences, I have studied the contribution of T92 and the influence of different substitutions of this residue, and also the contribution of T87. These two groups of mutations represent two different ways to generate fast ADP-releasing kinesin.

Moreover, high resolution crystal structures on these mutants in nucleotide-free state were obtained, as well as that of nucleotide-depleted WT kinesin. Interestingly, these apo-kinesins adopt two different conformations. By analyzing these structures, I found that microtubule accelerates ADP dissociation from kinesin by both interfering with magnesium binding and destabilizing the P-loop.

2.2 Paper: “The structural switch of nucleotide-free kinesin.”

The structural switch of nucleotide-free kinesin

Kinesin-1 is a dimeric ATP-dependent motor protein that moves towards microtubules (+)-ends. Whereas structures of ADP-kinesin and of two forms (nucleotide-free and complexed to an ATP analog) of a monomeric construct bound to tubulin have been determined, structures of apo-kinesin-1 in the absence of tubulin are still missing. Therefore, the role of nucleotide release in the structural cycle of kinesin-1 is left unsettled. Here we identified mutations in the kinesin P-loop nucleotide-binding motif that led to kinesin unable to bind ADP (T92V mutant) or releasing nucleotide 100-fold faster than the parental construct (T87A mutant). The structures of these two single amino acid mutants in their apo form were either isomorphous to ADP-kinesin-1 or to tubulin-bound apo-kinesin-1. Remarkably, both structures were also obtained from the nucleotide-depleted wild-type protein. Our results lead to a model in which, detached from microtubules, apo-kinesin alternates between the two conformations we characterized, whereas microtubule binding stabilizes the tubulin-bound apo-kinesin one. This conformation is primed to bind ATP and, therefore, to run through the natural nucleotide cycle of kinesin-1.

Keywords: Intracellular transport/Kinesin/Nucleotide release/P-loop/Structure

Kinesins are a family of microtubule-based motors that play important roles in intracellular transport and cell division. Kinesin-1 transports cargo within cells, a process tightly coupled with ATP hydrolysis (Svoboda et al. 1993; Coy, Wagenbach, and Howard 1999). Single-molecule studies have shown that dimeric kinesin-1 moves in a hand-over-hand manner by alternately translocating its two motor domains (Hackney 1994; Kaseda, Higuchi, and Hirose 2003). Whereas kinesin-1 in solution is mostly loaded with ADP, ADP release is accelerated several thousand-fold upon microtubule binding (Hackney 1988; Cross 2004). ATP binding then triggers a conformational change in the microtubule-bound leading motor domain, following which the rear head is drawn forward in the direction of the (+)-end of the microtubule. The moving head then binds to the microtubule 16 nm ahead from its previous position, whereas the (now) rear head hydrolyzes ATP and eventually detaches from microtubule, achieving a step (Andreasson et al. 2015b; Hancock 2016; Isojima et al. 2016).

X-ray crystallographic studies have defined the structures of an ADP-loaded kinesin-1 motor domain (Kull et al. 1996; Kozielski et al. 1997). Structural changes in the nucleotide-binding site upon binding of a non-hydrolysable ATP analog were then identified in the kinesin-5 Eg5 (Parke et al. 2010a). Most recent X-ray structural studies have shown that a kinesin-1 motor domain comprises 3 subdomains that reorient as a function of the nucleotide content and upon binding to tubulin (Cao et al. 2014; Gigant et al. 2013). Because the three nucleotide-binding motifs (the P-loop, Switch 1 and Switch 2) do not belong to the same subdomain, the nucleotide environment gets remodeled along with the kinesin mechanochemical cycle. The P-loop is embedded in the so-called “P-loop subdomain” that comprises elements of the N-terminal and of the C-terminal parts of the

motor domain. The C-terminal part of Switch 1, together with the first residue of the Switch 2 motif, has been ascribed to the “Switch 1/2 subdomain”, internal in the sequence of the motor domain, whereas most of Switch 2 is N-terminal to the $\alpha 4$ helix, one of the main elements of the “tubulin-binding subdomain” (Cao et al. 2014). These X-ray structural studies have been conducted in parallel with electron microscopy characterizations of what occurs in a motor domain as a function of its nucleotide, culminating in about 6 Å studies of kinesin bound to microtubules that were broadly consistent with the X-ray results, either when conducted on kinesin-1 (Shang et al. 2014; Sindelar and Downing 2010; Atherton et al. 2014) or on a kinesin-3 (Atherton et al. 2014).

One of the points that remained uncertain from these studies is that microtubule binding and nucleotide release were characterized in the same structure and, therefore, it was difficult to ascertain which structural changes were due to each of the two steps of the mechanism. To answer this question, apo-kinesin in the absence of microtubule has to be studied. Mutations have been identified that accelerate nucleotide release by a kinesin from several times (Cao et al. 2014; Higuchi et al. 2004; Heuston et al. 2010; Rice et al. 1999) to several thousand-fold (Rice et al. 1999) but the structural consequences of these mutations on the kinesin apo-form are not known. Here we characterized P-loop mutations in kinesin-1 that interfere with ADP binding and determined the structure of the corresponding mutated nucleotide-free kinesins. Notably, these structures are mostly similar to those of ADP-kinesin or of tubulin-bound nucleotide-free kinesin. Most remarkably these conformations are also adopted by the parental, nucleotide-depleted, wild-type protein. The consequences of these findings will be discussed.

Results

Mutational approach to enhance nucleotide release from kinesin-1.

Mutations in two general areas of kinesin have been found to facilitate nucleotide release. The first ones are in the environment of the Mg^{2+} ion that interacts with the ADP ligand in most kinesins (see, for instance, (Kull et al. 1996)). Indeed, initial studies demonstrated that modulating the Mg^{2+} free concentration changes the ADP release rate in kinesin-1 (Cheng, Jiang, and Hackney 1998) and in kinesin-3 (Nitta, Okada, and Hirokawa 2008). In kinesin-1, the only residue that interacts directly with the Mg^{2+} ion is T92 (Supplementary Fig. 1), the last residue of the P-loop motif. Either a threonine or a serine, this residue is conserved in all nucleotide-binding proteins' P-loop motif (GxxxxGK(S/T)), which is known as Walker A motif and required for coordinating α and β phosphates (Walker et al. 1982). In kinesins, when a serine is found at the last P-loop position, a higher ADP release rate is observed. Such is the case of the kinesin-3 Kif14, where a high ADP release rate was deduced from the spontaneous ATPase rate of the isolated motor domain (0.88 sec^{-1}) (Arora et al. 2014). As expected, when the T92S mutation was introduced in kinesin-1, ADP release was substantially accelerated, about 10-fold from 0.034 s^{-1} in wild-type kinesin to 0.33 s^{-1} in T92S (Table 1). Other mutations that interfere with the kinesin mechanism have been identified at this position in kinesin-1. It has been shown that when this residue is mutated to isoleucine or to asparagine, the corresponding kinesin binds to microtubules without dissociating, even in the presence of a large concentration of ATP (Nakata and Hirokawa 1995; Crevel et al. 2004). We also found that when T92 is mutated to a valine, the fluorescence of the kinesin does not increase upon incubation with mant-ADP, suggesting

that this kinesin mutant had lost its ability to bind ADP. To confirm this, we quantified the nucleotide content of the same amount of mutant and wild-type kinesin on an ion exchange column. We found indeed that the T92V kinesin has essentially lost its ability to bind ADP (Fig. 1A).

An initial indication that residues on the other side of ADP as compared to Mg^{2+} are important for ADP binding came from the study of the kinesin E236A mutant, which releases ADP about 100-fold faster than wild-type kinesin (Rice et al. 1999), a result we were able to confirm (Fig. 1B, Table 1). In ADP-kinesin-1, E236 forms two hydrogen bonds with T87 in the P-loop motif, one with the main chain and the other one with the side-chain (Supplementary Fig. 1), whereas these interactions do not exist in tubulin-bound apo-kinesin (Cao et al. 2014). Kinetic studies show that the kinesin conserved T87 residue is important for ADP binding, though it does not interact directly with the nucleotide: the T87S mutant releases ADP 10 times faster than wild-type (Fig. 1B, Table 1), similar to the equivalent mutation in drosophila kinesin-1 (Higuchi et al. 2004) and in kinesin-14 (Heuston et al. 2010). More importantly, when more mutations of residue 87 were tested, the T87A and T87G mutants were found to release ADP much faster than wild-type ($k_{off} = 2.77 \text{ s}^{-1}$ and 4.80 s^{-1} , respectively) (Fig. 1B, Table 1).

To gain further understanding of the effect of nucleotide release on the kinesin, we have determined the nucleotide-free structures of the two single amino acid mutants of kinesin-1, T87A and T92V. Remarkably, we were also able to remove the nucleotide from wild-type kinesin and to crystallize it in the same buffer conditions as the two previous mutants. The corresponding structures will now be presented.

Apo-kinesins in an ADP-kinesin like conformation.

We first determined the 2.0 Å resolution structure of apo-T92V in a P2₁ space group crystal form (Supplementary Table 1). There were two similar molecules in the asymmetric unit, with a root mean square deviation (r.m.s.d.) after superposition of 0.47 Å (305 C α s compared). The overall conformation of the protein is like that of ADP-kinesin-1 (r.m.s.d. = 0.72 Å over 300 C α s compared to the 1BG2 pdb data set (Kull et al. 1996), averaged value for the two molecules of the T92V asymmetric unit) (Fig. 2A) and much more different from the conformation of tubulin-bound apo-kinesin-1 (r.m.s.d. = 1.37 Å over 296 C α s compared to kinesin in the 4LNU pdb data set (Cao et al. 2014)) (Supplementary Fig. 2). Compared to ADP-kinesin-1, the three nucleotide binding motifs are conserved, as expected from the small deviation between the two structures: the Switch 1 and P-loop motifs superimpose very well, whereas a part of the L11 loop, where the Switch 2 motif is embedded is disordered in both structures (Fig. 2A). However, in apo-T92V, helix α 4, which is C-terminal to L11, is longer than that of ADP-kinesin-1 (pdb id 1BG2). Whereas in ADP-kinesin-1, the N-terminal part of α 4 is disordered up to residue K256, in apo-T92V, residues are ordered since D249 resulting in a two helix turns longer α 4 (Fig. 2A). In this case, the elongation of α 4 is likely to be due to a crystal contact. α 4 is nevertheless shorter than in tubulin-bound kinesin-1, whatever the nucleotide state, where it starts at position 246 (Cao et al. 2014; Gigant et al. 2013). Finally, whereas T92 interacts with D231 in wild-type ADP-kinesin-1 (Kull et al. 1996) (Supplementary Fig. 1), this hydrogen bond is not formed in the T92V mutant, as expected (Fig. 2B).

The main difference between T92V and wild-type ADP-kinesin is the missing nucleotide and magnesium ion in the T92V nucleotide binding cleft. Instead of the nucleotide, an electron density, well accounted for by a sulfate ion that likely comes from the crystallizing solution, is located close to the missing ADP β phosphate (Fig. 2C). Therefore, we conclude from these observations that the T92V mutation is sufficient to interfere with Mg^{2+} binding to the kinesin and, consequently, with ADP binding. This interference does not require an overall rearrangement of the structure of the kinesin motor domain. These results agree with an ADP release rate limited by that of Mg^{2+} (Cheng, Jiang, and Hackney 1998).

We were also able to crystallize in the same buffer conditions the nucleotide-free parental kinesin-1 (without the T92V mutation), following nucleotide digestion with apyrase, and to determine its structure (Supplementary Table 1, Supplementary Fig. 3). Remarkably this structure is isomorphous to that of ADP-kinesin (Kull et al. 1996). Therefore an ADP-kinesin like conformation can be adopted both by nucleotide-free wild-type kinesin and by the T92V mutant.

Isolated apo-kinesins in a tubulin-bound apo-kinesin-1 conformation.

Apo-T87A kinesin-1 was crystallized in a new crystal form following nucleotide digestion with apyrase and gel filtration to remove any trace of nucleotide. The crystals diffracted to 2.6 Å (Supplementary Table 1) and there were six identical molecules in the asymmetric unit (r.m.s.d. of C α s in pairs of molecules varies between 0.3 Å and 0.55 Å). Using these T87A crystals as seeds (see methods), we were also able to crystallize wild-type apo-kinesin-1, prepared as above by digestion of the nucleotide with apyrase followed by gel filtration, and the T92V mutant and to determine their structures (Supplementary Table 1,

Supplementary Fig. 3). Whereas most of the following analysis was performed taking the apo-T87A structure as a reference, identical conclusions could be reached from these wild-type apo-kinesin and T92V isomorphous structures.

The r.m.s.d. of C α s of the apo-T87A kinesin-1 compared to ADP-kinesin-1 (pdb id 1BG2) varies between 1.2 Å and 1.5 Å. By contrast, the conformation of apo-T87A is much more similar to that of apo wild-type kinesin-1 bound to tubulin (pdb id 4LNU), the r.m.s.d. of C α s being close to 0.8 Å whatever the apo-T87A molecule considered. Consistently, the secondary structure elements of both proteins superimpose very well (Fig. 3A) and very similar subdomain rearrangements are seen in both proteins as compared, for instance, to ADP-kinesin (Supplementary Fig. 2). The conformations of the three nucleotide-binding motifs are consistent with this scheme. In particular, the structure of the P-loop motif, which is part of the P-loop subdomain, does not change significantly between ADP-kinesin and apo-T87A or upon binding of kinesin-1 to tubulin. The structures of the Switch 1 and Switch 2 motifs, the N-terminal part of the former and the C-terminal part of the later not belonging to any of the subdomains (Cao et al. 2014), may differ in the kinesin-1 structures that have been determined. This is the case of a small portion of the L11 loop, a loop that comprises the Switch 2 motif, which is disordered in apo-T87A whereas interactions with tubulin stabilize it in the complex of apo-kinesin-1 with tubulin (Fig. 3B). By contrast, the tip of the L9 loop (the loop to which Switch 1 belongs to) is disordered both in T87A and in the initially determined apo-kinesin-1 structure (Cao et al. 2014).

There are two main additional differences between the structures of apo-T87A and that of apo-kinesin-1 bound to tubulin. The first one concerns residue E236, the last residue of the

Switch 2 motif, and its environment. As already mentioned, in ADP-kinesin-1 (and in apo-kinesin-1 in an ADP-kinesin like conformation, see Fig. 2B), this residue establishes two hydrogen bonds with T87. In apo-kinesin-1 bound to tubulin, the structure of L11, where this residue is embedded, changes and E236 interacts with residue R203, in the Switch 1 motif. But in apo-T87A, the structure of L11 has changed again (see above). As a consequence, the R203-E236 interaction is lost and the E236 side-chain is disordered and not visible beyond the C β (Fig. 3C). Since it is disordered in isolated T87A apo-kinesin-1, E236 does not make any visible interaction with the P-loop and with residue 87 in particular. It is therefore not surprising that the P-loop temperature factors become higher than those of the kinesin central β -sheet, taken as a reference, in apo-T87A (average temperature factor of the P-loop C α s is 47 Å², over the six molecules in the asymmetric unit, to be compared to an average temperature factor of 35 Å² for the central β -sheet C α s), whereas these temperature factors of the P-loop are much closer to that of the central β -sheet both in ADP-kinesin (Kull et al. 1996) and in apo-kinesin in an ADP-like conformation (this work) (Supplementary Table 2). Because in this last case kinesins are nucleotide-free, our temperature factors comparison rules out the possibility that the P-loop is mainly stabilized by ADP binding. The second difference between the structures of apo-T87A kinesin and that of apo-kinesin bound to tubulin concerns the N-terminal end of α 4. In a complex with tubulin, this part of the kinesin is close to the tubulin α subunit, with which residues at the C-terminal end of L11 (such as E244 and G242, Fig. 3B), i.e. close to α 4, interact. But in the structure of isolated apo-T87A kinesin-1, such an interaction is not made and, probably as a consequence, the temperature factors of residues in the first two turns of α 4 (residues 246 to 253) are significantly higher than those of residues in the rest

of the helix: the temperature factors of their C α s are larger than 70 Å² on average, whereas they are about 32 Å² in the rest of the helix. Such a difference of temperature factors is not observed among α 4 residues in tubulin-bound apo-kinesin-1 (average C α temperature factor for the C-terminal part of the helix is 44 Å² whereas that of the first two turns is 53 Å²).

The structure of isolated apo-kinesins similar to that of apo-kinesin-1 in its complex with tubulin provides an additional opportunity to probe the changes that occur when ADP-kinesin binds to tubulin (or microtubules). In particular, residue Q86 that interacts with residue N308 in the ADP-kinesin conformation, points towards the carbonyl of S235 when the tubulin-bound apo-kinesin like conformation is adopted (Fig. 3D). Mutating the Q86 residue to an alanine would clearly destabilize the interaction of this residue with N308 in ADP-kinesin, favoring ADP release, as witnessed by an increase of this reaction rate (from 0.034 s⁻¹ to 0.14 s⁻¹). This effect is further confirmed by the observation that the rate of ADP release by the double mutant Q86A-T87A is higher than that of the T87A point mutant (3.5 s⁻¹ vs. 2.77 s⁻¹, Table 1).

Apart from the T92V substitution, which leads to a kinesin unable to bind nucleotides, the rates of ADP release by all the mutants tested so far remain much lower than the rate of microtubule-stimulated ATP hydrolysis by kinesin-1 ($k_{\text{cat}}=50$ s⁻¹, see (Gigant et al. 2013)). These mutants involve in particular mutations at two positions in the P-loop, 87 and 92, as described above. Since most of ADP is embedded in the P-loop subdomain and interacts with the P-loop, it is not surprising that interactions of that loop with the rest of the motor domain that are lost in the tubulin-bound apo-kinesin-1 conformation are important for

ADP binding. As a consequence, ADP release is accelerated when they are prevented. This is in particular the case of the interactions of T87 and T92 (in the P-loop) with E236 and D231, respectively (Fig. 2B, Supplementary Fig. 1). Interestingly, a substantially higher rate of ADP release was reached by the T87A-T92S kinesin double mutant ($k_{\text{off}}=19 \text{ s}^{-1}$) compared to the single mutants (Fig. 1, Table 1).

Discussion

ADP release from kinesin is a slow process that is accelerated upon microtubule binding. Here we have studied the effect of several mutations on spontaneous ADP release and determined the structures of two point mutants and of wild-type kinesin-1 in the apo form. Our results point to two features of ADP binding. The first one is the importance of Mg^{2+} stabilization. In particular, mutating the Mg^{2+} interacting residue T92 to a valine leads to an intrinsically nucleotide-free kinesin (Fig. 1A) without the need of an overall structural change towards the tubulin-bound apo-kinesin conformation (Fig. 2A). An intermediate effect is observed with the T92S mutation. When this mutation is introduced in kinesin-1, ADP release is accelerated 10 times (Table 1) to reach a rate similar to those of kinesin-3s, as deduced from the spontaneous ATP hydrolysis rate of these kinesins (Arora et al. 2014; Nitta, Okada, and Hirokawa 2008). Additionally, the mutation to an alanine of residue 231, which interacts with T92, also accelerates ADP release substantially (Cao et al. 2014). These results are consistent with a spontaneous dissociation of ADP from wild-type kinesin that is limited by that of Mg^{2+} (Cheng, Jiang, and Hackney 1998). The second feature is the importance of P-loop stabilization for ADP binding. Although the most obvious direct

interactions of ADP with the P-loop are with the side chain of K91 and with the peptidic nitrogens of residues 88 and 90 to 93 (Supplementary Fig. 1) (Kull et al. 1996), mutations of T87 to alanine or glycine have among the strongest effects measured so far on ADP release; the effect of the destabilization of the interactions of Q86 (through a mutation of this residue to an alanine) is intermediate (Table 1). P-loop destabilization, together with the removal of the nucleotide, leads to a tubulin-bound apo-kinesin like conformation, as seen in the structure of the T87A kinesin (Fig. 3A).

It is remarkable that both crystal forms of apo-kinesin characterized here were also obtained from wild-type kinesin, following removal of the nucleotide, using crystallization conditions similar to those for the T92V and T87A mutants. In a natural context, the release of ADP from kinesin upon microtubule binding proceeds in two steps, a transition from weak to strong microtubule binding followed by ADP release (Cross 2004; Ma and Taylor 1997). The corresponding structural changes lead both to the destabilization of the P-loop and of Mg^{2+} binding, hence ADP release is favored (Cao et al. 2014; Shang et al. 2014). Interestingly, a double mutant (T87A-T92S) of kinesin, in which Mg^{2+} binding and the P-loop are destabilized, releases ADP spontaneously at a rate similar to that of tubulin-stimulated ATP hydrolysis by the kinesin (Gigant et al. 2013).

Whereas our results demonstrate that, in the absence of microtubules, apo-kinesin-1 may adopt two conformations (ADP-kinesin like and tubulin-bound apo-kinesin like), the effect of tubulin binding is to shift the balance between them and to stabilize the tubulin-bound apo-kinesin conformation, which is primed to bind ATP. The wild-type sequence also ensures that kinesin-1's interaction with microtubules is modulated by the bound

nucleotide. During processive movement, multiple cycles are performed, where this nucleotide gets hydrolyzed then replaced by ATP, as required.

Methods

Constructs and protein purification

The constructs and mutants used in this study were obtained by standard molecular biology from a monomeric cys-light version of human kinesin-1 (Rice et al. 1999). These constructs comprise the motor domain and the neck linker (construct 1-149, used for kinetic experiments) or the motor domain catalytic core only (construct 1-325, used for crystallization). Proteins were produced in BL21 *Escherichia coli* cells grown in 2YT medium. The expression was induced with 0.3 mM isopropyl β -D-1-thiogalactopyranoside at 18 °C overnight, after the absorbance at 600 nm of the culture reached 0.7 to 0.8. Cells were harvested and suspended in buffer A (25 mM Pipes pH 6.8, 1 mM MgCl₂, 0.5 mM EGTA, 25 μ M ATP, 1 mM DTT) plus 1 mM phenylmethylsulfonyl fluoride and protease inhibitors mix (complete EDTA free, Roche Applied Science). Two ion exchange columns were used for purification, a Hitrap SP FF column (GE Healthcare), using 20% buffer B (buffer A + 1 M NaCl) for the elution, then a Mono Q column (GE Healthcare) with a 10 to 40% buffer B gradient for elution.

To generate nucleotide-free kinesin-1 (wild-type and T87A mutant), the proteins were treated with apyrase (Sigma, 0.5 U/ml) at 4 °C overnight. For crystallization, an additional gel filtration column (Superdex 200 10/300 GL, GE Healthcare) in a buffer consisting of 16 mM Pipes pH 6.8, 0.5 mM MgCl₂, 0.2 mM EGTA, 100 mM NaCl was performed. The protein

was then concentrated, quantified using the absorbance value at 280 nm and stored in liquid nitrogen until use.

Crystallization and structure determination

Crystallizations were performed at 293 K by vapor diffusion using the hanging drop method. T92V and nucleotide-depleted wild-type kinesin were crystallized in the ADP-kinesin like form in a buffer consisting of 0.1 M Na-acetate pH 4.5 to 5.5, 20 to 25% (W/V) polyethylene glycol 4000, 0.2 M $(\text{NH}_4)_2\text{SO}_4$ and 0.1 mM SrCl_2 . Apo-T87A was crystallized in a tubulin-bound apo-kinesin like conformation in a buffer containing 50 mM Mes pH 6.5, 0.16 to 0.2 M $(\text{NH}_4)_2\text{SO}_4$ and 30% (W/V) polyethylene glycol 5000 monomethyl ether. T92V and wild-type apo-kinesin-1 were also crystallized in these same conditions following streak seeding using T87A crystals as seeds. Crystals were harvested in the crystallization buffer supplemented with 20% glycerol, then flash-cooled in liquid nitrogen until data collection.

Data sets were collected at 100 K at the Proxima1 and Proxima 2 beam lines (Soleil Synchrotron, Saint Aubin, France). The data were processed with XDS (Kabsch 2010) and Aimless (Winn et al. 2011). The structures were solved by molecular replacement with PHASER (McCoy et al. 2007) using either ADP-kinesin (pdb id 1BG2 (Kull et al. 1996)) or tubulin-bound apo-kinesin (pdb id 4LNU (Cao et al. 2014)) as starting models. The structures were iteratively refined with Buster (Bricogne et al. 2011) with model building in Coot (Emsley et al. 2010). Some refinement cycles were also performed using Phenix (Adams et al. 2010). Data collection and refinement statistics are reported in

Supplementary Table 1. Figures of structural models were generated with PyMOL (DeLano 2010).

Nucleotide content analysis

T92V (60 μ l at about 350 μ M) and wild-type (100 μ l at about 200 μ M) kinesins were denatured with 1 μ l Trifluoroacetic acid. After removal of the denatured protein by centrifugation, the pH of the supernatant containing released nucleotide was neutralized and the supernatant was loaded on a Mono Q column (GE Healthcare) equilibrated with 20 mM Tris-HCl pH 8.0. The nucleotide was eluted using a NaCl gradient. ADP and ATP solutions were injected as references to calibrate the column.

Mant-ADP release rate measurement

As a means to evaluate the ADP release rate (Cheng, Jiang, and Hackney 1998), kinesin constructs were loaded with mant-ADP and the fluorescence decrease associated with mant-ADP dissociation from kinesin was monitored using a SX20 stopped-flow spectrometer (Applied Photophysics) at 25°C. Specifically, kinesin was first desalted using a Micro Bio-spin 6 column (BioRad) equilibrated with 25 mM Pipes pH 6.8, 2 mM MgCl₂, 1 mM EGTA and 1 mM DTT to remove excess nucleotide. Then kinesin was incubated with a fourfold excess of mant-ADP on ice for about one hour. In the case of the mutants, because the release of ADP could be very fast, the excess mant-ADP was not removed and 0.5 μ M kinesin was mixed with an equal volume of a 1 mM ADP-containing buffer in the stopped-flow cell, resulting in an ADP:mant-ADP ratio of 500:1. The fluorescence intensity (excitation at 355 nm) was recorded using a 400 nm long-pass filter. The experimental data were fitted to an exponential decay to yield the dissociation rate constant k_{off} .

References

1. Svoboda K, Schmidt CF, Schnapp BJ, Block SM (1993) Direct observation of kinesin stepping by optical trapping interferometry. *Nature* **365**: 721-727
2. Coy DL, Wagenbach M, Howard J (1999) Kinesin takes one 8-nm step for each ATP that it hydrolyzes. *J Biol Chem* **274**: 3667-3671
3. Hackney DD (1994) Evidence for alternating head catalysis by kinesin during microtubule-stimulated ATP hydrolysis. *Proc Natl Acad Sci U S A* **91**: 6865-6869
4. Kaseda K, Higuchi H, Hirose K (2003) Alternate fast and slow stepping of a heterodimeric kinesin molecule. *Nat Cell Biol* **5**: 1079-1082
5. Hackney DD (1988) Kinesin ATPase: rate-limiting ADP release. *Proc Natl Acad Sci U S A* **85**: 6314-6318
6. Cross RA (2004) The kinetic mechanism of kinesin. *Trends Biochem Sci* **29**: 301-309
7. Andreasson JO, Milic B, Chen GY, Guydosh NR, Hancock WO, Block SM (2015) Examining kinesin processivity within a general gating framework. *Elife* **4**: e07403
8. Hancock WO (2016) The Kinesin-1 chemomechanical cycle: stepping toward a consensus. *Biophys J* **110**: 1216-1225
9. Isojima H, Iino R, Niitani Y, Noji H, Tomishige M (2016) Direct observation of intermediate states during the stepping motion of kinesin-1. *Nat Chem Biol* **12**: 290-297
10. Kull FJ, Sablin EP, Lau R, Fletterick RJ, Vale RD (1996) Crystal structure of the kinesin motor domain reveals a structural similarity to myosin. *Nature* **380**: 550-555
11. Kozielski F, Sack S, Marx A, Thormahlen M, Schonbrunn E, Biou V, Thompson A, Mandelkow EM, Mandelkow E (1997) The crystal structure of dimeric kinesin and implications for microtubule-dependent motility. *Cell* **91**: 985-994
12. Parke CL, Wojcik EJ, Kim S, Worthylake DK (2010) ATP hydrolysis in Eg5 kinesin involves a catalytic two-water mechanism. *J. Biol. Chem.* **285**: 5859-5867
13. Cao L, Wang W, Jiang Q, Wang C, Knossow M, Gigant B (2014) The structure of apo-kinesin bound to tubulin links the nucleotide cycle to movement. *Nat Commun* **5**: 5364
14. Gigant B, Wang W, Dreier B, Jiang Q, Pecqueur L, Pluckthun A, Wang C, Knossow M (2013) Structure of a kinesin-tubulin complex and implications for kinesin motility. *Nat Struct Mol Biol* **20**: 1001-1007
15. Shang Z, Zhou K, Xu C, Csencsits R, Cochran JC, Sindelar CV (2014) High-resolution structures of kinesin on microtubules provide a basis for nucleotide-gated force-generation. *Elife* **3**: e04686

16. Sindelar CV, Downing KH (2010) An atomic-level mechanism for activation of the kinesin molecular motors. *Proc Natl Acad Sci U S A* **107**: 4111-4116
17. Atherton J, Farabella I, Yu IM, Rosenfeld SS, Houdusse A, Topf M, Moores CA (2014) Conserved mechanisms of microtubule-stimulated ADP release, ATP binding, and force generation in transport kinesins. *Elife* **3**: e03680
18. Higuchi H, Bronner CE, Park HW, Endow SA (2004) Rapid double 8-nm steps by a kinesin mutant. *EMBO J* **23**: 2993-2999
19. Heuston E, Bronner CE, Kull FJ, Endow SA (2010) A kinesin motor in a force-producing conformation. *BMC Struct Biol* **10**: 19
20. Rice S, Lin AW, Safer D, Hart CL, Naber N, Carragher BO, Cain SM, Pechatnikova E, Wilson-Kubalek EM, Whittaker M, *et al.* (1999) A structural change in the kinesin motor protein that drives motility. *Nature* **402**: 778-784
21. Cheng J-Q, Jiang W, Hackney DD (1998) Interaction of mant-adenosine nucleotides and magnesium with kinesin. *Biochemistry* **37**: 5288-5295
22. Nitta R, Okada Y, Hirokawa N (2008) Structural model for strain-dependent microtubule activation of Mg-ADP release from kinesin. *Nat Struct Mol Biol* **15**: 1067-1075
23. Walker JE, Saraste M, Runswick MJ, Gay NJ (1982) Distantly related sequences in the α - and β -subunits of ATP synthase, myosin, kinases and other ATP-requiring enzymes and a common nucleotide binding fold. *EMBO J* **1**: 945-951
24. Arora K, Talje L, Asenjo AB, Andersen P, Atchia K, Joshi M, Sosa H, Allingham JS, Kwok BH (2014) KIF14 binds tightly to microtubules and adopts a rigor-like conformation. *J Mol Biol* **426**: 2997-3015
25. Nakata T, Hirokawa N (1995) Point mutation of adenosine triphosphate-binding motif generated rigor kinesin that selectively blocks anterograde lysosome membrane transport. *J Cell Biol* **131**: 1039-1053
26. Crevel IM, Nyitrai M, Alonso MC, Weiss S, Geeves MA, Cross RA (2004) What kinesin does at roadblocks: the coordination mechanism for molecular walking. *EMBO J* **23**: 23-32
27. Ma YZ, Taylor EW (1997) Kinetic mechanism of a monomeric kinesin construct. *J Biol Chem* **272**: 717-723
28. Kabsch W (2010) Xds. *Acta Crystallogr D Biol Crystallogr* **66**: 125-132
29. Winn MD, Ballard CC, Cowtan KD, Dodson EJ, Emsley P, Evans PR, Keegan RM, Krissinel EB, Leslie AG, McCoy A, *et al.* (2011) Overview of the CCP4 suite and current developments. *Acta Crystallogr D Biol Crystallogr* **67**: 235-242
30. McCoy AJ, Grosse-Kunstleve RW, Adams PD, Winn MD, Storoni LC, Read RJ (2007) Phaser crystallographic software. *J Appl Crystallogr* **40**: 658-674

31. Bricogne G, Blanc E, Brandl M, Flensburg C, Keller P, Paciorek W, Roversi P, Sharff A, Smart OS, Vonrhein C, *et al.* (2011) BUSTER version 2.10.0 Cambridge, United Kingdom: Global Phasing Ltd.,
32. Emsley P, Lohkamp B, Scott WG, Cowtan K (2010) Features and development of Coot. *Acta Crystallogr D Biol Crystallogr* **66**: 486-501
33. Adams PD, Afonine PV, Bunkoczi G, Chen VB, Davis IW, Echols N, Headd JJ, Hung LW, Kapral GJ, Grosse-Kunstleve RW, *et al.* (2010) PHENIX: a comprehensive Python-based system for macromolecular structure solution. *Acta Crystallogr D Biol Crystallogr* **66**: 213-221
34. DeLano WL (2010) The PyMOL Molecular Graphics System.

Table 1. Mant-ADP release rate from kinesins, estimated by fluorescence spectroscopy ^(a).

Construct	Wild-type	Q86A	T87S	T87A	T87G	Q86A T87A	T92S	T87A T92S	E236A
k_{off} (s⁻¹)	0.034	0.14	0.32	2.77	4.8	3.5	0.33	19	1.43
	±0.001	±0.001	±0.002	±0.037	±0.13	±0.065	±0.005	±0.97	±0.017

^(a) Kinetic parameters are given as value ±s.e. (calculated from the fit).

Figure legends.

Figure 1. The interference of kinesin-1 mutations with ADP binding and release. **(A)** The T92V mutant does not bind ADP. The nucleotide content of equivalent amounts of T92V and wild-type kinesin-1 was analyzed by ion exchange chromatography. Whereas in the case of wild-type kinesin-1 a chromatographic peak is eluted at the expected position for ADP, in the case of the T92V mutant, the peak at this position is hardly detected and no other peaks are detected. mAU, milliabsorbance units. **(B)** Dissociation of mant-ADP from kinesin-1 or from several point mutants and a double mutant, as indicated. The curves are the fit of the experimental data points

with a monoexponential decay function which accounts for the fluorescence decrease corresponding to the dissociation of mant-ADP from kinesin and yields the rate constant for ADP release (Table 1). The fit in the case of the wild-type protein, which releases ADP much more slowly, is presented in Supplementary Fig. 4. a.u., arbitrary units.

Figure 2. ADP-kinesin like structure of nucleotide-free kinesin-1. **(A)** Superposition of ADP-kinesin-1 (pdb id 1BG2, blue, with the side chain of residues T87 and T92 highlighted in darker blue) (Kull et al. 1996) and of the T92V mutant (pink, P2₁ crystal form), indicating that both motor domains share the same overall conformation. In both ADP-kinesin-1 and apo T92V, Loop 11 (L11), in which the third conserved nucleotide-binding motif, Switch 2, is embedded, is flexible. In T92V, several residues at the C terminal end of L11 are ordered and elongate $\alpha 4$. The $\alpha 4$ extension tilts by a few degrees to avoid a clash with Loop 7 (L7). **(B)** A close look at the T92V P-loop mutation. The valine of one of the two T92V molecules in the asymmetric unit, which is best defined (see panel C), is shown here. The T87-E236 interactions are shown both in ADP-kinesin and in T92V. **(C)** The $2 F_{\text{obs}} - F_{\text{calc}}$ electron density map (contoured at the 1σ level) in the nucleotide-binding site of T92V (ADP-kinesin like form) with a modeled sulfate ion. ADP and the Mg^{2+} ion from ADP-kinesin (pdb id 1BG2) are shown for reference. Stereo images of the electron density maps of nucleotide-depleted wild-type kinesin-1 in the ADP-kinesin like and tubulin-bound apo-kinesin like forms are presented in Supplementary Fig. 3.

Figure 3. Isolated apo-kinesin-1 in a tubulin-bound apo-kinesin-1 conformation. **(A)** Apo-T87A kinesin-1 mutant (green) superimposed on apo-kinesin-1 (wheat, the side chain of residues T87 and T92 is drawn) in complex with tubulin (blue) (pdb id 4LNU). In both structures, L9 is disordered whereas most of L11 is ordered, leading to full elongation of the $\alpha 4$ helix. **(B)** The structure of the L11 loop. Whereas in the absence of tubulin, a stretch of the kinesin L11 loop

remains flexible, in tubulin-bound apo-kinesin, this stretch interacts with tubulin and L11 is fully ordered. (C) The side chain of residue E236 is disordered in apo-T87A. In the complex with tubulin of apo-kinesin-1, E236 is ordered and interacts with the Switch 1 residue R203. In T87A, R203 stays at a position similar to that in tubulin-bound apo-kinesin-1 and establishes a hydrogen bond with E250 in $\alpha 4$, but the E236 side-chain is disordered beyond C β . (D) The Q86 interaction changes in apo-kinesin-1. The structures of nucleotide-depleted wild-type kinesin-1 in the ADP-kinesin like conformation (pink) and in the tubulin-bound apo-kinesin like conformation (green) have been superimposed (taking the P-loop subdomain as a reference).

Supplementary Figure 1. View of the ADP-kinesin nucleotide-binding site (pdb id 1BG2). T87 and T92 P-loop residues, that have been extensively studied in this work, and some of their interactions are shown. The P-loop interactions with the ADP phosphates are also shown.

Supplementary Figure 2. The two conformations of apo-kinesin-1 studied here. (Top) Comparison of T92V (ADP-kinesin like, P2₁ crystal form) with tubulin-bound apo-kinesin-1 (pdb id 4LNU). The P-loop subdomains of both kinesins have been superimposed and are shown in the background. Color code: T92V: P-loop subdomain, light pink; Switch 1/2 subdomain, magenta; tubulin-binding subdomain, red. Tubulin-bound apo-kinesin-1: P-loop subdomain, wheat; Switch 1/2 subdomain, olive; tubulin-binding subdomain, yellow. (Bottom) Comparison of apo-T87A with ADP-kinesin-1 (pdb id 1BG2). The P-loop subdomains of T87A and ADP-kinesin-1 have been superimposed and are shown in the background. Color code: apo-T87A: P-loop subdomain, pale green; Switch 1/2 subdomain, forest green; tubulin-binding subdomain, bright green. ADP-kinesin-1: P-loop subdomain, pale cyan; Switch 1/2 subdomain, dark blue; tubulin-binding subdomain, cyan.

Supplementary Figure 3. Structures of nucleotide-depleted wild-type kinesin-1. (Top) Stereo view of the 2.0 Å resolution $2 F_{\text{obs}} - F_{\text{calc}}$ electron density map of nucleotide-depleted kinesin-1 in the ADP-kinesin like (P2₁2₁2₁) crystal form, contoured at the 1 σ level. ADP (cyan) and the Mg²⁺ ion (green) from ADP-kinesin-1 (pdb id 1BG2) are shown for reference, after superposition of the motor domain of the two kinesins. (Bottom) Stereo view of the 2.6 Å resolution $2 F_{\text{obs}} - F_{\text{calc}}$ electron density map of the nucleotide-depleted kinesin-1 in the tubulin-bound apo-kinesin like (P1) crystal form, contoured at the 1 σ level. ADP (cyan) and Mg²⁺ ion (green sphere) from ADP-kinesin-1 (pdb id 1BG2) are shown for reference, after superposition of the P-loop subdomains of the two kinesins.

Supplementary Figure 4. Kinetics of mant-ADP release from wild-type kinesin-1. The line is the fit by an exponential decay function with a linear component due to photobleaching.

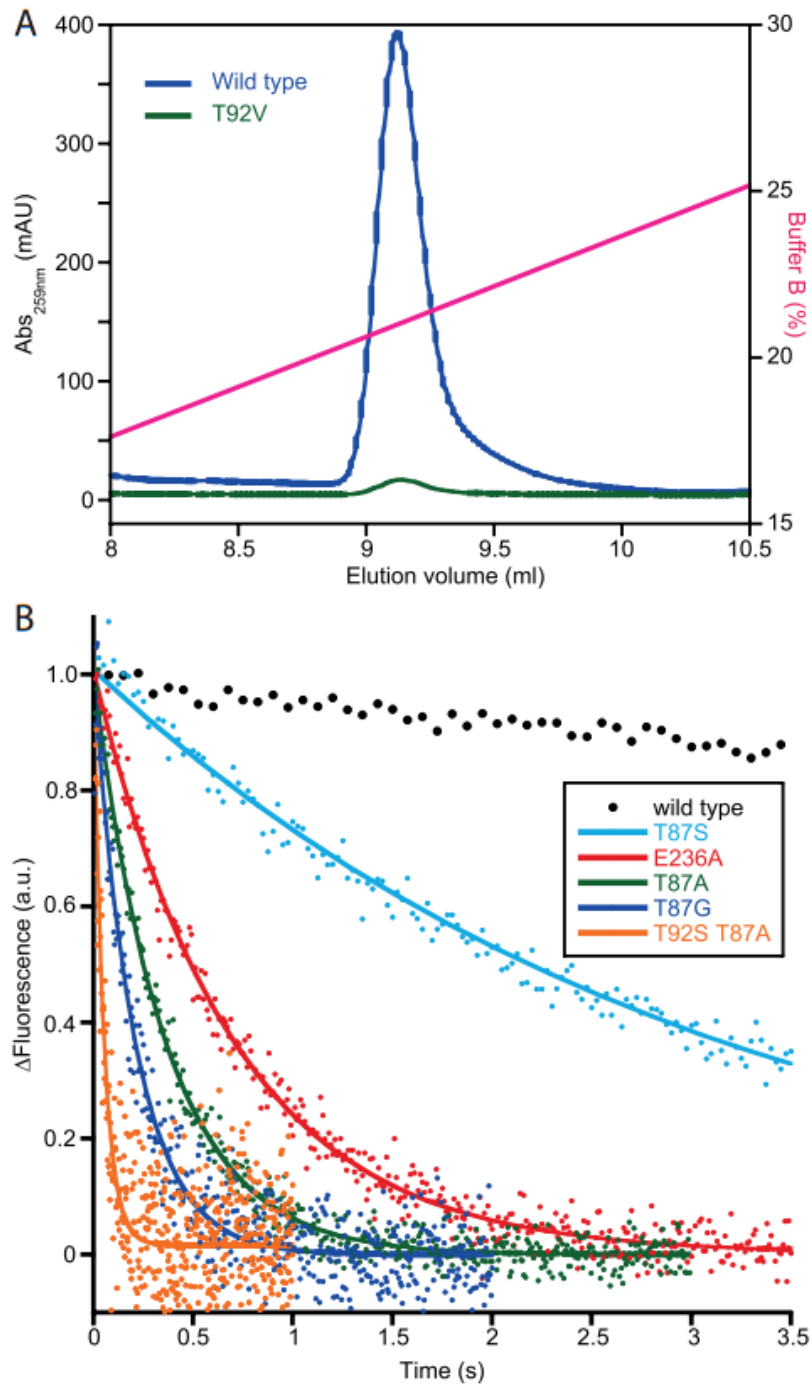


Figure .1

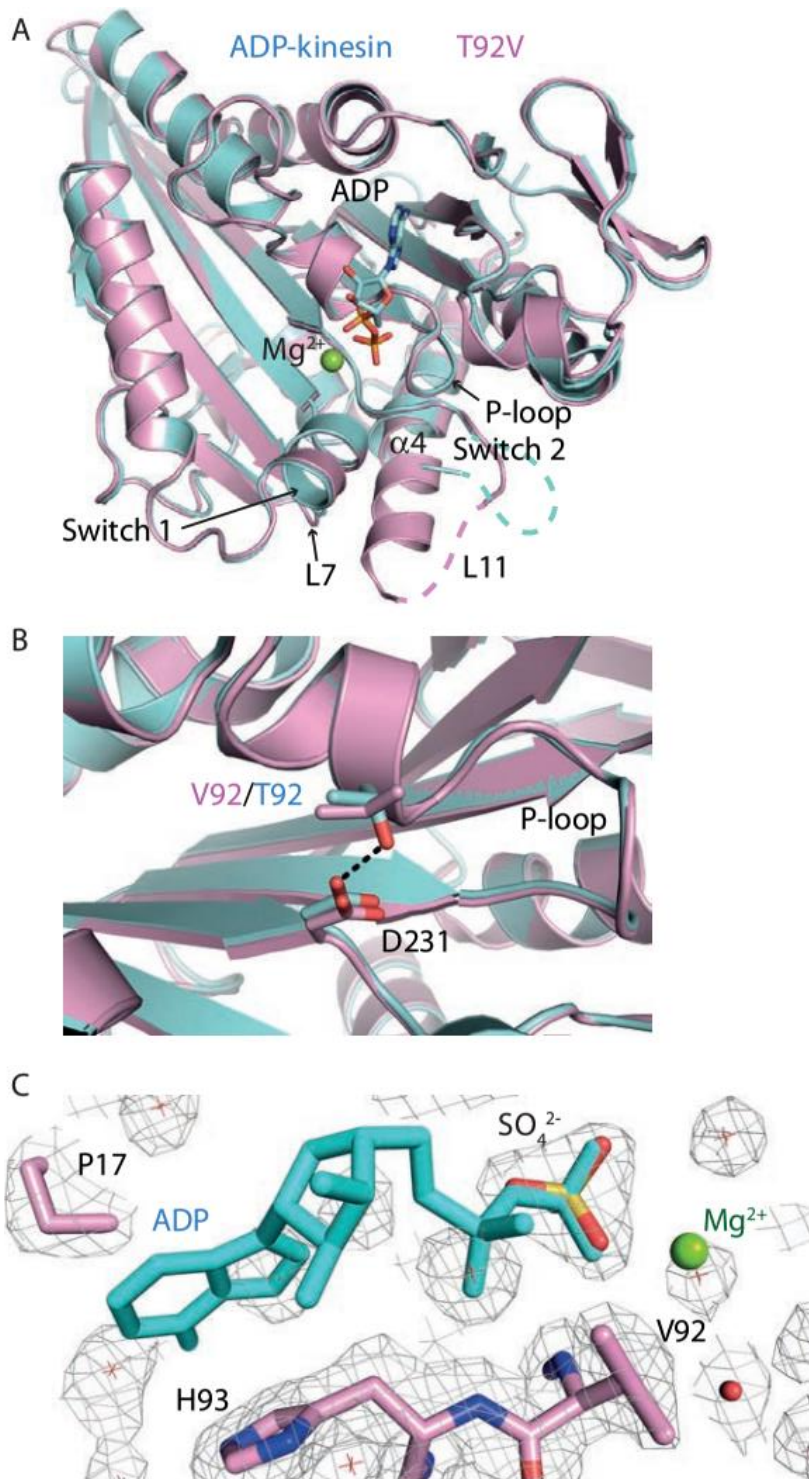


Figure. 2

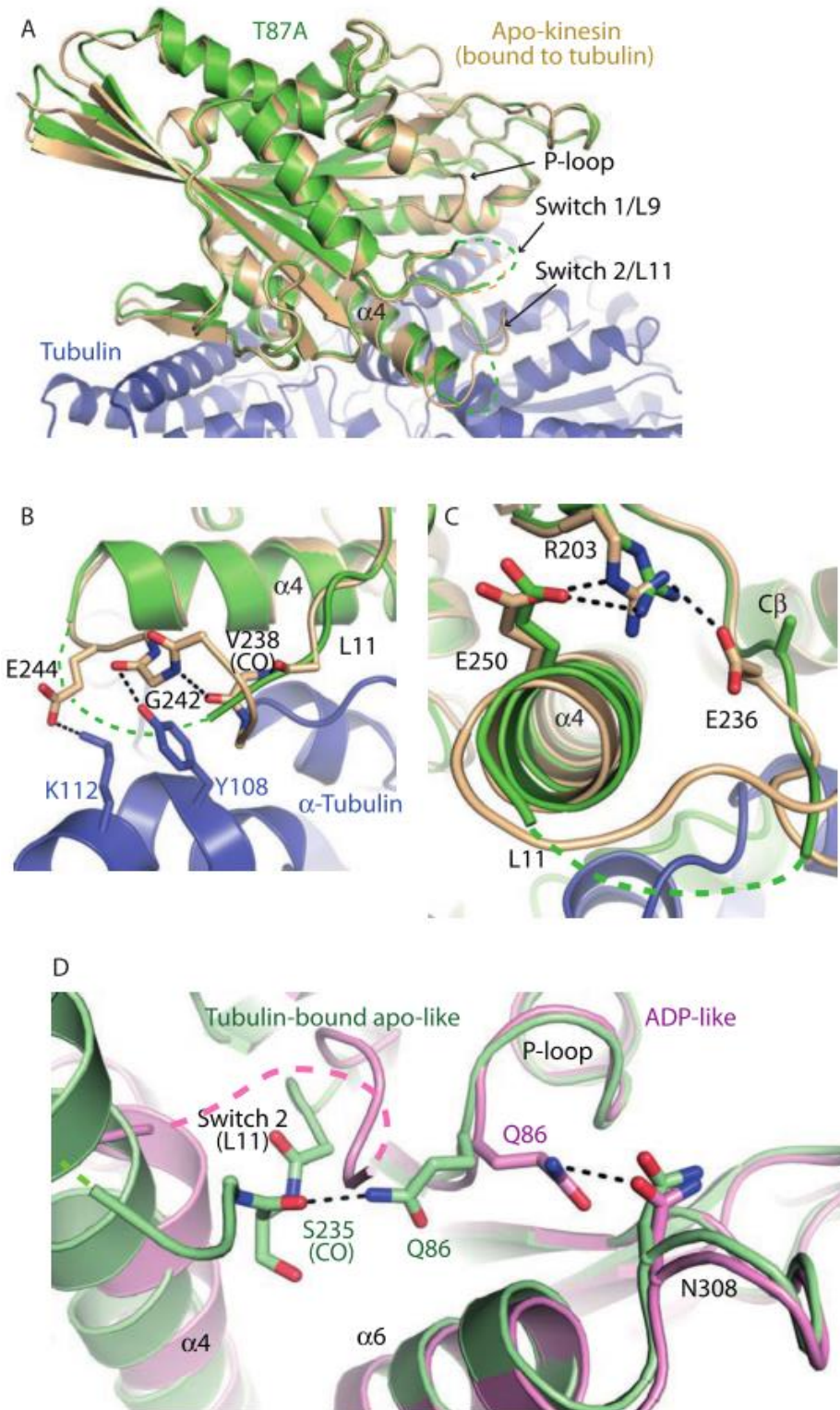
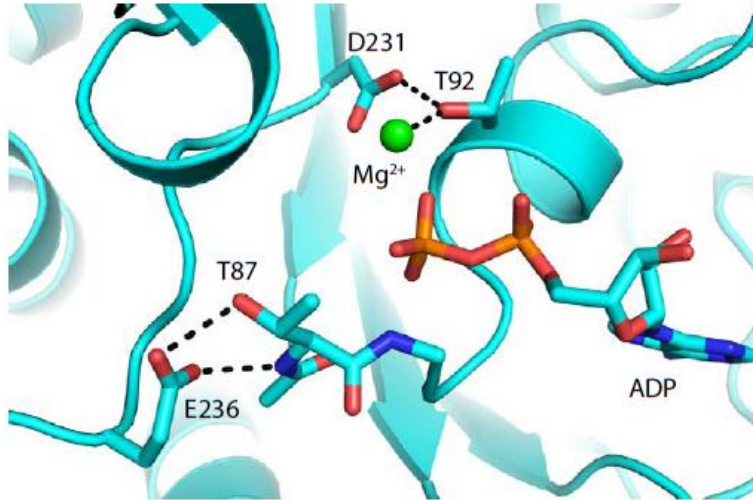
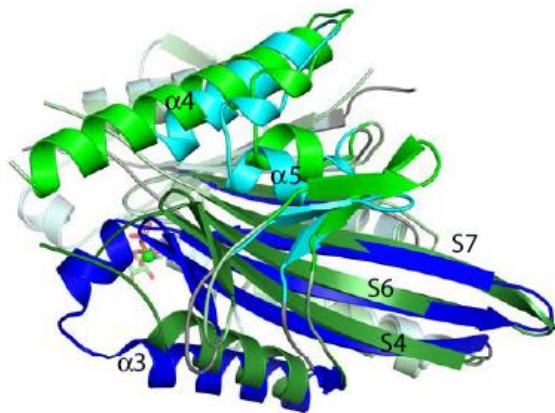
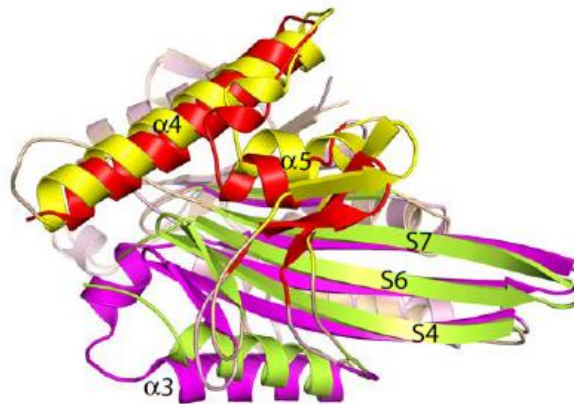


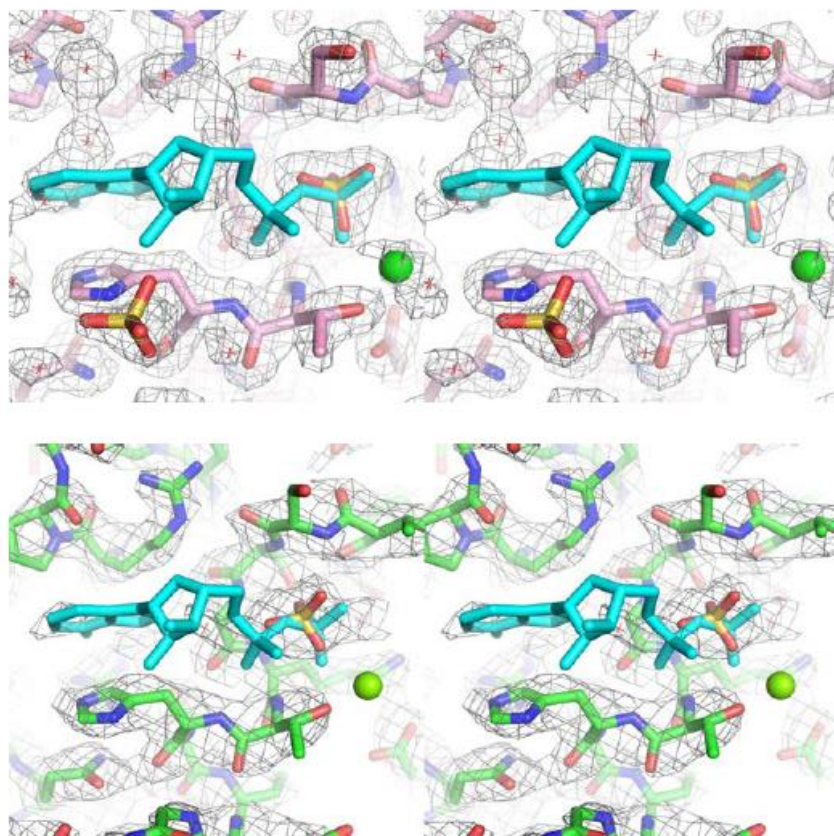
Figure. 3



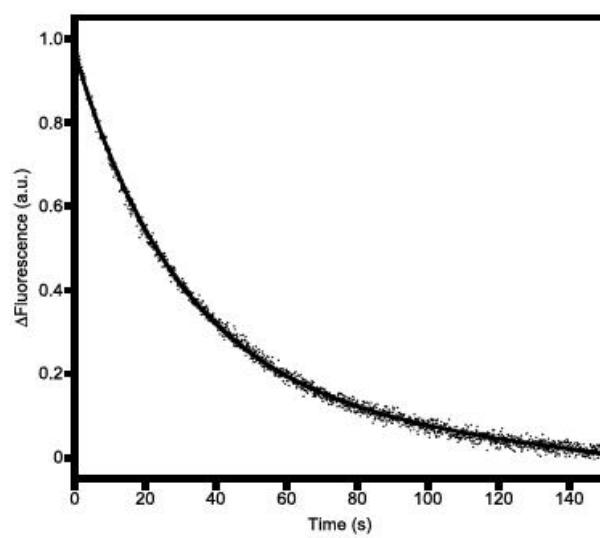
Supplementary Figure 1



Supplementary Figure 2



Supplementary Figure 3



Supplementary Figure 4

Supplementary Table 1. Data collection and refinement statistics for apo-kinesin structures.

	ADP-kinesin like form		Tubulin-bound apo-kinesin like form		
	T92V	Wild-type	T87A	Wild-type	T92V
Data collection^(a)					
Space group	P2 ₁	P2 ₁ 2 ₁ 2 ₁	P1	P1	P1
Cell dimensions					
a, b, c (Å)	53.9, 69.9, 100.1	49.0, 68.1, 112.4	56.7, 101.3, 101.5	56.7, 101.5, 101.6	57.2, 102.1, 102.1
α, β, γ (°)	90.0, 100.8, 90.0	90.0, 90.0, 90.0	119.6, 91.9, 91.8	119.2, 92.0, 92.0	119.5, 92.0, 92.0
Resolution (Å)	44-1.95 (2.00-1.95)	45.0-2.00 (2.05-2.00)	48.9-2.59 (2.66-2.59)	49.0-2.60 (2.67-2.60)	49.3-2.87 (2.98-2.87)
R _{meas}	0.20 (1.38)	0.17 (1.38)	0.29 (1.15)	0.23 (1.61)	0.32 (1.68)
I / σ I	4.8 (1.2)	9.2 (2.0)	3.8 (1.3)	6.8 (1.9)	4.5 (1.2)
CC _{1/2}	98.6 (40.6)	99.4 (67.1)	96.7 (49.0)	98.5 (60.3)	96.4 (30.8)
Completeness (%)	99.7 (95.9)	99.9 (99.9)	97.3 (91.0)	98.0 (97.6)	96.5 (80.1)
Multiplicity	3.7 (3.2)	6.4 (6.5)	2.9 (2.6)	3.5 (3.6)	3.4 (3.3)
Refinement					
Resolution (Å)	28.5-1.95	44.9-2.0	33.2-2.59	38.4-2.60	49.28-2.88
No. reflections	53434	26062	59275	59440	43981
Rwork / Rfree	0.214 / 0.234	0.170/0.213	0.197/0.274	0.187/0.258	0.188/0.285
No. atoms					
Protein	4874	2337	13771	13860	13923
Ligand/ion	53	44	40	55	60
Water	278	219	200	319	250

B factors					
Protein	29.6	33.7	49.5	57.7	58.3
Ligand/ion	68.6	99.5	90.6	117	103
Waters	32.2	49.2	37.7	45.2	47.5
Coordinate error (Å)	0.26	0.22	0.43	0.40	0.48
R.m.s.d.					
Bond lengths (Å)	0.010	0.007	0.009	0.009	0.010
Bond angles (°)	1.09	1.08	1.41	1.40	1.50
Ramachandran (%)					
Favored region	100	98.64	95.94	95.40	93.26
Allowed region	0	1.36	3.17	33.6	5.15
Outliers	0	0	0.89	1.3	1.59

^(a)Data were collected on a single crystal. Values in parentheses are for the highest-resolution shell.

Supplementary Table 2. Average temperature factors of the C α s of the P-loop and of the central β sheet in different structures.

Structure	Tubulin-bound apo-kinesin like ^(a)			ADP-kinesin like		ADP-kinesin (pdb id 1BG2)
	T87A	T92V	wild-type	T92V ^(b)	wild-type	
P-loop ^(c)	47 Å ²	58 Å ²	60 Å ²	16 Å ²	20 Å ²	15 Å ²
β sheet ^(d)	35 Å ²	43 Å ²	43 Å ²	19 Å ²	25 Å ²	21 Å ²
Overall (all C α s)	47 Å ²	56 Å ²	56 Å ²	24 Å ²	30 Å ²	29 Å ²

^(a) Averaged over the 6 molecules of the asymmetric unit.

^(b) Averaged over the 2 molecules of the asymmetric unit.

^(c) Residues 84 to 93.

^(d) Residues 9 to 15, 50 to 52, 79 to 84, 126 to 136, 141 to 144, 206 to 216, 222 to 231 and 295 to 302.

2.3 Discussion

To further study the mechanism of ADP dissociation from kinesin-1, I did mutagenesis study on kinesin-1 motor domain to generate mutants mimicking the conditions when it binds microtubule. Two series of mutants with high ADP dissociation rates represent two pathways to interfere with ADP binding. In addition, after ADP digestion by apyrase, I was able to prepare nucleotide-free kinesin (either WT or mutants) and to determine several structures in the absence of tubulin. Because isolated apo-kinesin was reported to be unstable (Cross 2004; Hackney 1996), I further studied the stability of the apo-kinesins I prepared.

Stability of kinesin and its mutants in the absence of nucleotide

Kinesins in nucleotide-free state were reported to be unstable (Sadhu and Taylor 1992; Hackney 1994). When the nucleotide in kinesin-1 is removed, some motor protein denatures and precipitates. The same instability of apo-kinesin was also observed in kinesin-14 (Lockhart and Cross 1994).

The observation that the intrinsically nucleotide-free T92V mutant could be purified suggests that apo-T92V is more stable and soluble than anticipated. So I tried to crystallize this mutant. The final success in the crystallization of apo-T92V convinced me that at least with T92 mutated, apo-kinesin is stable and well-folded. Furthermore, I obtained the crystal structure of another apo-kinesin mutant, T87A, after treatment with apyrase to remove the remaining nucleotide. It suggested that with T87 mutated kinesin is stable and well-folded as well, despite of its distinct crystal structure compared to T92V. These results make me wonder whether these mutations play a role in kinesin stability.

Therefore I have studied the stability of apo-kinesin mutants and apo-kinesin wild type by differential scanning calorimetry (DSC) with ADP-kinesin wild type as a control (Fig. 6.1). The results show that apo-kinesin is less stable and easier to denature than ADP-kinesin, as expected from results from the literature (Fig. 6.2). However the melting temperature is only 3 to 4°C lower in the case of apo-kinesin wild type compared to ADP-kinesin. In addition it is more stable than the T92V and T97A mutants. Overall these results indicated that apo-kinesin wild type, as well as its mutants, remains soluble and well-folded at 20°C, i.e. at the temperature where most of the biochemical experiments were performed, also where the protein was crystallized.

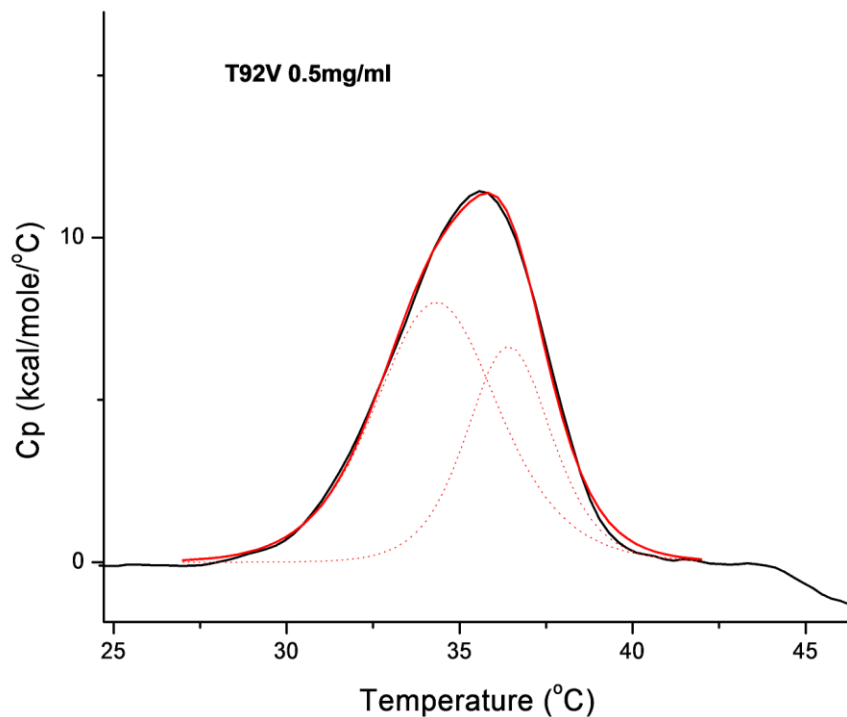


Figure 6.1 An example of DSC analysis of kinesin

The DSC thermographs (black) of kinesin are asymmetric; they were fitted (red) by two symmetric peaks with two melting temperature values (T_m) and two values of enthalpy of transition (ΔH) (red dash lines). The asymmetry of thermographs may be due to an intermediate state during the process of kinesin denaturation.

The solubility and stability of apo-kinesin, which is found higher than expected, could be due to the concentration of salt (150-300 mM NaCl) used. Indeed during purification kinesin elutes from the ion exchange columns at about 30% Buffer B, i.e. about 300 mM NaCl. I tried to desalt the samples when preparing them for crystallization, but I noticed some precipitation when the concentration of salt went down to 100 mM. Therefore for crystallization and DSC analysis, there was always 150 mM NaCl in the system to prevent kinesin from precipitating. In the ADP-release experiments, the concentration of kinesin is low (0.5 - 1 μ M) and there is always extra nucleotide in the system, so no salt is added during the measurement.

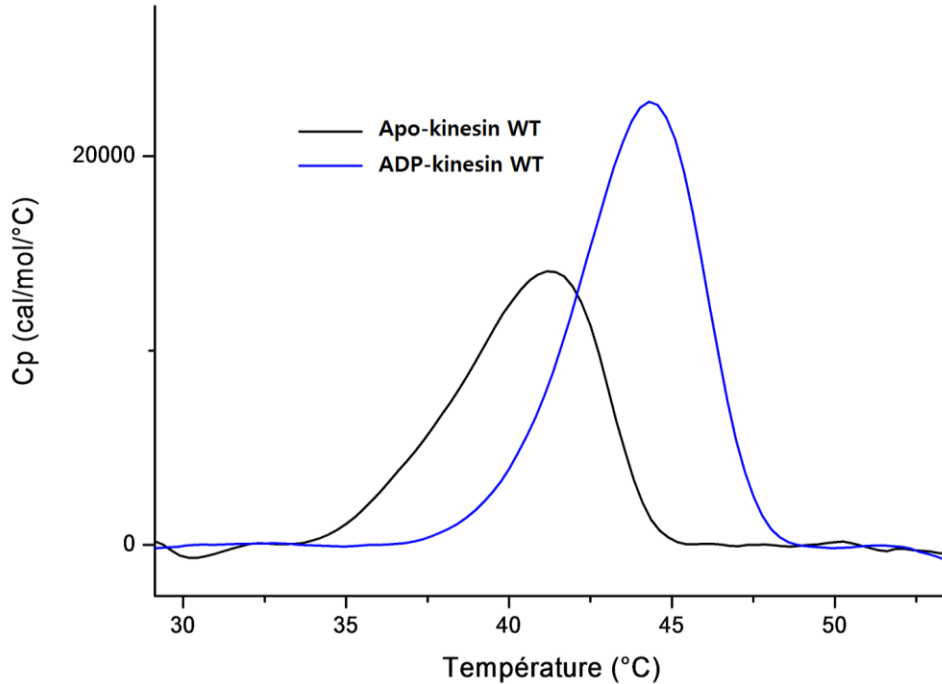


Figure 6.2 DSC analysis of kinesin-1 without or with the presence of ADP

Kinesin were treated with apyrase to generate apo-kinesin. The stability of apo-kinesin and ADP-kinesin are analyzed by differential scanning calorimetry parallelly. Compared to apo-kinesin, ADP-kinesin has higher melting temperature (T_m) and higher enthalpy of transition (ΔH). It means ADP-kinesin can survive higher temperature and consume more energy to denature. These results indicate that ADP-kinesin is more stable than apo-kinesin.

Table 6.1 DSC results of wild type kinesin and kinesin mutants

	T_{m1} (°C)	$\Delta H1$ (Kcal/mol)	T_{m2} (°C)	$\Delta H2$ (Kcal/mol)
ADP-WT	43	64	44.9	45
Apo-WT	39.4	46	41.8	31
Apo-T92V	34.3	38	36.4	22
Apo-T87G	36.1	39	38.1	25
Apo-T87A	35.7	39	37.7	30

The structural switch of nucleotide-free kinesin.

The DSC analysis indicates that the stability of apo-kinesin wild type is higher than that of apo-kinesin T92V and T87A mutants. Because useful crystals were obtained with these mutants, I wondered whether wild type apo-kinesin could be crystallized as well. I tried to crystallize it in the conditions where the apo-kinesin mutants crystallized spontaneously. Indeed, wild type apo-kinesin was crystallized and the structure indicates that it can adopt the two different conformations, ADP-like and tubulin-bound apo-like.

ADP-like apo-kinesin, with solvent replacing ADP in its nucleotide binding pocket, is able to crystallize spontaneously. It suggests that ADP-like is likely the dominant conformation in kinesin. It explains the stability and solubility of kinesin with the presence of salts as well.

Wild type apo-kinesin (so is T92V mutant) is able to be crystallized with an apo-like conformation only under the circumstance of seeded with apo-T87 mutants' crystals in the same condition where apo-T87 mutant is crystallized with apo-like conformation. This conformation of apo-kinesin with a relatively open nucleotide binding pocket, is probably a short-lived state which allowing apo-kinesin to rebind nucleotide. Binding to microtubule stabilizes this apo-like conformation by keeping the conformational changes of tubulin-binding subdomain, including the elongation of H4 helix.

Nevertheless, these results suggest the existence of various apo-kinesin conformations. More efforts should be made to investigate the states of apo-kinesin in the solution.

Structural study on kinesin motility

Kinesin-1 walks along microtubule as a homodimer in a hand-over-hand manner. That two motor domains go through the same cycle but in different states is crucial for kinesin's processive and unidirectional movement. Investigating the communication between two motor domains during kinesin movement will be interesting and meaningful.

So far, we obtained the crystal structure of kinesin monomer in different nucleotide states. The fact that T92V doesn't bind any nucleotide provides a possibility to study the communication between two motor domains of kinesin directly by having a structure of kinesin dimer with two motor domains in different nucleotide state, i.e. with one motor domain in nucleotide free state and the other in ATP-analog or ADP state.

Recent advancement on recombination and expression of tubulin suggests the possibility of obtaining a tubulin linear tetramer through introducing mutations into tubulin. In other words, one can obtain a tubulin polymer having two kinesin binding sites.

In general, a structure presented in figure 6.3 is accessible in theory and will bring new insights into kinesin's processive motility.

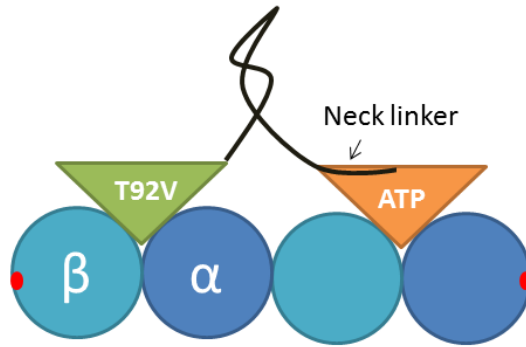


Figure 6.3 A model of kinesin-1 heterodimer in complex with tubulin tetramer.

T92V and wild type kinesin heterodimer may provide an opportunity to observe the communication between two motors domains in different mechanochemical states directly. With mutations (red points) introduced into recombined and expressed tubulin heterodimer, it's possible to generate heterodimeric tubulin heterodimer, a linear tubulin tetramer having two kinesin binding sites. Therefore, a complex, in which both kinesin motor domains bind tubulin but one in nucleotide-free state while the other in ATP-analog state (for example), can be generated. This work will be very challenging but possible theoretically.

3. Crystallization of kinesin-14 in complex with tubulin-DARPin

3.1 Objectives

To study the motility of kinesin-14, my objective is to obtain the crystal structure of a kinesin-14 in different nucleotide states complexed with a tubulin heterodimer, as presented in the introduction. I have worked with several constructs based on two well-studied kinesin-14 (Ncd from *Drosophila* and the yeast Kar3).

Ncd, as a representative of kinesin-14 has already been presented in the introduction of this these. Here, I will give a brief introduction on Kar3.

Kar3 is the only kinesin-14 member found in *Saccharomyces cerevisiae*. During karyogamy and mitosis, as Ncd, Kar3 is able to crosslink microtubules with its C-terminal motor domain bound to one microtubule and its N-terminal ATP-independent tail bound to another one.

Although *in vitro* Kar3 can form a homodimer as Ncd (Chu et al. 2005), *in vivo* it heterodimerizes with either Vik1 or Cik1 selectively to achieve distinct functions (Gonzalez et al. 2013). Vik1 and Cik1 are two kinesin-related proteins (they share at least 25% amino acid sequence identity (Manning et al. 1999)) but they are unable to bind a nucleotide. Kar3/Vik1 localizes at the poles of the mitotic spindle, crosslinking parallel microtubules, involved in spindle stabilization, whereas Kar3/Cik1 is capable of crosslinking antiparallel microtubules in the overlap zone, contributing to the spindle mid region geometry stabilization.

Previous studies indicated that both Kar3/Vik1 and Kar3/Cik1 go through a similar power stroke as the Ncd homodimer. The non-motor partner, Vik1 or Cik1 participates in the motile cycle directly by modulating the binding of the Kar3 motor domain to microtubules. ADP-Kar3 motor alone has a relatively low affinity for microtubules ($K_D = 233$ nM), while Vik1 head domain has a much higher affinity ($K_D = 43$ nM), similar to that of ADP-Kar3/Vik1 heterodimer ($K_D = 38$ nM). This suggests that the binding of ADP-Kar3/Vik1 to microtubules is first guided by the non-motor partner (Allingham et al. 2007). A kinetic study on Kar3/Cik1 leads to the same conclusion (Chen, Rayment, and Gilbert 2011). A model of Kar3/non-motor partner motility cycle is summarized in the following figure (Fig. 7.1).

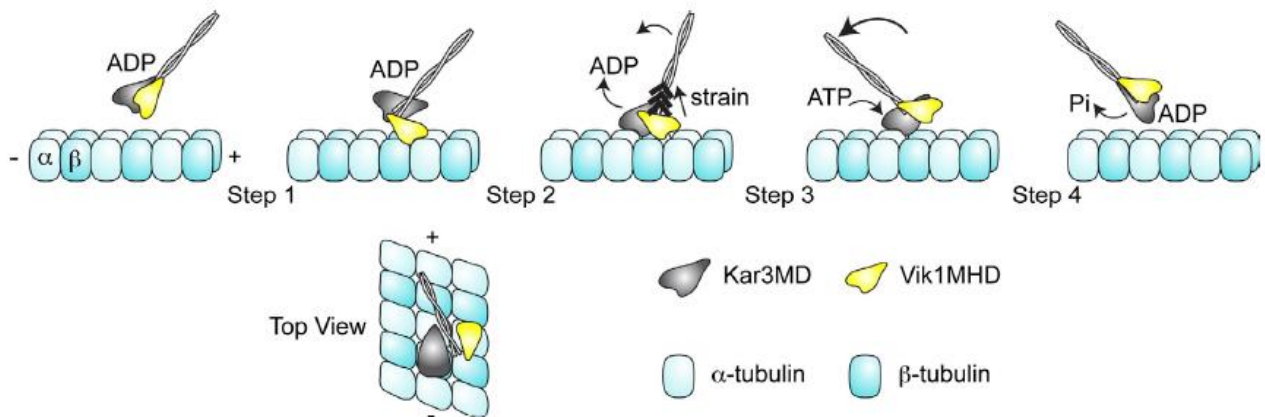


Figure 7.1 Motility model of Kar3/Vik1 heterodimer (Rank et al. 2012)

α/β tubulin heterodimers are colored in light and dark blue. Step 1, Vik1 binds to a microtubule, leading ADP-Kar3 to attach to the same microtubule too. Step 2, microtubule-bound Kar3 releases its ADP; meanwhile a strain with the coiled-coil is produced so that Vik1's tight contact with microtubule is ruined. Step 3, ATP binds nucleotide-free Kar3, causing a rotation of the stalk. Step 4, ATP hydrolysis occurs and ADP-Kar3 dissociates from microtubule. Previous studies also suggest that Kar3 motor domain and Vik1 bind to adjacent protofilaments with 'opposite orientations' on the lattice as shown in the bottom figure.

Structural studies on Kar3 will provide more insight into Kar3's partner-modulated motility. The first crystal structure published revealed that the Kar3 motor domain has a structure similar to those of other kinesin family members (Gulick et al. 1998). Vik1's crystal structure also shows that it has a fold similar to that of the kinesin catalytic core, while it lacks a functional ATP binding site (Allingham et al. 2007). The structure also points the conserved Gly373 Vik1 residue as a key residue for neck rotation (Fig. 7.2). It has suggested that the Kar3/Vik1 heterodimer may go through the same neck rotation as the Ncd homodimer (Cf. Introduction).

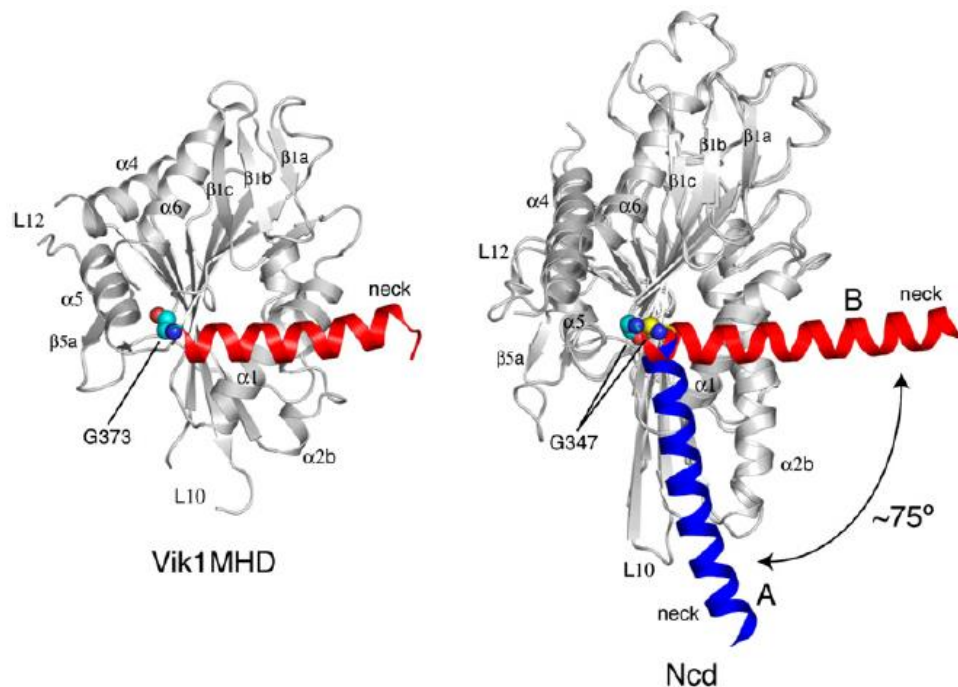


Figure 7.2 Comparison of the neck rotation in Ncd and Vik1 (Allingham et al. 2007).

The position of the neck (red) in Vik1 and the two different possible neck (red and blue) positions in Ncd are shown. For Ncd, the two motor domains' Cas of a Ncd mutant, N600K, with an asymmetric conformation (Cf, Introduction (Yun et al. 2003)) were superimposed. For Vik1, the Cas of Vik1's Motor-Homology Domain (MHD) without neck were superimposed with the motor domain of Ncd, but Ncd is not shown. The Gly373 in Vik1 and its equivalent residue in Ncd (Gly347) are highlighted.

The similarity between the Kar3/Vik1 heterodimer and the Ncd homodimer is also confirmed by the crystal structure of the Kar3/Vik1 heterodimer (Fig. 7.3).

To generate this structure, some artificial modifications were introduced in the heterodimer (Rank et al. 2012). First, different lengths of stalk were tried to generate a soluble and stable heterodimer. Second, a Synthetic HeteroDimer (SHD), with an acidic helix and a basic one, was added to the stalk in order to increase the yield and stability of Kar3/Vik1 heterodimer. These two peptides of SHD are able to form a dimer with hydrophobic interaction, while those charged residues on SHD prevent them from forming homodimers. Third, an intramolecular cross-link was introduced in Vik1, preventing Vik1's globular domain from moving relative to its helix.

The ADP-bound Kar3/Vik1 heterodimer is in a conformation similar to that of the asymmetric Ncd (cf. Introduction), which likely represents the pre-powerstroke position instead of the post-powerstroke one. The pre-powerstroke conformation was further supported by docking the heterodimer structure into the cryo-EM map of microtubule-bound Kar3/Vik1. ADP-Kar3/Vik1 heterodimer crystal structure, treated as a rigid body, was docked into both nucleotide-free and AMPPNP-Kar3/Vik1 decorated microtubule cryo-EM maps. The structure fitted well into the map of nucleotide-free Kar3/Vik1 bound to a microtubule. Docking of the Kar3/Vik1 heterodimer into the map of AMPPNP-Kar3/Vik1 decorated microtubule indicates there is a large structural rearrangement of Vik1 and the coiled-coil stalk. In ATP-analog-Kar3/Vik1, the stalk together with Vik1 rotates about 90° towards the minus end of microtubule (Rank et al. 2012). A similar rotation in ATP-analog-Ncd with the presence of microtubule has also been observed by cryo-EM (Endres et al. 2006).

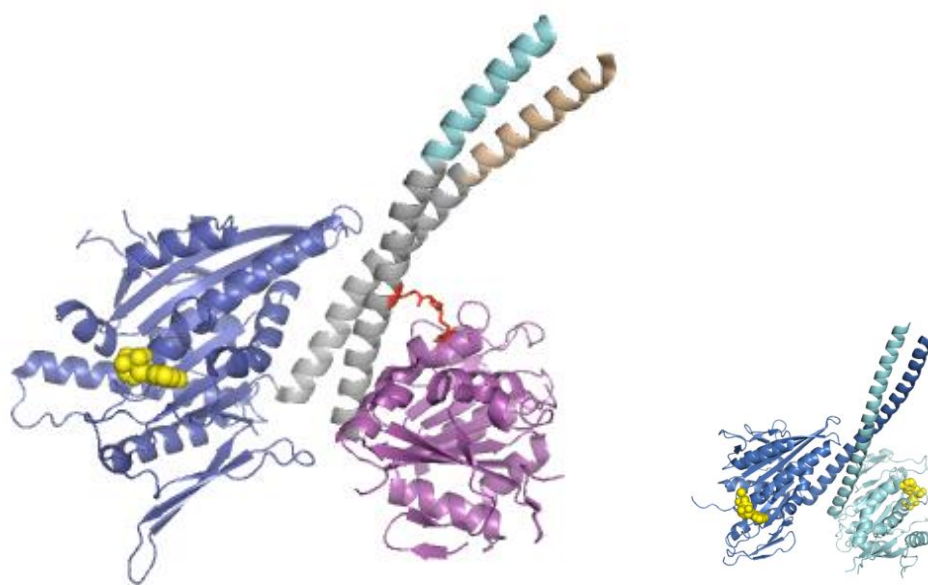


Figure 7.3 Kar3/Vik1 heterodimer (Rank et al. 2012)

Right: Kar3 motor domain is colored in dark blue with a bound ADP molecule (yellow). Vik1 kinesin-like domain without a nucleotide binding site is colored in magenta. Kar3 and Vik1 are dimerized with a coiled-coil stalk. Because Kar3 can form homodimer in vitro (Chu et al. 2005), an artificial heterodimerized leucine zipper (colored in cyan and wheat) is introduced to yield a Kar3/Vik1 heterodimer. In Vik1, an iodoacetamide based reagent (EBI) was used as a symmetric covalent cross-link between E355C and K423C (Red) in order to favor crystallization and improved crystal diffraction.

Left: The structure of an asymmetric Ncd homodimer (Liu, Pemble, and Endow 2012) is shown here, with two ADP molecules (yellow) binding to two motor domains. The similarity between Kar3/Vik1 and asymmetric Ncd homodimer is obvious.

Distinct from Kar3 and other motor proteins, Vik1 doesn't have a nucleotide binding site. In addition a non-conventional binding of Vik1 to microtubules, different from that of kinesins, has been proposed (Fig. 7.1, bottom). Moreover, the rotation of Vik1's neck hasn't been observed so far at an atomic level. A Vik1 motor-homology domain-tubulin complex structure may address these pending issues.

As in the case of Ncd, the structural information of Kar3 in different nucleotide states complexed with tubulin will be helpful to understand the details of Kar3 heterodimer's motility and more generally to gain insights into the motility of (-)-end directed kinesin-14s.

So, my main goal in this part was to crystallize Kar3 or Vik1 or Ncd in complex with a tubulin heterodimer.

3.2 Constructs

Motor or motor-homology domain

In the case of Vik1, the motor-homology domain (Vik1 MHD, Fig. 7.2) whose crystal structure has been published (Allingham et al. 2007) was purified and a complex with tubulin was prepared.

In the case of Kar3 and Ncd, my main objective is to study the dimers. As mentioned in the introduction, kinesin-14s require the dimeric stalk for movement. But Kinesin-14 homodimers (*in vitro* Kar3 can form a homodimer as well (Chu et al. 2005)) obviously have two microtubule binding sites, which may lead to the difficulty of co-crystallizing their complexes with tubulin. Therefore I have worked with Kar3 and Ncd heterodimers. Indeed previous experiments suggest that, as long as a dimeric stalk is formed, Ncd can still move at a normal speed even with only one functional motor domain (Fig. 7.4). Hence a one-motor kinesin-14 heterodimer construct is a suitable surrogate to study the kinesin-14 mechanochemical cycle.

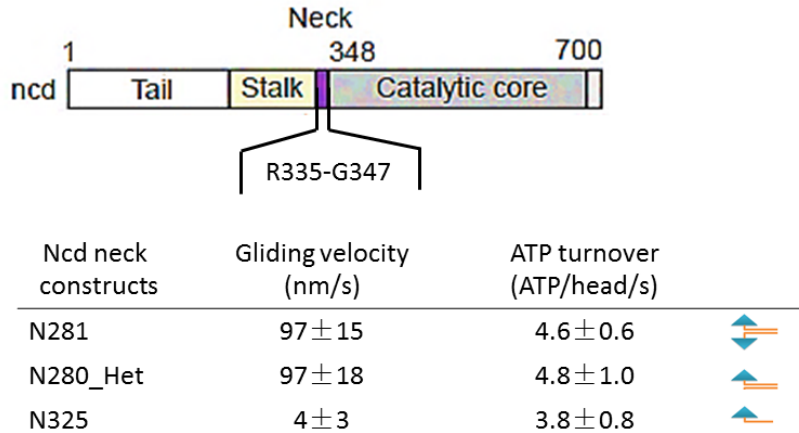


Figure 7.4 Different Ncd constructs and their characterization (Endres et al. 2006).

Top: Domain organization of full length Ncd. Ncd comprises an N-terminal tail, a coiled-coil stalk, a C-terminal catalytic core and a short neck linking the stalk and the catalytic core.

Bottom: ATPase activity and microtubule gliding velocity of an Ncd monomer, a one-motor heterodimer and of a homodimer. N281, comprising Ncd residues 281 to 700, forms a homodimer with two motor domains; N280_Het refers to an Ncd Heterodimer construct, with one chain comprising one motor domain (Ncd residues 281 to 700), the other chain being restricted to the C-terminal part of the stalk and to the neck region (residues 281 to 347); N325 (Ncd residues 325 to 700) is monomeric. The constructs' general structures are indicated by blue triangles (catalytic core) and orange lines (neck plus the C-terminal part of the stalk). The results indicate that a full length motor domain is responsible for ATP hydrolysis whereas a dimeric stalk with one motor domain only is necessary and sufficient for kinesin-14's movement.

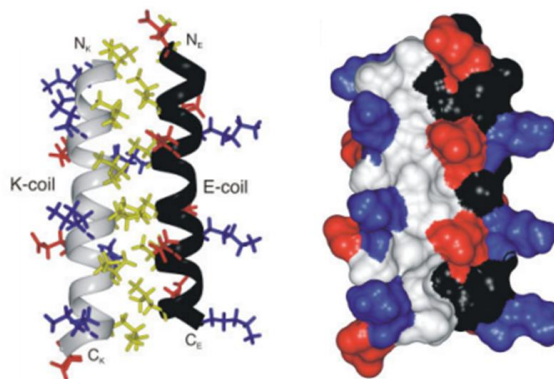


Figure 7.5 Synthesized Heterodimer (SHD)(Litowski and Hodges 2002).

The two SHD chains are in black and white. Hydrophobic residues are shown in yellow; acidic and basic residues are in red and blue, respectively.

The heterodimer was constructed by adding at the N-terminal end of the monomers one or the other of the two following SHD sequences:

Chain A: EIAALEKEIAALEKEIAALEKEI (also called E3)

Chain B: KIAALKEKIAALKEKIAALKEKI (also called K3)

They are able to dimerize by hydrophobic interaction (Fig. 7.5) whereas the homodimer formation is prevented because of the presence of charged residues. The same SHD was used to dimerize Kar3 and Vik1 to generate a Kar3-Vik1 dimer whose structure has been determined (Rank et al. 2012).

Fusion with AC2

As in the case of tubulin-kinesin-1 complexes, tubulin in complex with a kinesin-14 should be stabilized for crystallization experiments. Making ternary tubulin-kinesin-DARPin complexes is a suitable approach that has worked in the case of kinesin-1. In addition, in the case of kinesin-14 kinesins, I have designed DARPin-kinesin covalent constructs as a means to produce more stable complexes with tubulin. To this end, repeats of G4S (Gly-Gly-Gly-Gly-Ser) were used to link the C-terminus of the Kinesin-14 motor domain to the N-terminus of the DARPin named AC2, which has a high affinity for tubulin (K_D in the nanomolar range) (Ahmad et al. 2016). In addition, because the tubulin-AC2 structure has been determined, I am able to model the ternary complex in order to optimize the length of the G4S linker.

Summary

The following table lists all the kinesin-14 constructs I have tested.

Name	Description	Constructs	Nucleotide state
Hetero-Ncd 700	Heterodimer	K3-Ncd 321-700 (His-TEV)-E3-Ncd 321-347	Apo/ATP analog
Hetero-Ncd-AC2	Heterodimer	K3-Ncd 321-700-2G4S-AC2 (His-TEV)-E3-Ncd321-347	Apo/ATP analog
Hetero-Ncd 679	Heterodimer	K3-Ncd 321-679 (His-TEV)-E3-Ncd321-347	Apo/ATP analog
Ncd motor 700	Monomer	Ncd 325-700	Apo/ATP analog

Ncd motor-AC2	Monomer	Ncd 325-700-2G4S-AC2	Apo/ATP analog
Ncd motor 679	Monomer	Ncd 325-679	Apo/ATP analog
Hetero Kar3	Heterodimer	K3-Kar3 353-729 (His-TEV)-E3-Vik1 341-373	Apo/ATP analog
Hetero Kar3-AC2	Heterodimer	K3-Kar3 353-729-5G4S-AC2 (His-TEV)-E3-Vik1 341-373	Apo/ATP analog
Kar3 motor	Monomer	Kar3 353-729	Apo/ATP analog
Kar3 motor-AC2	Monomer	Kar3 353-729-5G4S-AC2	Apo/ATP analog
Vik1	Monomer	Vik1 353-647	Apo
Vik1-AC2	Monomer	Vik1 353-647-5G4S-AC2	Apo

3.3 Characterization

Expression and purification of Kinesin-14

Vik1 motor-homology domain was purified by a His-trap column then the His-tag was removed using TEV protease. This purification was polished by a gel filtration column. The molecular weight of Vik1 motor-homology domain was checked by mass spectrometry. The measured molecular weight (34688 ± 2 Daltons) matches the theoretical value deduced from the sequence (34687 Daltons).

In the case of kinesin-14 heterodimers, care should be exercised that both chains are present. In particular the detection of the motor-less SHD moiety is not conveniently recorded by SDS-PAGE analysis because of its small size. The first metal-affinity column is not a problem because this peptide comprises the His-tag. Then, after proteolysis of the TEV cleavage site and the subsequent gel filtration chromatography step, the presence of the SHD peptide in the case of the Hetero-Ncd 700 construct was checked by mass spectrometry. Mass spectrometry analysis confirmed the presence of two chains of molecular mass 44823 Daltons and 5203 Daltons, respectively. The experimental data match the theoretical mass of both chains of the heterodimer, indicating that proper kinesin-14 heterodimers can form and be purified. Although the stoichiometry of two chains has not been checked by experiment, a similar method was used to purify Kar3/Vik1

heterodimer which was crystallized finally. It suggests that the heterodimer is stable in the purification-crystallization process.

Afterwards, as the bigger chain of the kinesin-14 heterodimer is detected by SDS-PAGE, the small peptide is considered existing in the construct by default. However, the possibility that the small peptide may be lost later on cannot be ruled out.

Affinity to microtubules

To verify that the kinesin-14 heterodimers are functional, I first checked whether they bind microtubules and in which conditions the binding is favored. A centrifugation assay was used to analyze the interaction between microtubules and the Ncd heterodimers loaded with the ATP-analog, AMPPNP.

First, the binding ability of Ncd to microtubules was checked with various concentrations of microtubule (Fig. 7.6). The results suggested that in the presence of AMPPNP, Ncd is able to bind to microtubules tightly.

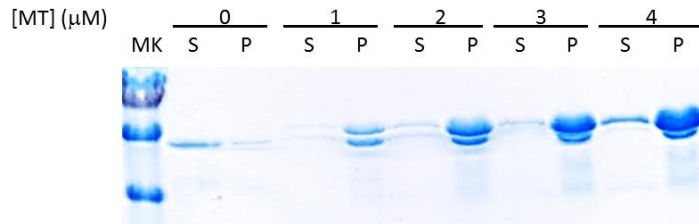


Figure 7.6 Ncd binds to microtubules (MT).

In the presence of 2 mM AMPPNP, 2 μM Ncd heterodimer was incubated with increasing amounts of microtubules (0 μM , 1 μM , 2 μM , 3 μM , 4 μM MT) at 25°C for 30 min. After centrifugation, the supernatant and pellet content were analyzed respectively by SDS Page.

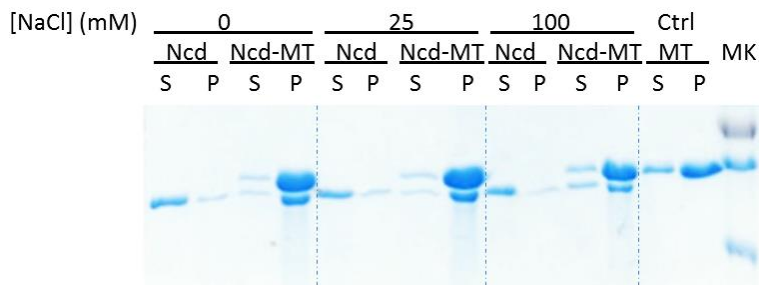


Figure 7.7 Ncd binding to microtubules (MT) under various salt concentrations.

In the presence of 2 mM AMPPNP, 4 μ M Ncd heterodimer alone or with 4 μ M microtubules were incubated at 25°C for 30 min at the indicated salt concentrations. The supernatant and pellet content were analyzed by SDS Page respectively after ultracentrifugation.

Then, I checked the influence of salt concentration because the stability of Ncd is slightly improved in the presence of salt. The results are presented in Fig. 7.7 and indicate that Ncd binds slightly less tightly to microtubules along with the increase of the salt concentration.

I have also tried to study the interaction without added nucleotide. To generate nucleotide-free Ncd heterodimer, the kinesin was incubated with 0.5 U/ml apyrase. After centrifugation all the motor protein went to the pellet even without microtubules having been added, indicating that spin down assay is not a proper method to study the interaction between nucleotide-free Ncd and microtubules. It also suggested that it may not be a good idea to generate an apo-kinesin-14 tubulin DARPIn complex by a treatment with apyrase. As a result, despite the fact that the ADP dissociation from kinesin-14 is slower than that from kinesin-1, I prepared apo-kinesin-14-tubulin-DARPIn complexes by simply mixing the components together without treating with apyrase, the same method which I used to generate an apo-kinesin-1-tubulin-DARPIn complex which I was able to crystallize (Cao et al. 2014). The nucleotide state of the complex generated was analyzed to confirm in the complex the kinesin-14 doesn't bind an ADP. The results will be presented later.

Complex

Kinesin-14 in different nucleotide states was mixed with tubulin-DARPIn complexes and the mixture was purified by a gel filtration chromatography. The gel filtration chromatography allowed me to 1) determine which DARPins are suitable candidates to make ternary complexes with kinesin-14 and tubulin; 2) have an idea on the motor protein:tubulin stoichiometry (a 1:1 complex is expected); 3) estimate the stability of the complexes.

Representative results are shown in Figures 7.8 and 7.9. They suggest that kinesin-14s, mentioned in the summary above, in different nucleotide states are able to form a complex with DARPIn-stabilized tubulin with a ratio of 1 to 1 to 1 (kinesin-14 to tubulin to DARPIn). However, kinesin-14 motor protein induces also some aggregation, which varies from batch to batch. So far, I haven't found a method to avoid the aggregation. For crystallization experiments, the main peak containing the expected complex was collected and concentrated.

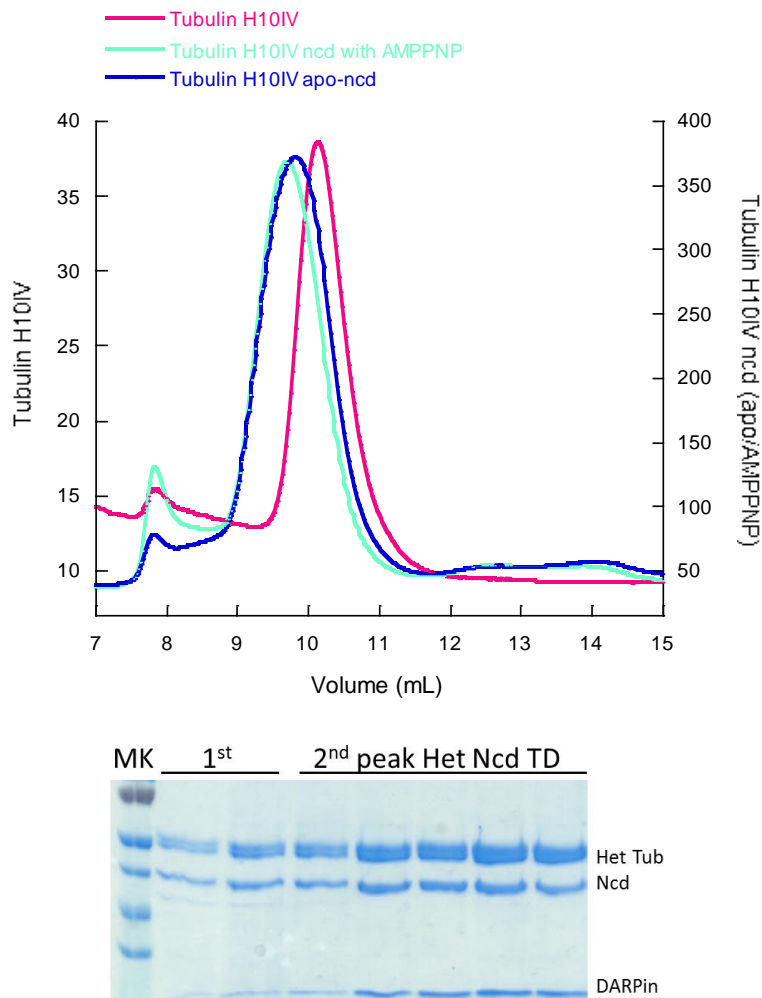


Figure 7.8 Ncd complex with tubulin stabilized by a DARPin (H10IV).

Top: gel filtration chromatography of Ncd (Hetero-Ncd 700) in different nucleotide states in complex with a tubulin-DARPin complex (tubulin-H10IV). The tubulin-DARPin complex was also injected as a control. Both apo- and AMPPNP-Ncd in complex with this tubulin-DARPin eluted at a similar position, earlier than tubulin-DARPin complex.

Bottom: SDS Page analysis of the AMPPNP-Ncd-tubulin-DARPin complex. The tubulin heterodimer (Het Tub), the Ncd motor domain and the DARPin are shown on the gel. The first two lanes correspond to the peak of aggregates (void volume of the column, about 8 ml). Fractions corresponding to the second and main peak were analyzed as well. The results confirmed that the main peak is composed of Ncd, tubulin and the DARPin proteins with a ratio around 1 to 1 to 1.

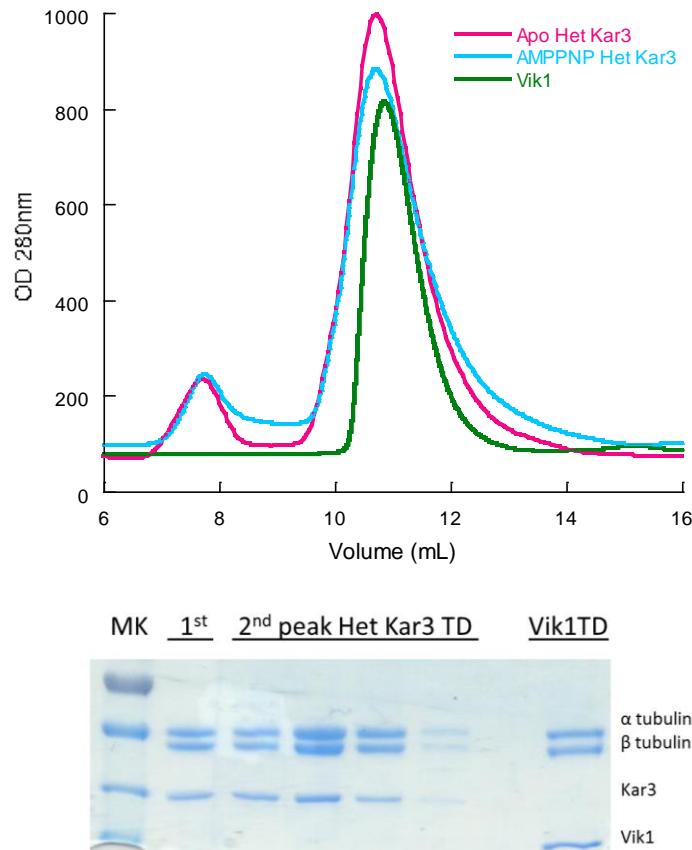


Figure 7.9 Hetero-Kar3 in different nucleotide states or Vik1 in complex with tubulin-DARPin.

Top: the gel filtration chromatography profile of Hetero-Kar3 in different nucleotide states in complex with tubulin and a DARPin (named H5II) is presented. The elution volumes of apo- and AMPPNP-Hetero Kar3 in complex with tubulin-DARPin are similar. By comparison, the peak of Vik1-Tubulin-DARPin complex is slightly shifted, as expected because Vik1 is smaller than Kar3 and does not comprise the hetero coiled-coil.

Bottom: SDS Page analysis confirmed the presence of Kar3 and tubulin (or Vik1 and tubulin) in the main peak (DARPin is not shown here) with a ratio about 1 to 1. For Kar3, there is still a part of the complex that came out as aggregation in the void volume of the column.

Nucleotide state analysis of the apo-ncd-tubulin-DARPin complex

I prepared the nucleotide-free kinesin-14 complex by mixing directly the kinesin construct with tubulin-DARPin, instead of treating kinesin-14 with apyrase to digest the nucleotide

trapped in the motor. There are several reasons for this procedure. First, in the absence of microtubules or of tubulin the nucleotide-free kinesin-14 motor is very unstable and aggregates easily (see above). Second, although apyrase digests ATP and ADP in priority, it also hydrolyzes GDP and GTP. Therefore apyrase treatment cannot be performed on the complex because hydrolysis of GDP or GTP may destabilize the tubulin heterodimer. Finally, this procedure has worked in the case of kinesin-1.

However, although the same method was used to produce the apo-kinesin-1 tubulin DARPIn complex, I wanted to check its efficiency in the case of a kinesin-14. The nucleotide content of a kinesin-14-tubulin-DARPIn complex was checked by ion exchange chromatography (Fig. 7.10), after protein denaturation to release the bound nucleotide. The results indicated that the complex contains only GDP and GTP that come from tubulin. Therefore mixing kinesin-14 with tubulin-DARPIn leads to a complex with nucleotide-free kinesin-14.

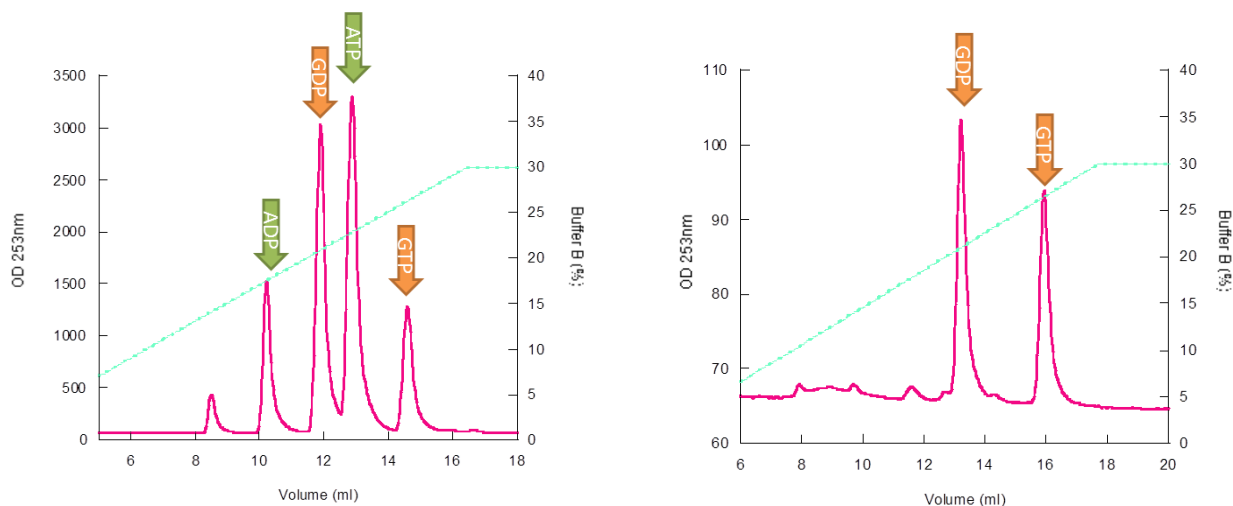


Figure 7.10 Nucleotide analysis of an “apo-”ncd tubulin-DARPIn complex.

Left: control with a mix of ADP, ATP, GDP and GTP injected to a Mono Q column and eluted with a salt gradient.

Right: nucleotide content analysis of apo-ncd-tubulin-DARPIn complex. By comparing the positions of peaks in the upper and lower figures, I could figure out the nucleotide component in an apo-ncd tubulin DARPIn complex.

3.4 Crystallization

Kinesin-14 constructs in different nucleotide states were mixed with tubulin stabilized by different DARPins, then the complexes were purified by gel filtration chromatography as

described above. Commercially available crystallization kits were used to screen for crystallization conditions of concentrated kinesin-14-tubulin-DARPin complexes. Some home-made kits were tried as well. However, whereas crystals have been obtained, they were of tubulin-DARPin complexes only and not of the ternary complexes.

As a means to increase the likelihood of obtaining crystals of kinesin-14-tubulin-DARPin complexes, I also digested tubulin with subtilisin. The C-terminal part of both tubulin subunits is flexible. Moreover, it is heterogeneous because of differences between tubulin isoforms and because of post-translational modifications. These features are a priori unfavorable for crystallization. These C-terminal tails can be removed by subtilisin limited proteolysis. Unfortunately it turned out to be unsuccessful as well. After several different DARPins and different commercial kits have been tried, there is no crystal of kinesin-14-DARPin in complex with subtilisin-treated tubulin has been obtained.

In addition I tried to crystallize Hetero-Kar3 in the AMPPNP state alone (without tubulin). The initial idea was to observe the effect of ATP binding on the orientation of the stalk. Crystals were obtained in several conditions and a high resolution dataset was collected. However, molecular replacement with the Kar3 motor domain failed, suggesting that these were probably not crystals of Kar3. I tried to analyze the component of crystals by SDS Page, but nothing was observed on the gel. What crystallizes is probably either a protein contaminant or the motor-less peptide of the heterodimer. But this should be confirmed by further analysis.

3.5 Discussion

Despite a lot of attempts, kinesin-14s still have not been successfully crystallized in complex with tubulin (and a DARPin). This could be due to several reasons, including the quality of the kinesin-14 constructs and the quality of the kinesin-14 tubulin DARPin complexes.

SHD heterodimer stability

A successful case where Kar3/Vik1 heterodimer was crystallized with the help of SHD has been reported. The Kar3/Vik1 heterodimer was purified and crystallized at a pH varying from 7.5 to 8 (Rank et al. 2012).

Another previous study indicated that the SHD is sensitive to pH, with a lower stability at pH 5 compared to pH 7 (Fig. 7.11). In my case, crystals were usually obtained at pH below 7, which may have led to the destabilization of the kinesin-14 heterodimer. In addition, the K3 peptide is linked to a small part of Vik1 stalk, without a motor-homology domain. What crystallized is probably the self-polymerized K3 Vik1 peptide. More sensitive methods should be used to check the components in the crystals.

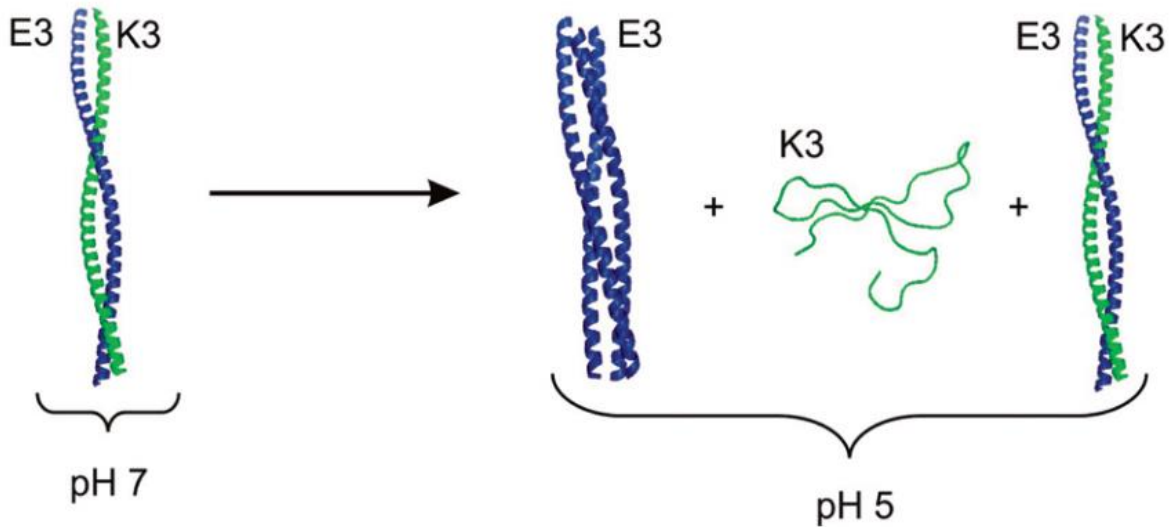


Figure 7.11 SHD conformation changes according to the pH. (Apostolovic and Klok 2008)

In neutral solution, the two peptides of SHD form a stable heterodimer. But at lower pH, the heterodimer is less stable and E3 homotrimer, K3 monomers and dimers (not shown here) as well as E3/K3 heterodimers coexist in the same solution.

Quality of Kinesin-14 motor domain

Kinesin-14 motor domains are much less stable than the conventional kinesin-1 motor domain. First, they are unstable in the nucleotide-free state, as shown above. Moreover, without excess nucleotide kinesin-14 motors precipitate easily. Precipitates are also observed even with excess nucleotide. Second, the solubility of kinesin-14 motors is salt dependent. Although a spin down assay with 4 μM Ncd did not indicate a substantial difference in solubility according to the salt conditions (Fig. 7.6), at the protein concentration needed for crystallization experiments (usually more than 100 μM), aggregates are observed when the concentration of salt is lower than 100 mM. Different salt or other additives may be tried to generate stable kinesin-14 motors.

Quality of Kinesin-14 in complex with tubulin-DARPin

Even in complex with tubulin-DARPin, kinesin-14 motors precipitate with its partner proteins. Both Kar3 and Ncd are able to form ternary complexes with tubulin-DARPin no matter the nucleotide state of the kinesin-14. But gel filtration chromatography indicates that some aggregates are formed. Even though the aggregates are separated from the 1:1:1 kinesin-14:tubulin:DARPin complex by gel filtration chromatography, aggregation may still happen later on, especially during concentration. The quality of kinesin-14-tubulin-DARPin

complex should be further checked in order to know the stability of complex during the process of crystallizing screening, i.e. the complex should be analyzed by gel filtration after concentration, after 1 day incubation at room temperature and after a few days incubation.

The case of Vik1 seems more favorable. The gel filtration chromatography indicates that a ternary complex with tubulin-DARPin is formed; no obvious aggregation was detected: a single peak was observed (Fig. 7.9). This result suggested that the vik1-tubulin-DARPin complex is stable and homogeneous. Nevertheless, so far, no useful crystal of Vik1-tubulin-DARPin has been obtained.

I think more efforts can be tried to crystallize a kinesin-14 complex. For example, more covalent DARPin-kinesin constructs can be generated. As ATP-analog kinesin-1 in complex with tubulin-D2 has been crystallized, how D2 binds tubulin is known. D2-kinesin constructs can be designed based on this information in order to generate a stable kinesin-14-tubulin-D2 complex. Moreover, I may also try screening with the crystallization kits at 4 °C, considering the complex is unstable. Lowering the crystallizing temperature could increase the chances of crystals growth.

Conclusions and Perspectives

During my thesis, I have been interested in three aspects of kinesins motility. The first one is the structural study of a kinesin-1-tubulin-DARPin complex in which kinesin is in its nucleotide-free state. This structure was the main missing one in the kinesin mechanochemical cycle. The second one is, through a mutagenesis approach, the study of the mechanism of ADP release by kinesin-1. In the course of this study, I have also determined the structure of apo-kinesins (both WT kinesin and mutants) in two different conformations. Finally I have tried to obtain the crystal structure of kinesin-14 in complex with tubulin-DARPin. This last part has not met success so far.

A summary on the structural basis of kinesin-1 motility

Together with previous studies of kinesin motility, my work has allowed me to summarize the kinesin-1 homodimer's movement corresponding to the mechanochemical cycle of its two motor domains (Fig. 8.1).

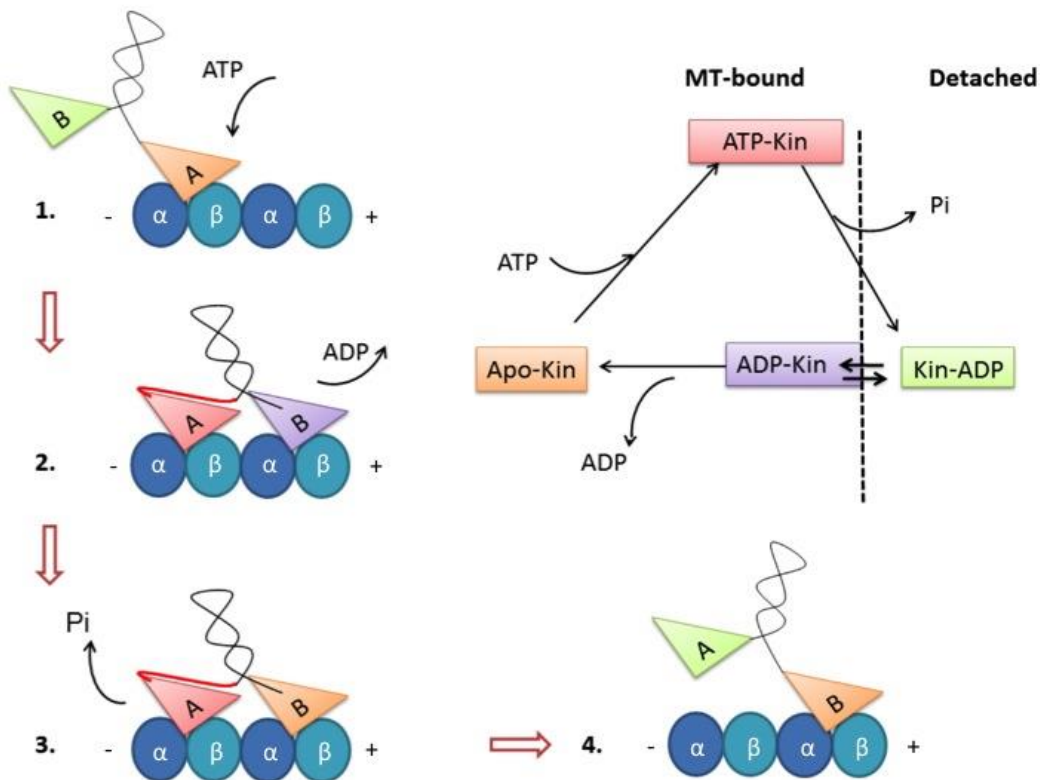


Figure 8.1 A model of kinesin-1's movement

Two motor domains (A and B) of Kinesin-1 homodimer are colored depending on their nucleotide states (with a same color pattern as presented in the kinesin cycle at the top right corner). Docked neck linker is shown in red.

Step 1: One motor domain (A) in nucleotide-free state binds to microtubule, with another motor domain (B) in ADP state detached.

Step 2: ATP binds to apo-motor A, causing the subdomain movement identified in this thesis. The movement of subdomains creates a space, which is remote from the nucleotide binding site, in motor A, allowing the first residue of neck linker (I325) to dock into.

In the meantime, ADP-motor B binds to microtubule. Microtubule brings conformational changes to motor B. In the tubulin binding subdomain, binding to microtubule makes the H4 helix extend and the whole L11 loop become ordered. Conformational changes in the tubulin binding subdomain induce the change of other parts. Elongation of H4 helix clashing with Switch 1 leads to the melting of L9 loop. The residue E236 located on L11 can no longer anchor the P-loop by forming hydrogen bonds with P-loop residue T87. P-loop destabilization together with P-loop subdomain rotation interferes with ADP binding. On the other hand, rotations of P-loop subdomain and Switch 1/2 subdomain, separating T92 and D231, disturb the magnesium binding environment. ADP release is further accelerated.

Step 3: In motor A, I325, as a pin, preventing subdomains from rotating back to the apo-like conformation, stabilizes the conformation in an ATP-like state where ATP can be hydrolyzed efficiently.

Step 4: Pi is released, ADP-motor-A detaches from microtubule with a flexible neck linker. The kinesin homodimer is reset back to the step 1 but with one step further.

The structure of apo-kinesin-1 in complex with tubulin

As the intermediate state between isolated ADP-kinesin and ATP-kinesin bound to microtubule in the kinesin cycle, the atomic structure of apo-kinesin bound to a microtubule (or tubulin) is expected to give insights into the mechanism of microtubule-stimulated ADP release, of the conformational changes accompanying ATP binding and leading to neck linker docking, and of ATP hydrolysis.

When I started this work, the structures of isolated ADP-kinesin (Kull et al. 1996; Sindelar et al. 2002; Sack et al. 1997) and of tubulin-bound ATP-like kinesin (Gigant et al. 2013) were known. These structures were very useful to precise the kinesin conformational changes upon microtubule binding, whose general features had been previously inferred from EM studies (Sindelar and Downing 2007; Goulet et al. 2012). These data led somehow to the division of the kinesin motor domain into two subdomains: a tubulin-binding one and a second and main block comprising the Switch1/2 and the P-loop subdomains. Because these two subdomains rotate roughly along the same axis when going from microtubule-bound ATP-kinesin to isolated ADP-kinesin (see Fig. 3 of Article 1), they were not discriminated at that time. In addition, the elements that interact with microtubule undergo a substantial conformational change upon binding (this includes in particular the

ordering of L11 and the lengthening of the H4 helix), that might have precluded the identification of more subtle changes. By contrast, in ATP-like-kinesin-tubulin and apo-kinesin-tubulin complexes, kinesin is always attached to tubulin, so the tubulin-binding subdomain does not vary much and the main variable is whether ATP is bound or not.

By comparing these two high-resolution tubulin-bound kinesin structures, the kinesin's three subdomains have been identified. ATP, located between the Switch 1/2 subdomain and the P-loop subdomain, is able to induce distinct rotations of these subdomains. Furthermore, the three-subdomain movement provides a structural explanation for the docking of the neck linker and for the efficiency of ATP hydrolysis in microtubule-bound ATP kinesin.

When ADP-kinesin and apo-kinesin-tubulin are compared, the nucleotide state is not the only variable. Having a structure of kinesin with nucleotide in the absence of tubulin and another one of tubulin-bound kinesin but without nucleotide, I found it's hard to isolate the conformational changes caused by tubulin binding or by nucleotide dissociation. Consequently, further studies were necessary to understand the kinesin's ADP dissociation mechanism and to dissociate the structural consequences linked to ADP release from those linked to microtubule binding. That's the reason I further did the mutagenesis study and structural study of isolated kinesin-1.

Moreover, it is worth trying to obtain the crystal structure of ADP-kinesin in complex with tubulin. As presented in the introduction part of this thesis, in kinesin-1's mechanochemical cycle, ADP-kinesin-1 binds to a microtubule, following which ADP is released. After ATP hydrolysis and the release of Pi, there is also a (transient) ADP-kinesin-microtubule complex. It is therefore of interest to obtain such a structure. By comparing isolated and tubulin-bound ADP-kinesin, we can have direct information on how microtubule binding and ADP binding influences each other. Whereas the affinity between ADP-kinesin and microtubules is relatively low, the K_D being about 10-20 μM (Cross 2004), and the ADP dissociation rate is high (about 50 s^{-1}), using highly concentrated protein and high concentration of ADP, it might be possible to crystallize an ADP-kinesin-tubulin-DARPin complex. There are several EM structures of different ADP-kinesins bound to microtubule reported, indicating that it's possible to generate such stable ADP-kinesin microtubule complexes so that it might be also possible to have a stable ADP-kinesin tubulin complex (Atherton et al. 2014; Goulet et al. 2012).

Another step of the kinesin cycle which could be studied structurally with apo-kinesin-tubulin crystals is the hydrolysis of ATP *in crystallo*. Because in this complex the kinesin is nucleotide-free, it might be possible to soak crystals with ATP. By freezing crystals in liquid nitrogen using different lengths of soaking time, theoretically, different stages of ATP hydrolysis can be observed. By analyzing these series of structures, we may obtain

structural information from nucleotide-free kinesin accepting ATP up to ADP-kinesin tending to detach from tubulin. There are several prerequisites for this experiment to work. First, the hydrolysis rate there should be slow enough to trap an ATP state or some intermediate states. Then, the ATP molecule should be able to diffuse up to the kinesin nucleotide-binding site. Moreover the kinesin structural changes upon ATP binding should be compatible with the crystal packing.

Mutagenesis study on kinesin-1

A mutagenesis study on kinesin-1 was performed to precise further the ADP release mechanism in kinesin motor domain. Residues, predicted to be involved in the mechanism of microtubule-stimulated ADP dissociation based on structural studies, were mutated in order to mimic the effect of microtubule binding. Furthermore, structures of some mutants in nucleotide-free state were determined. These results indicate that microtubule binding interferes with ADP binding in kinesin mainly through 1) disturbing its magnesium binding environment and 2) breaking the anchor which stabilizes the P-loop.

Interestingly, during this study I found that isolated wild type kinesin-1 in nucleotide-free state can be generated by ADP digestion with apyrase. Furthermore, with the presence of extra salt in the solution, apo-kinesin-1 can be almost as stable as ADP-bound kinesin-1, although it was reported that apo-kinesin can denature easily (Sadhu and Taylor 1992; Hackney 1994). Remarkably I crystallized apo-WT kinesin-1 in the conditions where apo-kinesin mutants have been crystallized and I obtained two apo-WT kinesin-1 structures, one of which has an ADP-like conformation and the other one is similar to that of tubulin-bound apo-kinesin. These results suggest that, in solution, apo-kinesin probably alternates between these two conformations. One possibility is that kinesin-1 with the apo-like conformation is less stable, probably a short-lived state with a relatively open nucleotide binding pocket which facilitates nucleotide rebinding; while kinesin-1 with the ADP-like conformation is as stable as ADP-kinesin with solvent replacing nucleotide occupying the binding pocket, guaranteeing the stability of apo-kinesin-1. In my opinion, it's accessible and worthy to further investigate the states of apo-kinesin-1 in solution.

These results also raise the following question: could ADP-kinesin adopt an apo-like conformation? When kinesin switches to the tubulin-bound apo-like conformation, upon subdomain rotation, the E236 interaction with the P-loop is broken so that the P-loop becomes unstable. In addition the magnesium binding environment is also disrupted. As a result, ADP dissociates from kinesin. Nevertheless, without microtubule binding, there is no stimulus favoring the conformational change. Interestingly, in the case of the kinesin-3 Kif14, an "apo-like" conformation of isolated Kif14 was obtained with bound ADP (but without magnesium) (Arora et al. 2014). In this case, although the E236 equivalent residue still interacts with the ADP-bound P-loop, the loop where the glutamic acid is embedded is

drawn with the movement of P-loop subdomain instead that P-loop is anchored by the glutamic acid. By contrast such a conformation has not been seen in the many other ADP-kinesin structures that have been determined. Is this a specific feature of Kif14? To try answering this question, I soaked the “apo-like” apo-kinesin crystals with nucleotides. But after incubation with 1mM ADP or AMPPNP for about 12 hours, no signal could be attributed to a bound nucleotide in the electron density maps, suggesting that kinesin-1 may not share this Kif14 feature. Alternatively the crystal packing might have precluded the entrance of the nucleotide. Therefore, to confirm this result, if different apo-like apo-kinesin crystals are obtained, it will be interesting to try to soak them with nucleotide.

In my opinion, conformations of apo-kinesin and ADP-kinesin in solution should be checked by experiments. If possible, apo or ADP kinesin in solution may be simulated by dynamic simulation. It may provide supporting evidence to our theory on kinesin’s ADP dissociation. It will bring an idea on how kinesin exchanges its nucleotide in a dynamic system as well.

Crystallization of kinesin-14 in complex with tubulin-DARPin

Kinesin-14s are peculiar because they move towards the microtubule minus end, a property shared by the dyneins whereas the other motile kinesins move towards the plus end. In addition they are the only members in the kinesin superfamily that have the motor domain positioned at the C-terminal end of the protein. Therefore a structure of tubulin-bound kinesin-14 would be very useful to gain insights not only into how the movement in kinesin-14 is generated but also into the direction control in kinesin superfamily. Although substantial efforts have been made, kinesin-14s or its non-motor partner vik1 haven’t been co-crystallized with tubulin-DARPin successfully yet. Several reasons could be invoked, including the instability of kinesin-14s per se and the instability of the complex.

Nonetheless I have shown that kinesin-14s are able to form complexes with tubulin-DARPin and that these complexes are stable enough to be purified by gel filtration. Based on these results, I think it’s worth trying to obtain a kinesin-14-tubulin crystal structure. Among different possibilities that have not been tested so far, kinesin-14s different from Ncd or Kar3 could be tried. In addition, other DARPins could be used to stabilize the kinesin-14-tubulin complex for crystallization. Similarly, tubulin-stabilizing proteins targeting other tubulin surfaces compared to the current DARPins that bind the tubulin longitudinal interface could be tried as well. All these approaches should provide us with different kinesin-14-tubulin complexes, therefore with new chances to obtain useful crystals.

However, I think before more crystallizing conditions are screened and more DARPins are tried, the character of kinesin-14s and kinesin-14-tubulin-DARPin complexes should be

further studied. Efforts should be made to find a condition where more stable homogeneous kinesin-14-tubulin-DARPin complexes can be formed and be maintained.

One option would be to generate additional kinesin-14-DARPin chimerical constructs, in which the two proteins are linked together. Beside from D1, D2 is another DARPin whose binding site on tubulin has been determined (Gigant et al. 2013). D2 forms a stable complex with tubulin heterodimer. It should be possible to design a D2-kinesin-14 covalent construct in order to generate stable and homogenous 1:1:1 tubulin:kinesin-14:D2 complexes.

Finally another possibility to study kinesin-14 interacting with microtubule would be through cryo-electron microscopy. Recent development on cryo-EM pushes the resolution for protein structure determined by this method to new levels. Especially, impressive progress has been achieved on EM studies of microtubule and microtubule associated proteins. Rui ZHANG *et al.* determined 3.5 Å resolution microtubule structures in different nucleotide states (Zhang et al. 2015). Microtubule-bound kinesins in different nucleotide state have also been studied. The resolution achieved is in the 6 to 7 Å range (Atherton et al. 2014; Shang et al. 2014) and even an ADP-kinesin bound to microtubule has been studied at a 7 Å resolution (Atherton et al. 2014). A key feature in cryo-EM studies is the possibility to prepare homogenous samples for averaging. In particular, in the case of microtubule-decorated kinesins, microtubule should be saturated as much as possible and the kinesin molecules should be in very similar conformations. If homogenous samples can be prepared, the recent developments on cryo-EM provide an exciting and promising future for the structural study of kinesin-14 in complex with microtubule.

Materials and Methods

1. Differential Scanning Calorimetry assay on kinesin-1 and its mutants

Samples were prepared for Differential Scanning Calorimetry assay (DSC) by dialysis for the following goals. 1) to generate wild type and mutated kinesin (KHC 349) in nucleotide-free state, in addition to an ADP-bound wild type kinesin control; 2) to move the samples into a buffer whose pKa doesn't vary significantly with temperature, since during the experiment the system temperature increases; 3) to adjust the samples in the same condition.

1 μ l*200 U/ml Apyrase and 4 μ l * 0.25 M EDTA were added respectively into the T87A KHC 349, T87G KHC 349, T92V KHC 349 and WT KHC 349 samples with a volume about 200 μ l and a concentration around 200 μ M. Then, the samples were dialyzed against 400 ml buffer containing 30 mM NaH₂PO₄ pH 7.0, 150 mM NaCl, 0.5 mM EGTA, 1 mM MgCl₂ with a Dialysis Cassette 10,000 MWCO (Thermo™) at 4 °C overnight. In the same condition, about the same amount of ADP-kinesin was dialyzed against the same buffer without Apyrase and EDTA added.

Samples were diluted until ~0.5 mg/ml before loaded to the Differential Scanning Calorimetry. The dialyzing buffer served as blank.

2. Purification of Kinesin-14 heterodimer

2.1 Constructs

Kar3 and Ncd

Two types of kinesin-14 are tried in co-crystallization assays with tubulin-DARPin complexes. One is Ncd, a *Drosophila* kinesin-14; the other is Kar3, the only kinesin-14 in *Saccharomyces cerevisiae*. Both of them are regarded as kinesin-14 models and well-studied biochemically. Ncd is a homodimer, having two catalytic cores locating at its C-terminus. Kar3 in cells works as a heterodimer with one catalytic core dimerized with a non-motor domain, Vik1 or Cik1.

For kinesin-14, the conformational change leading to movement is associated with its coiled-coil stalk rotation. So I designed kinesin-14 heterodimers containing one catalytic core plus a C-terminal part of dimeric coiled-coil. In other words, for ncd homodimer, one

catalytic motor is truncated; for Kar3 heterodimer, the motor-homology domain of Vik1 is deleted (Fig. 9.1).

Because both Ncd and Kar3 are able to form homodimers *in vitro* (Sablin et al. 1998; Chu et al. 2005), to generate the heterodimer, a synthetic heterodimer (SHD) is introduced at the N-terminus of the constructs, one half of the SHD in each chain (Rank et al. 2012). The SHD containing an acidic helix and a basic helix is supposed to form a stable heterodimer with hydrophobic interactions between their paired leucine and isoleucine residues. For the short helix without motor domain, a His-tag is added to its N-terminal, followed by a cleavable TEV site, in order to purify the heterodimeric protein.

Moreover, for Ncd, two different lengths of motor domain are tried, Ncd 700 stop and Ncd 679 stop. One is the full length Ncd motor domain; in the other construct, the C-terminal part of Ncd (from 680 to 700), which is not observed in the crystal structures of either wild type ADP-Ncd or Ncd mutants which mimic Ncds in different nucleotide state, is truncated to facilitate crystallization.

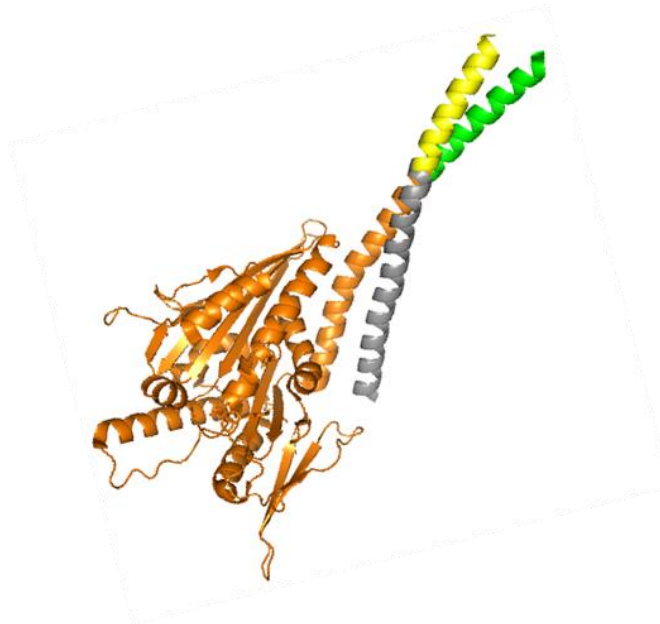


Figure 9.1 A model of Kar3 heterodimer

*Kar3's catalytic motor domain and a part of its N-terminus stalk, both colored in orange, are dimerized with Kar3's non-motor partner Vik1 (grey) by forming a coiled-coil. The motor-homology domain of Vik1 is deleted; otherwise, this domain is able to bind another tubulin heterodimer. To improve the yield of heterodimer, as Kar3 can form a homodimer *in vitro*, a synthetic heterodimer (SHD) is introduced into the construct. An acidic helix (green) and a basic helix (yellow) in a SHD tend to bind each other and reinforce the helix-helix interaction.*

Constructs for Hetero Ncd:

Chain A: MEIAALEKEIAALEKE + Ncd 321-end (679 stop, 700 stop)

Chain B: MKHHHHHHHPMSDYDIPTTENLYFQ/GAMGKIAALKEKIAALKEK + Ncd 321-347

Constructs for Hetero Kar3:

Chain A: MEIAALEKEIAALEKEIAALEKEI+Kar3 353-end (729 stop)

Chain B: MKHHHHHHHPMSDYDIPTTENLYFQ/GAMGKIAALKEKIAALKEKIAALKEKI + Vik1 341-373

In addition, Ncd (325-700), Ncd (325-679) and Kar3 (353-729) motor domain monomers are tried in co-crystallization experiments with tubulin-DARPin complexes.

Vik1

Vik1 is the motor-homology partner of Kar3. It is supposed to form a heterodimer with Kar3 in cells and modulate the binding of the Kar3 motor domain to microtubules. Its motor-homology domain alone, whose crystal structure has been determined (Allingham et al. 2007), is able to bind microtubules itself with a high affinity ($K_D = 43$ nM). But there is neither an EM structure nor a crystal structure of Vik1 bound to a microtubule or to tubulin. How the motor-homology domain interacts with microtubules is unclear. Therefore, I also tried to obtain the crystal structure of Vik1 motor-homology domain (353-647) in complex with tubulin-DARPin.

2.2 Plasmid construction

Monomer

Ncd-GFP was a gift from Dr. Ron Vale (Addgene plasmid # 24507). Plasmids containing full length Vik1 and Kar3 gene are gifts from Dr. Stefan Westermann.

Ncd 325-700, Kar3 353-729 and Vik1 353-647 were amplified by PCR; restriction sites were added to both sides of the sequence. The amplified genes were then inserted into pET-M11 plasmid, right after a His-tag and a TEV cleavage site.

Ncd 325-679 plasmid was generated by inserting a stop codon after that of residue 679.

The sequences of inserting fragments were checked with T7 (TAATACGACTCACTATAGGG) and pET-RP (CTAGTTATTGCTCAGCGG) as sequencing primers.

Heterodimer

In order to express the two chains of the heterodimer in a same cell, pET-Duet1 with two T7 promoters is used as a vector. It has two ribosome binding sites, each of which is followed by an independent open reading frame (Fig. 9.2).

DNA sequence coding for SHD' was added to the N-terminus of Ncd321-347 (or Vik1 341-373) by two rounds of PCR, then the fragment was inserted into pET-M11, right after a His-tag and a TEV cleavage site. Another round of PCR was performed to clone the full sequence of His-TEV-SHD'- Ncd321-347 (or Vik1 341-373). The amplified fragment was inserted into the first open reading frame of pET-Duet1.

DNA sequence coding SHD is introduced into the N-terminus of NCD 321-700 (or Kar3 353-729) by two rounds of PCR. The amplified fragment was inserted into the second open reading frame of the vector.



Figure 9.2 pETDuet-1 cloning/expression regions

There are two open reading frames in the pETDuet-1 plasmid, each of which is following an independent pair of T7 promoter and ribosome binding site. As a consequence, both inserted constructs can be expressed independently in the same system at the same time.

The sequences of inserting fragments were checked with T7 (TAATACGACTCACTATAGGG), DuetUP2 (TTGTACACGGCCGCATAATC) and pET-RP (CTAGTTATTGCTCAGCGG) as sequencing primers. The positions where these primers bind to are shown in figure 9.2.

Ncd 679 stop

The codon of residue 680 in Ncd was mutated to a stop codon to generate a short Ncd construct by QuikChange II Site-directed Mutagenesis Method (Fig. 9.3). The same method was used to generate single mutations in Kinesin-1 as well.

A 45 bp DNA fragment, containing the target mutation in the middle of the sequence, and its reverse complement fragment are synthesized as primers for PCR amplification. A plasmid containing the mother construct is used as template. Here, both Hetero-Ncd 700 plasmid and Ncd 700 motor plasmid were used as templates.

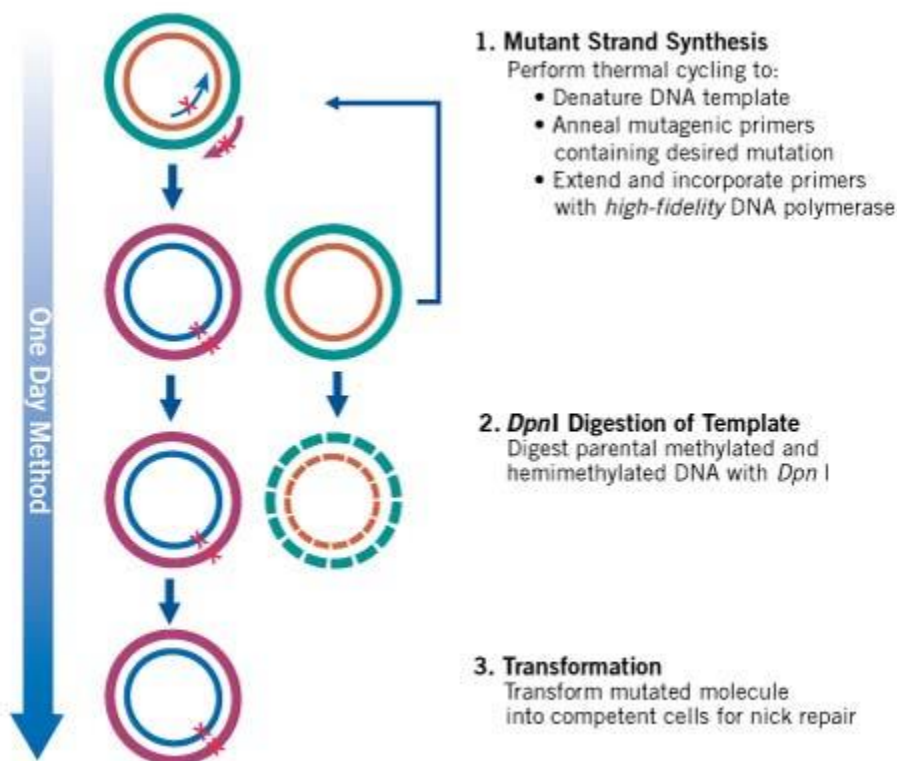


Figure 9.3 Overview of the QuikChange II Site-directed Mutagenesis Method (Agilent Technology™).

*A pair of mutagenic primers containing the desired mutation is designed to produce linear fragment of the whole sequence of the plasmid. After treated by *Dpn*I, the original plasmids are digested, while only the plasmid fragment produced by PCR is left. The linear fragment is*

transformed into competent cells directly. Normal plasmids with the desired mutation will be formed by nick repair in vivo.

PCR procedure:

Step 1: 95°C, 2 min

Step 2: 95°C, 30 s

55°C, 1 min

68°C, 6 min 30 s

For 20 cycles

Step 3: 68°C, 15 min

Step 4: 4°C, forever

The PCR products are purified with a GeneJET Gel Extraction and DNA Cleanup Micro Kit (Thermo Scientific™). Then, a fast digest enzyme DpnI is used to digest the initial template which contains methylated and hemi-methylated DNA. Fragments are purified again with GeneJET Gel Extraction and DNA Cleanup Micro Kit (Thermo Scientific™) and transformed into XL1-Blue competent cells by a heat shock reaction (45 seconds at 42°C).

Sequence of the constructs containing target mutations are checked by sequencing the plasmid with T7 (TAATACGACTCACTATAGGG) as a forward primer and pET-RP (CTAGTTATTGCTCAGCGG) as a reverse primer.

2.3 Expression and purification

Transformation and Pre-culture

The competent bacteria (homemade) are transformed with the target plasmid by heat shock. *E. coli* Rosetta are used as competent cells because they contain plasmids (with chloramphenicol as selective antibiotics) for tRNA of rare codons as found in kinesin-14's sequence. 1 µL plasmid is mixed with 100 µL Rosetta and incubated on ice for 30 minutes. Then, a heat shock (45 seconds at 42°C) is applied and afterwards the cells are incubated on ice immediately for about 2 minutes. Add 850 µL preheated 2YT and incubate in a shaker (250 RPM, 37 °C) for about one hour. 2YT is an enriched medium which consists of Bacto Trypton 16 mg/mL, Yeast extract 5 mg/mL, NaCl 5 mg/mL. Streak at least 50 µL on a LB agar plate containing antibiotics. 100 µg/mL ampicillin and 25 µg/mL chloramphenicol serve as antibiotics to select positive colonies for heterodimers (carried by pET-Duet1). Or

50 µg/mL kanamycin and 25 µg/mL chloramphenicol serve as antibiotics to select positive colonies for monomers (carried by pET-M11). The plates were incubated overnight at 37 °C.

A single colony was picked and pre-cultured in 20 mL LB liquid medium (10 mg/mL tryptone, 5 mg/mL yeast extract, 10 mg/mL NaCl) with relevant antibiotics. Pre-culture system is kept on a shaker with a speed of 200 rpm overnight at 37°C.

Culture and Inducement

The second day, 10 mL pre-culture cell is added into 1 L 2YT medium containing the same concentration of the same antibiotics as the pre-culture system. Cells are cultured on a shaker at 37°C (usually for about 3h) until its OD₆₀₀ reaches 0.8-1.

0.5 mM IPTG is added to induce the expression of the target protein. The bacterial cultures are moved to 18°C overnight (about 16-18 hours).

Afterwards, cells are harvested by centrifugation 20 min at 5000g at 4°C.

Extraction

Cells are resuspended with 20 mL Lysis buffer containing Hepes pH 7.2 25 mM, NaCl 150 mM, DTT 1 mM, PMSF (Phenylmethylsulfonyl fluoride) 1mM and a tablet of EDTA free protease inhibitor cocktail (Roche™). Then, the cells are frozen and lysed using a French pressure cell press. DNase (1µg/mL) is added after the sample has been thawed. Finally, the mixture is centrifuged at 30000g at 4°C for one hour and the pellet is discarded. The supernatant is filtered with a 0.2 µm filter right before injected into a column.

Purification

Kinesin-14s are initially purified by an affinity chromatography. The N-terminal His-tag allows kinesin-14s to bind to a Ni-column (HisTrap HP 5 ml, GE Healthcare™). The loading buffer contains Hepes pH 7.2 25 mM, MgCl₂ 2 mM, EGTA 1 mM, 150 mM NaCl, 20 mM Imidazole, 1 mM DTT and ATP 25 µM. The elution buffer is prepared by adding 0.5 M Imidazole to the loading buffer. For the first purification step, the sample is eluted by a gradient elution (0% to 40% in 10 min). Target protein elutes at about 30% elution buffer. TEV (homemade) is added to the peak collected with an estimated ratio about 1:20 (w/w), in order to remove the His-tag. Then, the collected fractions mixed with TEV are dialyzed against the loading buffer overnight at 4 °C to dilute the imidazole in the solution.

For the second purification step, protein is injected to the same column. But this time, the flow through is collected. Small fragments with the cut His-tag and TEV and fragments with an uncut His-tag as well will be trapped on the column.

Protein purified is finally concentrated to 300-500 µM and kept at -80°C.

3. Production of Kinesin-Tubulin-DARPin complex

3.1 DARPin purification

Several DARPins that bind tubulin with high affinity, K_D ranges from 100 nM (or lower) to 200 nM, without interfering with kinesin binding were available in the laboratory.

Transformation

cf. Transformation of kinesin-14. To express DARPin, XL1 blue (Invitrogen™) are used as competent cells. 50 µg/mL Ampicillin is used as antibiotics to select positive colonies.

Pre-culture

Inoculate 30 mL LB containing 50 µg/mL Ampicillin and 1% Glucose with a single colony and incubate the pre-culture overnight at 37 °C in a shaker.

Culture

Inoculate 1 L LB containing 50 µg/mL Ampicillin with the overnight pre-culture to make the initial OD₆₀₀ around 0.1. The culture is then incubated at 37 °C under shaking until its OD₆₀₀ reaches 0.6 to 0.8. 0.5 mM IPTG is added to induce the expression of the DARPin. The culture is kept in the same conditions as pre-culture for four hours. Finally, the cells are harvested by centrifugation at 6000 g for 15 minutes at 4 °C. If the protein is not extracted immediately, the harvested cells are stored at -80 °C.

Extraction

Use 50 mL Lysis buffer containing Tris pH 8 50 mM, NaCl 300 mM, MgCl₂ 5 mM, imidazole 10 mM, lysozyme 0.5 mg/mL, beta-mercaptoethanol 10 mM which is added extemporaneously together with a complete pill of EDTA free anti-protease inhibitor cocktail (Roche™) to resuspend the pellet. Cells are kept on ice and sonicated 6 times for 30 seconds at 40 W with 30 seconds intervals. Then, the supernatant and pellet are separated by centrifugation at 20000 g at 4 °C for 20 minutes. The pellet is discarded. The supernatant is filtered with a 0.2 µm filter right before injected into a column.

Purification

DARPin is purified in two steps: the first one is by affinity chromatography on a Ni-column (HisTrap HP 5 ml, GE Healthcare™). Then a gel filtration chromatography on a Superdex 75 column (GE Healthcare™) is performed.

For the HisTrap column, the loading buffer contains Tris pH 8 50 mM, NaCl 300 mM, Imidazole 15 mM and beta-mercaptoethanol 1 mM; the high salt buffer contains Tris pH 8

50 mM, NaCl 1 M and Imidazole 15 mM; and the elution buffer contains Tris pH 8 50 mM, NaCl 100 mM and Imidazole 0.5 M. After loading the sample in loading buffer conditions, the column is washed with 100% high salt buffer. Then the DARPin is eluted with 50% elution buffer and the peak is collected. Finally, the sample collected is concentrated to a volume of 2 mL to improve the efficiency of gel filtration.

The gel filtration buffer contains K-phosphate pH 7.2 20 mM, EGTA 0.5 mM, MgCl₂ 1 mM and KCl 100 mM.

Purified DARPin is concentrated until the concentration reaches at least 500 μM, then stored at -80°C.

3.2 Tubulin DARPin complex

Tubulin recycling

An aliquot of 500 μL purified sheep tubulin in Mes pH 6.8 50 mM, GTP 0.1 mM and 1/3 Glycerol (v/v) at about 30 mg/mL is recycled by one cycle of “polymerization-depolymerization” (Castoldi and Popov 2003; Dorleans, Knossow, and Gigant 2007). A PD-10 column is then used to exchange the buffer to Pipes-K pH 6.8 50 mM, EGTA 0.4 mM, MgCl₂ 0.5 mM and GDP 10 μM. This procedure is to recover fully functional tubulin.

Reaction

DARPin and tubulin are mixed with a ratio of 1.2 to 1, and the complex is stored in liquid nitrogen until being used.

3.3 Subtilisin-cleaved tubulin

Tubulin is treated with subtilisin protease VIII (Sigma™) so that the flexible C-termini of the two tubulin chains are removed. Subtilisin-cleaved tubulin is reported to have a higher homogeneity. Therefore, subtilisin treatment should be tried to increase the likelihood of complexes crystallization.

First, recycled tubulin at whatever concentration (usually 100 μM) is diluted to guarantee a low salt condition (e.g. 12.5 mM Mes pH6.8, 0.25 mM MgCl₂, 0.25 mM EGTA). GDP is added to reach a final concentration of 0.5 mM.

The tubulin solution is equilibrated at 25 °C about 5 min before subtilisin is added. The ratio between subtilisin:tubulin is 1:100 (W/W). Then the mixture of tubulin and subtilisin is incubated at 25 °C about 20 min. Usually, after the incubation, the solution becomes turbid.

PMSF is added to reach a final concentration of 0.1 % (W/V) in order to stop the reaction. The solution is incubated on ice for 5 min.

DARPin is added to subtilisin-treated tubulin, with a ratio about 1.2:1 (DARPin:tubulin). The solution is still cloudy, due to some precipitated PMSF. Centrifugation 15000 rpm * 15 min is performed to get rid of the precipitant. Then the DARPin-bound cleaved tubulin is mixed with kinesin-14. The complex is further purified by a gel filtration chromatography.

4. Nucleotide state analysis

In theory, the nucleotide-free Kinesin-tubulin-DARPin complex shouldn't contain any ADP or ATP, while the two subunits of tubulin bind a GTP (α tubulin) and a GDP or a GTP (β tubulin), depending on the way tubulin has been prepared. The nucleotide content of the complex is analyzed by anion exchange chromatography on Mono Q (GE Healthcare TM). The nucleotides are detected by the absorbance at 253 nm.

Tris-HCl pH 8 20 mM is used as loading buffer, while elution buffer is the same as loading buffer supplemented with 1 M KCl. As a control, 500 μ L mixtures of ADP, ATP, GDP and GTP is injected and eluted by a 0 to 30% gradient of elution buffer in 15 minutes (with a flow 1 ml/min).

10 μ L concentrated Kinesin-tubulin-DARPin (Abs_{280} between 20 and 30) is diluted to 30 μ L so that the desalting microBiospin 6 column (Bio-Rad TM) can be used to remove unbound nucleotide. The protein is then denatured by adding 0.5 μ L Trifluoroacetic acid at room temperature, which denatures the protein and releases nucleotides. The sample is centrifuged (15000g * 15 min) and the supernatant (free of denatured protein) is neutralized with KOH and injected. The sample is eluted by a 0 to 30 % gradient of elution buffer in 15 minutes (with a flow 1 ml/min).

5. Spin down assay

50 μ L Ncd (2 μ M or 4 μ M) is incubated with various concentrations of microtubules (from 0 to 4 μ M) in the buffer containing 50 mM Pipes pH 6.8, 2 mM $MgCl_2$, 1 mM EGTA, 2 mM AMPPNP at 25 °C for at least 30 min. 1 μ M Taxol is added to prevent microtubules from depolymerizing.

Then, supernatant and pellet are separated by ultracentrifugation at 85 000 rpm for 15 min at 35 °C. The pellet is resuspended in 50 μ L buffer.

The separated supernatant and the pellet are analyzed by SDS-PAGE respectively.

References

- Adams, P. D., P. V. Afonine, G. Bunkoczi, V. B. Chen, I. W. Davis, N. Echols, J. J. Headd, L. W. Hung, G. J. Kapral, R. W. Grosse-Kunstleve, A. J. McCoy, N. W. Moriarty, R. Oeffner, R. J. Read, D. C. Richardson, J. S. Richardson, T. C. Terwilliger, and P. H. Zwart. 2010. 'PHENIX: a comprehensive Python-based system for macromolecular structure solution', *Acta Crystallogr D Biol Crystallogr*, 66: 213-21.
- Ahmad, S., L. Pecqueur, B. Dreier, D. Hamdane, M. Aumont-Nicaise, A. Pluckthun, M. Knossow, and B. Gigant. 2016. 'Destabilizing an interacting motif strengthens the association of a designed ankyrin repeat protein with tubulin', *Sci Rep*, 6: 28922.
- Allingham, J. S., L. R. Sproul, I. Rayment, and S. P. Gilbert. 2007. 'Vik1 modulates microtubule-Kar3 interactions through a motor domain that lacks an active site', *Cell*, 128: 1161-72.
- Amos, L. A., and D. Schlieper. 2005. 'Microtubules and maps', *Adv Protein Chem*, 71: 257-98.
- Andreasson, J. O., B. Milic, G. Y. Chen, N. R. Guydosh, W. O. Hancock, and S. M. Block. 2015. 'Examining kinesin processivity within a general gating framework', *Elife*, 4: e07403.
- Apostolovic, B., and H. A. Klok. 2008. 'pH-sensitivity of the E3/K3 heterodimeric coiled coil', *Biomacromolecules*, 9: 3173-80.
- Arora, K., L. Talje, A. B. Asenjo, P. Andersen, K. Atchia, M. Joshi, H. Sosa, J. S. Allingham, and B. H. Kwok. 2014. 'KIF14 binds tightly to microtubules and adopts a rigor-like conformation', *J Mol Biol*, 426: 2997-3015.
- Asbury, C. L. 2005. 'Kinesin: world's tiniest biped', *Curr Opin Cell Biol*, 17: 89-97.
- Atherton, J., I. Farabella, I. M. Yu, S. S. Rosenfeld, A. Houdusse, M. Topf, and C. A. Moores. 2014. 'Conserved mechanisms of microtubule-stimulated ADP release, ATP binding, and force generation in transport kinesins', *Elife*, 3: e03680.
- Bhabha, G., G. T. Johnson, C. M. Schroeder, and R. D. Vale. 2016. 'How Dynein Moves Along Microtubules', *Trends Biochem Sci*, 41: 94-105.
- Block, S. M. 2007. 'Kinesin motor mechanics: binding, stepping, tracking, gating, and limping', *Biophys J*, 92: 2986-95.
- Bricogne, G., E. Blanc, M. Brandl, C. Flensburg, P. Keller, W. Paciorek, P. Roversi, A. Sharff, O.S. Smart, C. Vornrhein, and T.O. Womack. 2011. 'BUSTER version 2.10.0 Cambridge, United Kingdom: Global Phasing Ltd.'
- Brouhard, G. J. 2015. 'Dynamic instability 30 years later: complexities in microtubule growth and catastrophe', *Mol Biol Cell*, 26: 1207-10.
- Cao, L., W. Wang, Q. Jiang, C. Wang, M. Knossow, and B. Gigant. 2014. 'The structure of apo-kinesin bound to tubulin links the nucleotide cycle to movement', *Nat Commun*, 5: 5364.
- Castoldi, M., and A. V. Popov. 2003. 'Purification of brain tubulin through two cycles of polymerization-depolymerization in a high-molarity buffer', *Protein Expr Purif*, 32: 83-8.
- Cecchini, M., A. Houdusse, and M. Karplus. 2008. 'Allosteric communication in myosin V: from small conformational changes to large directed movements', *PLoS Comput Biol*, 4: e1000129.
- Chen, C. J., I. Rayment, and S. P. Gilbert. 2011. 'Kinesin Kar3Cik1 ATPase pathway for microtubule cross-linking', *J Biol Chem*, 286: 29261-72.

- Cheng, Jing-Qui, Wei Jiang, and David D. Hackney. 1998. 'Interaction of mant-adenosine nucleotides and magnesium with kinesin', *Biochemistry*, 37: 5288-95.
- Chu, H. M., M. Yun, D. E. Anderson, H. Sage, H. W. Park, and S. A. Endow. 2005. 'Kar3 interaction with Cik1 alters motor structure and function', *EMBO J*, 24: 3214-23.
- Conde, C., and A. Caceres. 2009. 'Microtubule assembly, organization and dynamics in axons and dendrites', *Nat Rev Neurosci*, 10: 319-32.
- Cormier, A., M. Knossow, C. Wang, and B. Gigant. 2010. 'The binding of vinca domain agents to tubulin: structural and biochemical studies', *Methods Cell Biol*, 95: 373-90.
- Coureux, P. D., A. L. Wells, J. Menetrey, C. M. Yengo, C. A. Morris, H. L. Sweeney, and A. Houdusse. 2003. 'A structural state of the myosin V motor without bound nucleotide', *Nature*, 425: 419-23.
- Coy, D. L., M. Wagenbach, and J. Howard. 1999. 'Kinesin takes one 8-nm step for each ATP that it hydrolyzes', *J Biol Chem*, 274: 3667-71.
- Crevel, I. M., A. Lockhart, and R. A. Cross. 1996. 'Weak and strong states of kinesin and ncd', *J Mol Biol*, 257: 66-76.
- Crevel, I. M., M. Nyitrai, M. C. Alonso, S. Weiss, M. A. Geeves, and R. A. Cross. 2004. 'What kinesin does at roadblocks: the coordination mechanism for molecular walking', *EMBO J*, 23: 23-32.
- Cross, R. A. 2004. 'The kinetic mechanism of kinesin', *Trends Biochem Sci*, 29: 301-9.
- DeLano, W.L. 2010. 'The PyMOL Molecular Graphics System'.
- Dogan, M. Y., S. Can, F. B. Cleary, V. Purde, and A. Yildiz. 2015. 'Kinesin's front head is gated by the backward orientation of its neck linker', *Cell Rep*, 10: 1967-73.
- Dorleans, A., M. Knossow, and B. Gigant. 2007. 'Studying drug-tubulin interactions by X-ray crystallography', *Methods Mol Med*, 137: 235-43.
- Downing, K. H., and E. Nogales. 1998. 'Tubulin and microtubule structure', *Curr Opin Cell Biol*, 10: 16-22.
- Dutcher, S. K. 2001. 'The tubulin fraternity: alpha to eta', *Curr Opin Cell Biol*, 13: 49-54.
- Emsley, P., B. Lohkamp, W. G. Scott, and K. Cowtan. 2010. 'Features and development of Coot', *Acta Crystallogr D Biol Crystallogr*, 66: 486-501.
- Endres, N. F., C. Yoshioka, R. A. Milligan, and R. D. Vale. 2006. 'A lever-arm rotation drives motility of the minus-end-directed kinesin Ncd', *Nature*, 439: 875-8.
- Gigant, B., W. Wang, B. Dreier, Q. Jiang, L. Pecqueur, A. Pluckthun, C. Wang, and M. Knossow. 2013. 'Structure of a kinesin-tubulin complex and implications for kinesin motility', *Nat Struct Mol Biol*, 20: 1001-7.
- Gonzalez, M. A., J. Cope, K. C. Rank, C. J. Chen, P. Tittmann, I. Rayment, S. P. Gilbert, and A. Hoenger. 2013. 'Common mechanistic themes for the powerstroke of kinesin-14 motors', *J Struct Biol*, 184: 335-44.
- Goulet, A., W. M. Behnke-Parks, C. V. Sindelar, J. Major, S. S. Rosenfeld, and C. A. Moores. 2012. 'The structural basis of force generation by the mitotic motor kinesin-5', *J Biol Chem*, 287: 44654-66.
- Gulick, A. M., H. Song, S. A. Endow, and I. Rayment. 1998. 'X-ray crystal structure of the yeast Kar3 motor domain complexed with Mg.ADP to 2.3 Å resolution', *Biochemistry*, 37: 1769-76.
- Hackney, D. D. 1988. 'Kinesin ATPase: rate-limiting ADP release', *Proc Natl Acad Sci U S A*, 85: 6314-8.

- Hackney, D. D. 1994. 'Evidence for alternating head catalysis by kinesin during microtubule-stimulated ATP hydrolysis', *Proc Natl Acad Sci U S A*, 91: 6865-9.
- Hackney, D. D. 1996. 'The kinetic cycles of myosin, kinesin, and dynein', *Annu Rev Physiol*, 58: 731-50.
- Hackney, D. D., M. F. Stock, J. Moore, and R. A. Patterson. 2003. 'Modulation of kinesin half-site ADP release and kinetic processivity by a spacer between the head groups', *Biochemistry*, 42: 12011-8.
- Hammer, J. A., 3rd, and J. R. Sellers. 2012. 'Walking to work: roles for class V myosins as cargo transporters', *Nat Rev Mol Cell Biol*, 13: 13-26.
- Hancock, W. O. 2016. 'The Kinesin-1 chemomechanical cycle: stepping toward a consensus', *Biophys J*, 110: 1216-25.
- Heuston, E., C. E. Bronner, F. J. Kull, and S. A. Endow. 2010. 'A kinesin motor in a force-producing conformation', *BMC Struct Biol*, 10: 19.
- Higuchi, H., C. E. Bronner, H. W. Park, and S. A. Endow. 2004. 'Rapid double 8-nm steps by a kinesin mutant', *EMBO J*, 23: 2993-9.
- Hirokawa, N., and Y. Noda. 2008. 'Intracellular transport and kinesin superfamily proteins, KIFs: structure, function, and dynamics', *Physiol Rev*, 88: 1089-118.
- Hirokawa, N., Y. Noda, Y. Tanaka, and S. Niwa. 2009. 'Kinesin superfamily motor proteins and intracellular transport', *Nat Rev Mol Cell Biol*, 10: 682-96.
- Howard, J. 1996. 'The movement of kinesin along microtubules', *Annu Rev Physiol*, 58: 703-29.
- Huang, T. G., and D. D. Hackney. 1994. 'Drosophila kinesin minimal motor domain expressed in Escherichia coli. Purification and kinetic characterization', *J Biol Chem*, 269: 16493-501.
- Hunter, A. W., M. Caplow, D. L. Coy, W. O. Hancock, S. Diez, L. Wordeman, and J. Howard. 2003. 'The kinesin-related protein MCAK is a microtubule depolymerase that forms an ATP-hydrolyzing complex at microtubule ends', *Mol Cell*, 11: 445-57.
- Isojima, H., R. Iino, Y. Niitani, H. Noji, and M. Tomishige. 2016. 'Direct observation of intermediate states during the stepping motion of kinesin-1', *Nat Chem Biol*, 12: 290-7.
- Kaan, H. Y., D. D. Hackney, and F. Kozielski. 2011. 'The structure of the kinesin-1 motor-tail complex reveals the mechanism of autoinhibition', *Science*, 333: 883-5.
- Kabsch, W. 2010. 'Xds', *Acta Crystallogr D Biol Crystallogr*, 66: 125-32.
- Kaseda, K., H. Higuchi, and K. Hirose. 2003. 'Alternate fast and slow stepping of a heterodimeric kinesin molecule', *Nat Cell Biol*, 5: 1079-82.
- Kozielski, F., S. Sack, A. Marx, M. Thormahlen, E. Schonbrunn, V. Biou, A. Thompson, E. M. Mandelkow, and E. Mandelkow. 1997. 'The crystal structure of dimeric kinesin and implications for microtubule-dependent motility', *Cell*, 91: 985-94.
- Krylyshkina, O., I. Kaverina, W. Kranewitter, W. Steffen, M. C. Alonso, R. A. Cross, and J. V. Small. 2002. 'Modulation of substrate adhesion dynamics via microtubule targeting requires kinesin-1', *J Cell Biol*, 156: 349-59.
- Kull, F. J., E. P. Sablin, R. Lau, R. J. Fletterick, and R. D. Vale. 1996. 'Crystal structure of the kinesin motor domain reveals a structural similarity to myosin', *Nature*, 380: 550-5.
- Litowski, J. R., and R. S. Hodges. 2002. 'Designing heterodimeric two-stranded alpha-helical coiled-coils. Effects of hydrophobicity and alpha-helical propensity on protein folding, stability, and specificity', *J Biol Chem*, 277: 37272-9.

- Liu, H. L., C. W. th Pemble, and S. A. Endow. 2012. 'Neck-motor interactions trigger rotation of the kinesin stalk', *Sci Rep*, 2: 236.
- Lobert, S., and J. J. Correia. 1992. 'Subtilisin cleavage of tubulin heterodimers and polymers', *Arch Biochem Biophys*, 296: 152-60.
- Lockhart, A., and R. A. Cross. 1994. 'Origins of reversed directionality in the ncd molecular motor', *EMBO J*, 13: 751-7.
- Ma, Y. Z., and E. W. Taylor. 1997. 'Kinetic mechanism of a monomeric kinesin construct', *J Biol Chem*, 272: 717-23.
- Mackey, A. T., and S. P. Gilbert. 2000. 'Moving a microtubule may require two heads: a kinetic investigation of monomeric Ncd', *Biochemistry*, 39: 1346-55.
- Mandelkow, E. M., E. Mandelkow, and R. A. Milligan. 1991. 'Microtubule dynamics and microtubule caps: a time-resolved cryo-electron microscopy study', *J Cell Biol*, 114: 977-91.
- Manning, B. D., J. G. Barrett, J. A. Wallace, H. Granok, and M. Snyder. 1999. 'Differential regulation of the Kar3p kinesin-related protein by two associated proteins, Cik1p and Vik1p', *J Cell Biol*, 144: 1219-33.
- Maravillas-Montero, J. L., and L. Santos-Argumedo. 2012. 'The myosin family: unconventional roles of actin-dependent molecular motors in immune cells', *J Leukoc Biol*, 91: 35-46.
- Marszalek, J. R., and L. S. Goldstein. 2000. 'Understanding the functions of kinesin-II', *Biochim Biophys Acta*, 1496: 142-50.
- McCoy, A. J., R. W. Grosse-Kunstleve, P. D. Adams, M. D. Winn, L. C. Storoni, and R. J. Read. 2007. 'Phaser crystallographic software', *J Appl Crystallogr*, 40: 658-74.
- Milic, B., J. O. Andreasson, W. O. Hancock, and S. M. Block. 2014. 'Kinesin processivity is gated by phosphate release', *Proc Natl Acad Sci U S A*, 111: 14136-40.
- Morikawa, M., H. Yajima, R. Nitta, S. Inoue, T. Ogura, C. Sato, and N. Hirokawa. 2015. 'X-ray and Cryo-EM structures reveal mutual conformational changes of Kinesin and GTP-state microtubules upon binding', *EMBO J*, 34: 1270-86.
- Nakata, T., and N. Hirokawa. 1995. 'Point mutation of adenosine triphosphate-binding motif generated rigor kinesin that selectively blocks anterograde lysosome membrane transport', *J Cell Biol*, 131: 1039-53.
- Nawrotek, A., M. Knossow, and B. Gigant. 2011. 'The determinants that govern microtubule assembly from the atomic structure of GTP-tubulin', *J Mol Biol*, 412: 35-42.
- Nitta, R., Y. Okada, and N. Hirokawa. 2008. 'Structural model for strain-dependent microtubule activation of Mg-ADP release from kinesin', *Nat Struct Mol Biol*, 15: 1067-75.
- Nogales, E., and H. W. Wang. 2006. 'Structural intermediates in microtubule assembly and disassembly: how and why?', *Curr Opin Cell Biol*, 18: 179-84.
- Nogales, E., S. G. Wolf, and K. H. Downing. 1998. 'Structure of the alpha beta tubulin dimer by electron crystallography', *Nature*, 391: 199-203.
- Oakley, B. R. 2000. 'An abundance of tubulins', *Trends Cell Biol*, 10: 537-42.
- Ovechkina, Y., and L. Wordeman. 2003. 'Unconventional motoring: an overview of the Kin C and Kin I kinesins', *Traffic*, 4: 367-75.
- Parke, C. L., E. J. Wojcik, S. Kim, and D. K. WorthyLake. 2010. 'ATP hydrolysis in Eg5 kinesin involves a catalytic two-water mechanism', *J. Biol. Chem.*, 285: 5859-67.

- Pechatnikova, E., and E. W. Taylor. 1997. 'Kinetic mechanism of monomeric non-claret disjunctional protein (Ncd) ATPase', *J Biol Chem*, 272: 30735-40.
- Pecqueur, L., C. Duellberg, B. Dreier, Q. Jiang, C. Wang, A. Pluckthun, T. Surrey, B. Gigant, and M. Knossow. 2012. 'A designed ankyrin repeat protein selected to bind to tubulin caps the microtubule plus end', *Proc Natl Acad Sci U S A*, 109: 12011-6.
- Pollard, T. D., and E. D. Korn. 1973. 'Acanthamoeba myosin. I. Isolation from *Acanthamoeba castellanii* of an enzyme similar to muscle myosin', *J Biol Chem*, 248: 4682-90.
- Rank, K. C., C. J. Chen, J. Cope, K. Porche, A. Hoenger, S. P. Gilbert, and I. Rayment. 2012. 'Kar3Vik1, a member of the kinesin-14 superfamily, shows a novel kinesin microtubule binding pattern', *J Cell Biol*, 197: 957-70.
- Ravelli, R. B., B. Gigant, P. A. Curmi, I. Jourdain, S. Lachkar, A. Sobel, and M. Knossow. 2004. 'Insight into tubulin regulation from a complex with colchicine and a stathmin-like domain', *Nature*, 428: 198-202.
- Rayment, I. 1996. 'Kinesin and myosin: molecular motors with similar engines', *Structure*, 4: 501-4.
- Rice, S., A. W. Lin, D. Safer, C. L. Hart, N. Naber, B. O. Carragher, S. M. Cain, E. Pechatnikova, E. M. Wilson-Kubalek, M. Whittaker, E. Pate, R. Cooke, E. W. Taylor, R. A. Milligan, and R. D. Vale. 1999. 'A structural change in the kinesin motor protein that drives motility', *Nature*, 402: 778-84.
- Sablin, E. P., R. B. Case, S. C. Dai, C. L. Hart, A. Ruby, R. D. Vale, and R. J. Fletterick. 1998. 'Direction determination in the minus-end-directed kinesin motor ncd', *Nature*, 395: 813-6.
- Sablin, E. P., F. J. Kull, R. Cooke, R. D. Vale, and R. J. Fletterick. 1996. 'Crystal structure of the motor domain of the kinesin-related motor ncd', *Nature*, 380: 555-9.
- Sack, S., F. J. Kull, and E. Mandelkow. 1999. 'Motor proteins of the kinesin family. Structures, variations, and nucleotide binding sites', *Eur J Biochem*, 262: 1-11.
- Sack, S., J. Muller, A. Marx, M. Thormahlen, E. M. Mandelkow, S. T. Brady, and E. Mandelkow. 1997. 'X-ray structure of motor and neck domains from rat brain kinesin', *Biochemistry*, 36: 16155-65.
- Sadhu, A., and E. W. Taylor. 1992. 'A kinetic study of the kinesin ATPase', *J Biol Chem*, 267: 11352-9.
- Schliwa, M., and G. Woehlke. 2003. 'Molecular motors', *Nature*, 422: 759-65.
- Shang, Z., K. Zhou, C. Xu, R. Csencsits, J. C. Cochran, and C. V. Sindelar. 2014. 'High-resolution structures of kinesin on microtubules provide a basis for nucleotide-gated force-generation', *Elife*, 3: e04686.
- Shipley, K., M. Hekmat-Nejad, J. Turner, C. Moores, R. Anderson, R. Milligan, R. Sakowicz, and R. Fletterick. 2004. 'Structure of a kinesin microtubule depolymerization machine', *EMBO J*, 23: 1422-32.
- Sindelar, C. V., M. J. Budny, S. Rice, N. Naber, R. Fletterick, and R. Cooke. 2002. 'Two conformations in the human kinesin power stroke defined by X-ray crystallography and EPR spectroscopy', *Nat Struct Biol*, 9: 844-8.
- Sindelar, C. V., and K. H. Downing. 2007. 'The beginning of kinesin's force-generating cycle visualized at 9-A resolution', *J Cell Biol*, 177: 377-85.
- Sindelar, C. V., and K. H. Downing. 2010. 'An atomic-level mechanism for activation of the kinesin molecular motors', *Proc Natl Acad Sci U S A*, 107: 4111-6.

- Song, Y., and S. T. Brady. 2015. 'Post-translational modifications of tubulin: pathways to functional diversity of microtubules', *Trends Cell Biol*, 25: 125-36.
- Svoboda, K., C. F. Schmidt, B. J. Schnapp, and S. M. Block. 1993. 'Direct observation of kinesin stepping by optical trapping interferometry', *Nature*, 365: 721-7.
- Sweeney, H. L., and A. Houdusse. 2010. 'Myosin VI rewrites the rules for myosin motors', *Cell*, 141: 573-82.
- Tantama, M., J. R. Martinez-Francois, R. Mongeon, and G. Yellen. 2013. 'Imaging energy status in live cells with a fluorescent biosensor of the intracellular ATP-to-ADP ratio', *Nat Commun*, 4: 2550.
- Vale, R. D., and R. A. Milligan. 2000. 'The way things move: looking under the hood of molecular motor proteins', *Science*, 288: 88-95.
- Vale, R. D., T. S. Reese, and M. P. Sheetz. 1985. 'Identification of a novel force-generating protein, kinesin, involved in microtubule-based motility', *Cell*, 42: 39-50.
- Verhey, K. J., and J. W. Hammond. 2009. 'Traffic control: regulation of kinesin motors', *Nat Rev Mol Cell Biol*, 10: 765-77.
- Walker, J. E., M. Saraste, M. J. Runswick, and N. J. Gay. 1982. 'Distantly related sequences in the α - and β -subunits of ATP synthase, myosin, kinases and other ATP-requiring enzymes and a common nucleotide binding fold', *EMBO J*, 1: 945-51.
- Walker, R. A., E. T. O'Brien, N. K. Pryer, M. F. Soboeiro, W. A. Voter, H. P. Erickson, and E. D. Salmon. 1988. 'Dynamic instability of individual microtubules analyzed by video light microscopy: rate constants and transition frequencies', *J Cell Biol*, 107: 1437-48.
- Wang, W., L. Cao, C. Wang, B. Gigant, and M. Knossow. 2015. 'Kinesin, 30 years later: Recent insights from structural studies', *Protein Sci*, 24: 1047-56.
- Winn, M. D., C. C. Ballard, K. D. Cowtan, E. J. Dodson, P. Emsley, P. R. Evans, R. M. Keegan, E. B. Krissinel, A. G. Leslie, A. McCoy, S. J. McNicholas, G. N. Murshudov, N. S. Pannu, E. A. Potterton, H. R. Powell, R. J. Read, A. Vagin, and K. S. Wilson. 2011. 'Overview of the CCP4 suite and current developments', *Acta Crystallogr D Biol Crystallogr*, 67: 235-42.
- Wloga, D., and J. Gaertig. 2010. 'Post-translational modifications of microtubules', *J Cell Sci*, 123: 3447-55.
- Yajima, J., M. C. Alonso, R. A. Cross, and Y. Y. Toyoshima. 2002. 'Direct long-term observation of kinesin processivity at low load', *Curr Biol*, 12: 301-6.
- Yildiz, A., and P. R. Selvin. 2005. 'Kinesin: walking, crawling or sliding along?', *Trends Cell Biol*, 15: 112-20.
- Yildiz, A., M. Tomishige, R. D. Vale, and P. R. Selvin. 2004. 'Kinesin walks hand-over-hand', *Science*, 303: 676-8.
- Yokoyama, H., J. Sawada, S. Katoh, K. Matsuno, N. Ogo, Y. Ishikawa, H. Hashimoto, S. Fujii, and A. Asai. 2015. 'Structural basis of new allosteric inhibition in Kinesin spindle protein Eg5', *ACS Chem Biol*, 10: 1128-36.
- Yun, M., C. E. Bronner, C. G. Park, S. S. Cha, H. W. Park, and S. A. Endow. 2003. 'Rotation of the stalk/neck and one head in a new crystal structure of the kinesin motor protein, Ncd', *EMBO J*, 22: 5382-9.
- Zhang, R., G. M. Alushin, A. Brown, and E. Nogales. 2015. 'Mechanistic Origin of Microtubule Dynamic Instability and Its Modulation by EB Proteins', *Cell*, 162: 849-59.

Titre : Bases structurales de la motilité des kinésines

Mots clés : kinésine, tubuline, motilité

Résumé : Les kinésines sont des protéines moteur liées au cytosquelette de microtubules. Elles convertissent l'énergie provenant de l'hydrolyse de l'ATP en un travail mécanique. Leur fonction typique est de se déplacer le long du microtubule pour véhiculer des charges. La plupart des kinésines sont des dimères. Elles comprennent un domaine moteur, qui porte à la fois les sites de liaison du nucléotide et du microtubule, un domaine intermédiaire de dimérisation et une partie dite « queue » qui confère la spécificité des charges à transporter. Mon objectif est d'établir le mécanisme moléculaire à la base de la motilité, avec un intérêt particulier pour la détermination des variations structurales du domaine moteur de la kinésine le long de son cycle mécano-chimique. Au cours de ma thèse, mon objet d'étude principal a été la kinésine-1 humaine, encore appelée kinésine conventionnelle.

J'ai étudié plus particulièrement deux aspects du cycle mécano-chimique de la kinésine-1, en combinant des approches de biologie structurale et l'étude de mutants. Les deux aspects concernent l'étude de la fixation de la kinésine-ADP au microtubule, conduisant à l'éjection du nucléotide et à une liaison forte de la kinésine au microtubule. Dans un premier temps, j'ai déterminé la structure du domaine moteur de la kinésine-1, dépourvue de nucléotide, et sous forme d'un complexe avec la tubuline. La tubuline est la protéine constitutive des microtubules. Cette structure était la donnée principale qui nous manquait dans le cycle structural de la kinésine. En comparant cette structure avec celle de la kinésine dans un état ATP, on peut rendre compte des changements de conformation de la kinésine selon le mouvement de trois sous-domaines du domaine moteur. Cette analyse explique notamment le lien entre la fixation de l'ATP et l'ouverture d'une poche hydrophobe distante de 28 Å du site du nucléotide. Cette cavité va accommoder le premier résidu du neck linker, conduisant à la stabilisation de ce peptide situé en partie C-terminale du domaine moteur. En s'ordonnant, le neck linker va faire avancer la charge ainsi que l'autre domaine moteur de la kinésine dimérique. Il lie ainsi la fixation de l'ATP au mouvement. L'étude de l'effet de mutations du neck linker montre aussi comment, réciproquement, le neck linker bloque la kinésine dans la conformation active pour l'hydrolyse de l'ATP. Ceci diminue la probabilité que l'ATP soit hydrolysé avant que l'étape mécanique se soit produite; cet aspect est essentiel pour rendre compte de la processivité de la kinésine-1.

Ces données structurales suggèrent également comment la fixation de la kinésine-ADP au microtubule accélère l'éjection de l'ADP. Pour étudier cet aspect plus en détail, j'ai étudié l'effet de mutations sur la vitesse de largage de l'ADP. L'idée était de mimer à l'aide de mutations la fixation au microtubule. J'ai identifié ainsi deux séries de mutants qui présentent une vitesse accélérée de largage spontané de l'ADP, ce qui suggère deux voies pour interférer avec la fixation du nucléotide. J'ai ensuite déterminé la structure de deux de ces mutants dépourvus de nucléotide, ainsi que celle de la kinésine de départ également dans une forme apo, obtenue par digestion de l'ADP. En absence de microtubule, la kinésine dépourvue de nucléotide adopte une conformation soit à l'image de celle de la kinésine-ADP, ou proche de celle de la kinésine-apo liée à la tubuline. Dans un contexte naturel, seule la deuxième conformation est compatible avec la fixation au microtubule. L'ensemble de ces résultats suggère que le microtubule accélère l'éjection du nucléotide par un double mécanisme : en interférant avec la liaison du magnésium et en déstabilisant le motif P-loop de liaison du nucléotide.



Title : Structural Basis Of Kinesin Motility

Keywords : kinesin, microtubule, motility,

Abstract : Kinesins are a family of microtubule-interacting motor proteins that convert the chemical energy from ATP hydrolysis into mechanical work. Many kinesins are motile, walking along microtubules to fulfill different functions. Most kinesins are dimers, the monomer comprising a motor domain, a dimerizing stalk domain, and a tail domain. The motor domain contains both the nucleotide-binding site and the microtubule-binding site. I am interested in the molecular mechanism of kinesin's motility. In particular I want to establish the structural variations of the kinesin motor domain along with the mechanochemical cycle of this motor protein. During my thesis, I have focused my work on the human kinesin-1, also named conventional kinesin, which is the best characterized kinesin.

I have studied two aspects of the kinesin mechanochemical cycle, by combining structural and mutational approaches. Both aspects rely on the binding of ADP-kinesin to a microtubule, which leads to the release of the nucleotide and to a tight kinesin-microtubule association. First I determined the crystal structure of nucleotide-free kinesin-1 motor domain in complex with a tubulin heterodimer, which is the building block of microtubule. This structure represented the main missing piece of the structural cycle of kinesin. Three subdomains in the kinesin motor domain were identified through the comparison of this complex structure with ATP-analog kinesin-1-tubulin structure. The relative movements of these subdomains explain how ATP binding to apo-kinesin bound to microtubule triggers the opening of a hydrophobic cavity, 28 Å distant from the nucleotide-binding site. This cavity accommodates the first residue of the “neck linker”, a short peptide that is C-terminal to the motor domain, allowing the neck linker to dock on the motor domain. The docking of the neck linker is proposed to trigger the mechanical step, i.e. the displacement of the cargo and the stepping of the dimeric kinesin. By studying mutants of the neck linker, I have shown that, reciprocally, this peptide locks kinesin in the ATP state, which is also the conformation efficient for ATP hydrolysis. Doing so, it prevents the motor domain from switching back to the apo-state. It prevents also an untimely hydrolysis of ATP, before the mechanical step has occurred. These features are required for movement and processivity.

Second, these structural data also suggest how the binding of ADP-kinesin to tubulin enhances nucleotide release from kinesin. To further study this step of the kinesin cycle, I studied the effect of kinesin-1 mutations. These mutations were designed in isolated kinesin to mimic the state when kinesin is bound to a microtubule. I identified two groups of mutations leading to a high spontaneous ADP dissociation rate, suggesting that there are two ways to interfere with ADP binding. Then I determined the crystal structures of the apo form of two mutants as well as that of the nucleotide-depleted wild type kinesin. It showed that apo-kinesin adopts either an ADP-like conformation or a tubulin-bound apo-like one. In the natural context, the second one is stabilized upon microtubule binding. Overall, the mutational and structural data suggest that microtubules accelerate ADP dissociation in kinesin by two main paths, by interfering with magnesium binding and by destabilizing the nucleotide-binding P-loop motif.

